The Sun and Heliosphere In Three Dimensions

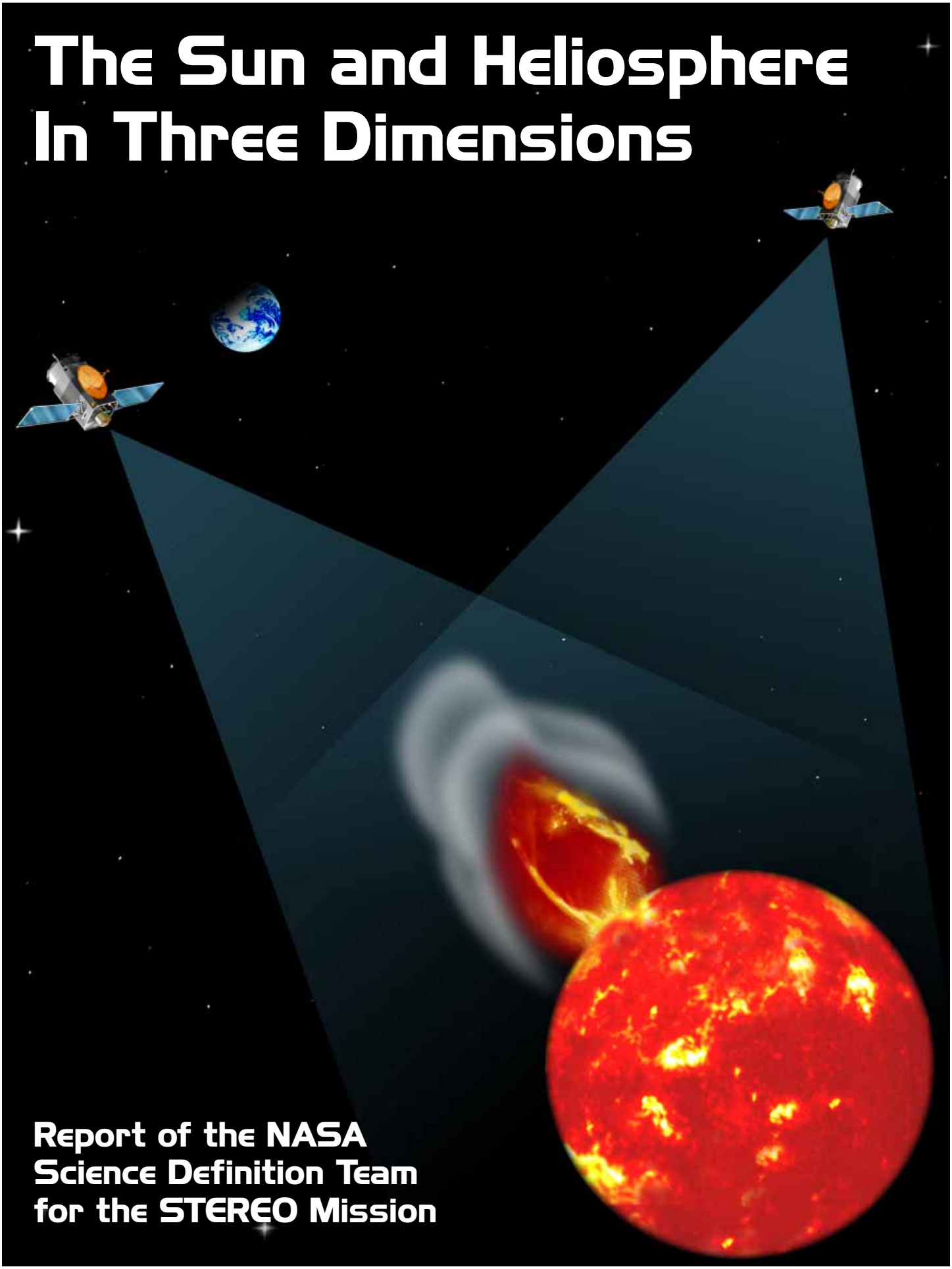

Report of the NASA Science Definition Team for the STEREO Mission

Table of Contents

Acknowledgements

We are grateful for the encouragement and support of so many of our colleagues in the solar and space physics community. In particular, we thank Bernie Jackson, Allen Gary, Don Reames, Barbara Thompson, John Davis, Jeff Hall, and Eric De Jong for illustrations, and Ralph McNutt and Tom Potemra for reviewing a draft of this report. Jim Watzin led the Goddard study team. Murrie Burgan, Eric Benfer, and Patrice Zurvalec helped in editing the manuscript and preparing it for publication.

Science Definition Team Members

Chairman
David Rust
The Johns Hopkins University
Applied Physics Laboratory
Laurel, Maryland

NASA Study Scientist
Joseph Davila
NASA/Goddard Space Flight Center
Greenbelt, Maryland

Members
Volker Bothmer
University of Kiel
Institut für Reine und Angewandte Kernphysik
Kiel, Germany

Lennard Culhane
Mullard Laboratory
University College
London, United Kingdom

Richard Fisher
NASA/Goddard Space Flight Center
Greenbelt, Maryland

John Gosling
Los Alamos National Laboratory
Los Alamos, New Mexico

Lika Guhathakurta
NASA/Goddard Space Flight Center
Greenbelt, Maryland

Hugh Hudson
Institute of Space and Astronautical Science
Kanagawa, Japan

Michael Kaiser
NASA/Goddard Space Flight Center
Greenbelt, Maryland

James Klimchuk
Naval Research Laboratory
Washington, D. C.

Paulett Liewer
Jet Propulsion Laboratory
Pasadena, California

Richard Mewaldt
California Institute of Technology
Pasadena, California

Marcia Neugebauer
Jet Propulsion Laboratory
Pasadena, California

Victor Pizzo
NOAA/Space Environment Laboratory
Boulder, Colorado

Dennis Socker
Naval Research Laboratory
Washington, D. C.

Keith Strong
Lockheed Martin Advanced Technology Center
Palo Alto, California

NASA Study Scientist
George Withbroe
NASA Headquarters
Washington, D. C.

Goddard Study Manager
James Watzin
NASA/Goddard Space Flight Center
Greenbelt, Maryland

1. Introduction

NASA's Sun-Earth Connections program aims to improve mankind's understanding of the origins of solar variability, how that variability transforms the interplanetary medium, how eruptive events on the Sun impact geospace, and how they might affect climate and weather.

STEREO is the third of five Solar-Terrestrial Probes called for in NASA's Space Science Enterprise Strategic Plan to accomplish the goals of the Sun-Earth Connections program. The first of these missions, the Thermosphere-Ionosphere-Mesosphere Energetics and Dynamics mission (TIMED) is scheduled for launch in 2000. The other missions are

- *Solar-B*, which will obtain high-resolution images of the solar magnetic field to determine how it emerges, evolves, and dissipates its energy at the solar surface. These processes are the drivers of the solar activity we observe.
- *STEREO*, which will obtain simultaneous images of the Sun from two spacecraft and build a three-dimensional (3-D) picture of coronal mass ejections (CMEs) and the complex structures around them. STEREO will also study the propagation of disturbances through the heliosphere and their effects at Earth orbit.
- *Magnetospheric Multiscale*, which will provide a network of *in situ* measurements of Earth's magnetosphere that can be combined to give a 3-D image of magnetic substorms and other activity in geospace.
- *Global Electrodynamics*, which will probe Earth's upper atmosphere to determine how variations in particle flux and solar electromagnetic radiation affect it.

While these missions individually will doubtless produce exciting discoveries about the complex Sun–Earth system, together they are a formidable fleet that will greatly improve our ability to predict weather in space, enhance our knowledge of solar influences on climate change, and give us fresh insight into the origins and future of life on Earth. Although the Sun is much quieter today than in the distant past —it was once a rapidly rotating, strongly magnetic, violently active star with a massive stellar wind—it is still capable of violent explosions and substantial variations in radiative output. Understanding present-day solar activity will help mankind understand the history of the Sun's climate and its possible influence on Earth's evolution and the development of life.

It is through CMEs that solar activity is most forcefully felt at Earth. CMEs are the most energetic eruptions on the Sun. They are responsible for essentially all of the largest solar proton events, and they are the primary cause of major geomagnetic storms. Unfortunately, no one can predict reliably when a CME will occur or what its effects will be.

In order to make progress in this area, we need to follow CME-generated disturbances from the Sun to at least the orbit of Earth and we need to know the state of the ambient solar wind in front of these disturbances. Coronal observations need to provide accurate measurements of the pre-CME corona and of CME timing, size, geometry, mass, speed (as a function of height), and direction at a minimum. Information about the strength and polarity of the field embedded within the CMEs would also be highly desirable. We need to track the evolution of the disturbances optically or by radio emissions through the interplanetary medium to 1 AU. The *in situ* observations need to provide accurate information about the state of the ambient wind and energetic particle populations ahead of the CMEs while also determining the plasma, magnetic field, and energetic particle characteristics of the interplanetary disturbances as they pass.

Unfortunately, the CMEs that most affect Earth are also the least likely to be detected with ground-based or Earth-orbiting telescopes. To understand CMEs better and to forecast their arrival and effects at Earth, a totally new perspective on CMEs and their sources in the solar atmosphere is needed. Achieving this perspective will require moving away from our customary lookout point. This report describes the scientific progress that can be achieved toward the goals of the Sun-Earth Connections program with two spacecraft at 1 AU, one drifting well ahead of Earth and one well behind. Together the two spacecraft comprise the Solar-TErrestrial Relations Observatory (STEREO).

2. Scientific Objectives

The principal science objectives to be addressed by the STEREO mission are as follows:

- Understand the origin and consequences of CMEs
- Determine the processes that control CME evolution in the heliosphere by tracking CME-driven disturbances from the Sun to Earth's orbit
- Discover the mechanisms and sites of solar energetic particle acceleration
- Determine the 3-D structure and dynamics of coronal and interplanetary plasmas and magnetic fields
- Probe the solar dynamo through its effects on the corona and heliosphere

Coronal Mass Ejections

A primary scientific motivation for studying CMEs stems from their enormous and difficult-to-explain spatial scales, masses, speeds, and energies. CMEs appear to be the means by which the corona evolves through the solar cycle. They may be the means of removing dynamo-generated magnetic flux from the Sun. They appear thus to be a crucial link to Earth from the solar dynamo. Further, the striking effects of CMEs on planetary magnetospheres, comets, and cosmic rays extend the interest in mass ejections well beyond the traditional realm of solar physics, as emphasized in the Sun-Earth Connection Roadmap. Finally, there may be astrophysical analogues of mass ejections, perhaps in accretion disks and active galactic nuclei, that will be better understood when we understand CMEs.

Explaining the sudden expulsion of a highly conducting plasma from the magnetized Sun presents a major challenge to space physics. The spectacular nature of these large mass ejections is illustrated in Figure 1 by a time sequence of images obtained with the Large Angle Spectroscopic Coronagraph (LASCO) flown on the SOHO mission. The bright, loop-like feature contains more than 10^{15} g of plasma. The energy required to lift the material off the Sun may be as high as 4×10^{32} ergs.

CMEs are complex and poorly understood. Nonetheless, it is now evident that many ejections involve

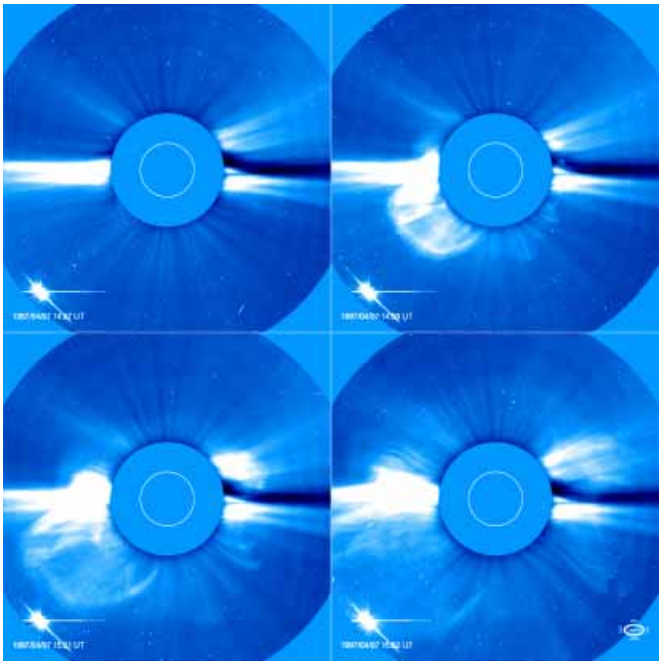

Figure 1. Four images from the LASCO coronagraph on SOHO, showing a CME on 7 April 1997.

the eruption of coronal and chromospheric plasma from a region pervaded by magnetic fields that are initially closed and possibly twisted. What triggers the eruption? How is the energy built up and over what scale? Which, if any, of the several competing models of CME origins is the correct physical description of what happens on the Sun?

CME Onset

Here are some of the many models for the origins of CMEs that have been proposed:

- Magnetic shear by surface motions, causing loss of equilibrium in the corona
- Magnetic helicity charging from beneath the surface, causing a kink instability in the corona
- Emerging magnetic flux, causing loss of equilibrium in a coronal arcade
- Magnetic helicity charging of the corona by flares, causing loss of equilibrium in a coronal arcade
- Thermally driven blast wave from a large flare, blowing the corona open
- Buoyancy, due to a low-density cavity in the corona

One should be able to distinguish among the models by careful examination of the structure of the pre-CME corona. CMEs frequently follow several days of "swelling" of a coronal helmet streamer. There may be corresponding changes in the low corona: magnetic shear (by differential rotation's effect on emerged coronal loops) or magnetic helicity charging (loop twisting by subsurface flows). Three-dimensional reconstructions by triangulation on coronal features should reveal the key signatures of these processes and even allow us to specify the density, temperature, and magnetic fields of the pre-event structures.

As the list of models suggests, several fundamental questions must be answered if we are to understand the physical causes of CME eruption:

- Are CMEs driven primarily by magnetic or nonmagnetic forces?
- What is the geometry and magnetic topology of CMEs?
- What key coronal phenomena accompany CME onset?
- What initiates CMEs?
- What is the role of magnetic reconnection?
- What is the role of evolving surface features?

These questions cannot be satisfactorily addressed with single-vantage-point observations of the type currently available. The corona is optically thin, both in the emissions seen by X-ray and UV imagers and in the Thompson-scattered photospheric light seen by coronagraphs. Line-of-sight integration effects are a major source of ambiguity and confusion. Only STEREO can provide the observations necessary to sort out the overlapping 3-D structures.

CME Geometry and Onset Signatures

The geometry of erupting CME structures is currently unknown. Several basic configurations have been proposed: a simple dipolar arcade, a quadrupolar multi-arcade system, a half-emerged flux rope, and a suspended flux rope. The different physical properties of these configurations predict different eruption scenarios, as discussed later. Detailed numerical models of CMEs have been developed, but nearly all of them have made the simplifying assumption that the field is two dimensional (e.g., an infinite arcade). In reality, of course, the erupting structures have finite extent, and 3-D effects must be important. *With the range of view angles accessible to the STEREO telescopes, CMEs and coronal structures can be reconstructed in three dimensions.*

A CME frequently starts with a sinuous brightening in the low corona and an outward movement of coronal structures on many scales. Chromospheric and coronal plasma is accelerated to 300 km s^{-1} or more. Observations with the Extreme-ultraviolet Imaging Telescope (EIT) on SOHO show that CMEs are often accompanied by a wave front in the corona. An example is shown in Figure 2. It was once thought that such waves are triggered only by flares, but now

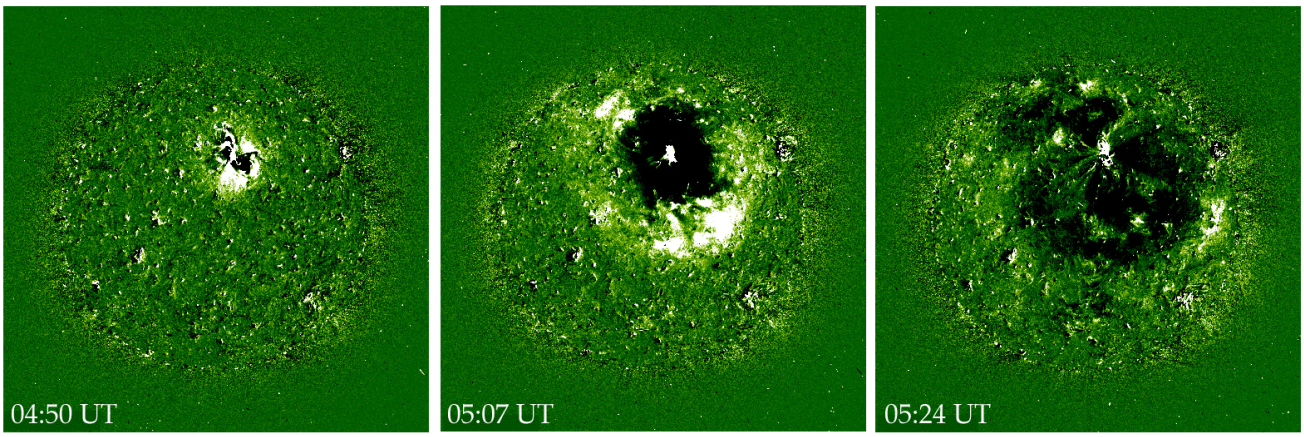

Figure 2. SOHO-EIT observations of a wave expanding from a CME initiation site on 12 May 1997. Images are successive differences of images in Fe XII 195 Å.

the whole issue must be reexamined. While the waves, variously called Moreton waves or EIT waves, do not appear to be "thermal blast waves," they seem to be intimately involved with CMEs. What is the relationship of the wave to the CME? Which is the trigger? In order to resolve these questions, STEREO should be designed to provide images with a much higher cadence than SOHO does.

It is well established that pre-eruption magnetic field configurations contain ample free energy to explain the gravitational and kinetic energies of CMEs. However, it is not so obvious that enough of this energy is released as the field is opened during the eruption. There can actually be an increase in the magnetic energy locally, even though the global magnetic energy may decrease. This has led some to argue that CMEs must be buoyancy driven, so it is important to be able to gauge the size and density of coronal cavities.

Many CMEs have a three-part structure that includes a dark cavity, a bright frontal loop, and an embedded core (probably erupting prominence material). There are, however, many examples of CMEs and pre-event streamers with no obvious cavity. If no cavity exists, then buoyancy can be ruled out, and CMEs must be magnetically driven. Whether or not cavities are present in these structures is difficult to know due to the possibility of overlapping bright features in the foreground and background. Only STEREO can provide the observations needed to unambiguously establish whether cavities are universal and, therefore, whether CMEs are magnetically or buoyancy driven. Determination of crucial physical parameters such as the density and pressure of the cavity will require simultaneous observations of emissions that are sensitive to density (white-light coronagraph) and to density squared (emission-line imager).

Reconnection

In many CME models, magnetic reconnection is necessary for the eruption to begin or to proceed. The physical role of reconnection varies from model to model, however, and it is possible that reconnection plays no active role whatsoever. In the dipolar arcade and suspended flux rope models, the stretched fields reconnect beneath the CME at the same time that the CME is lifting off. Without reconnection, a full eruption is not possible. In contrast, the quadrupolar model involves reconnection high in the corona above the erupting arcade, and no reconnection is necessary at low altitudes.

These different scenarios can be tested with STEREO observations. For example, reconnection in the dipole arcade and flux rope models produces closed magnetic loops under the CME that should be visible at the time of the eruption. If no loops are seen, then the models must be either rejected or modified. Existing observations suggest that the erupting magnetic fields in many events remain open to the surface for a considerable time after the eruption has begun. This would seem to contradict the models. However, the interpretation of the observations is open to debate, since the orientation of the arcade is not known. An end-on view should reveal closed loops if they exist, but a sideways view might not. Only STEREO can resolve this ambiguity.

Surface Evolution

It is widely believed that CMEs are a response to changes in the surface magnetic fields. These fields are constantly evolving, either by the twisting and shearing of existing flux or by the emergence of new flux from below the photosphere. These processes stress the overlying coronal field, and the field erupts whenever the stresses become too great. An understanding of how surface fields evolve leading up to eruption is vital if we are to understand why CMEs occur. It might also prove valuable for CME prediction, a long-term goal of the National Space Weather Program. At present, it is extremely difficult to study surface evolution in the days immediately proceeding a CME. Surface features, especially magnetic fields, are best observed near disk center, whereas CMEs are best observed near the limb. A STEREO coronagraph would be able to detect CMEs that originate above surface locations that are at solar disk center as viewed from Earth. This would allow us to study the role of surface evolution and, in particular, to address the recent suggestion that CMEs are triggered by emerging flux. The needed vector magnetograms will be available from Solar-B and the National Solar Observatory SOLIS magnetographs.

The Heliosphere Between the Sun and Earth

The heliosphere extending from 30 R_{Sun} to 1 AU (215 R_{sun}), i.e., from the edge of the widest-field LASCO coronagraph to Earth orbit, contains nearly 400 times the volume of the currently imaged region close to the Sun. This volume has remained unexplored, except during the Helios mission 20 years ago. The two Helios spacecraft carried solar wind analyzers and low-resolution photometers that mapped the solar wind density distribution in the heliosphere and proved that CMEs can be detected well beyond 30 R_{Sun}, even well into the heliosphere (see Figure 3). No such observations are available now.

In general, dense heliospheric structure follows the location of the heliospheric current sheet. However, this structure evolves and is segmented, with the dense segments generally being associated with regions of high solar activity. Thus, the heliosphere is populated not so much by a continuous dense "ballerina skirt" of slow-speed solar wind forming a wave around the Sun but, instead, by a set of spikes (see Figure 4) along the skirt that vary continually in strength.

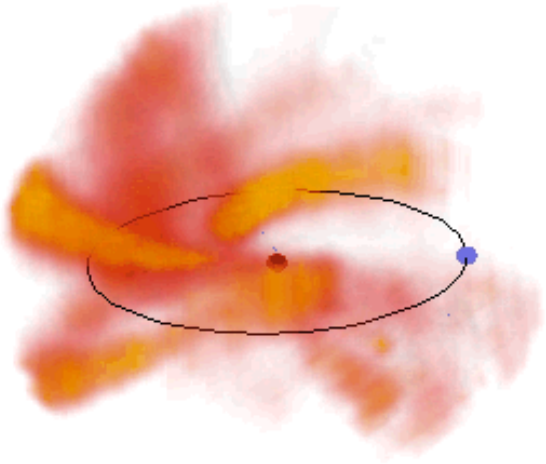

Figure 4. Perspective view of the corotating solar wind pattern for Carrington Rotation 1653. The ellipse indicates Earth's orbit. Solar wind densities, indicated by shades of gray, were derived by fitting a heliospheric model to Helios photometer observations of Thompson-scattering from solar wind electrons.

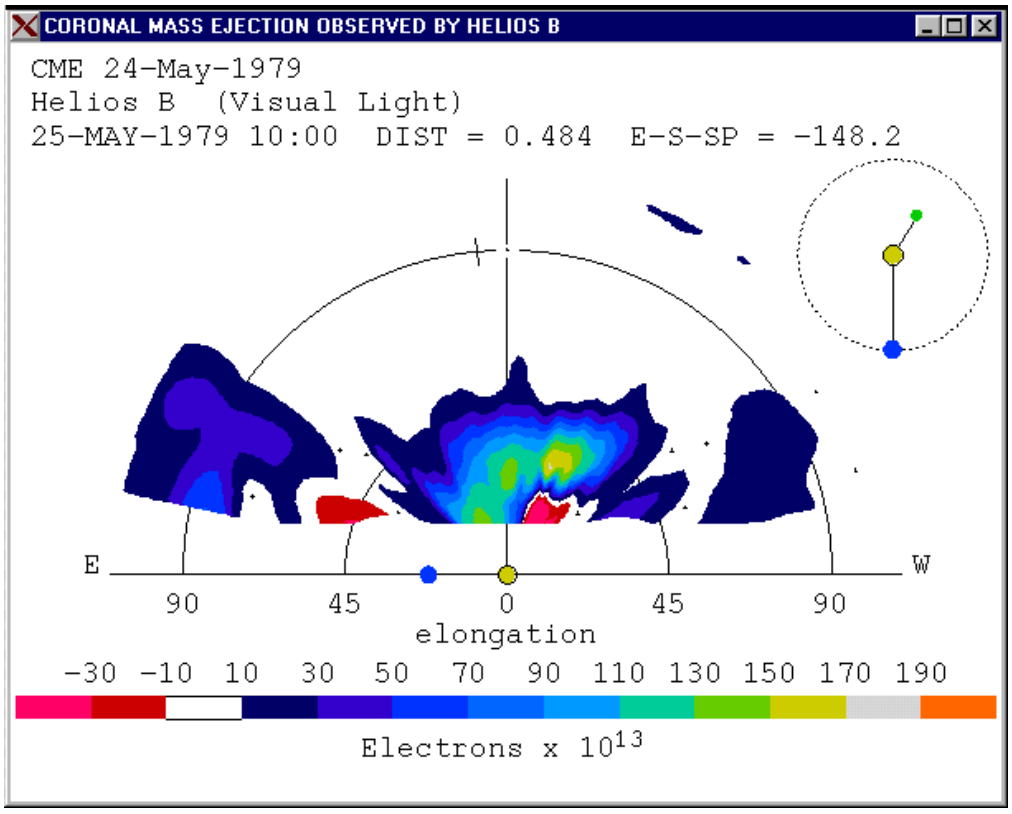

Figure 3. Polar plot of a CME recorded by the Helios B visible light photometer. Signal at 90° elongation corresponds to a CME passing overhead. The spacecraft was at 0.484 AU from the Sun at the time.

The quiet solar wind flows out nearly radially from the Sun in corotating patterns that evolve slowly with time. The distribution of matter in the heliosphere is never entirely certain because of a lack of timely 3-D information. Figure 5 shows what has been accomplished with Helios data analysis, but that image was built up under the assumption that the heliospheric density distribution was unchanged for a whole solar rotation. *Determination of the instantaneous distribution of matter in the heliosphere is an important goal for STEREO*. Solar wind density and velocity measured *in situ* at 1 AU can be related to 3-D reconstructions from STEREO heliosphere imagers and coronagraphs and traced almost all the way down to the solar surface. This is not currently possible.

Visibility of Earth-Directed CMEs

The quantities observed by coronagraphs are the polarized brightness *pB* and the brightness *B*, and they are related to the electron density through a line-of-sight integral over the light-scattering electrons. The (Thompson) scattering cross section is quite small and the density of the corona is very low. As a consequence, the white-light corona is very faint, and because the incident light is polarized by the scattering, one has to consider carefully how coronal visibility is affected by the angle between the Sun, the scattering electrons, and the observer. For a spherically symmetric coronal density distribution, roughly half of the total scattered light comes from within about ±20° of the plane of the sky. *Contributions of structures that are 60° in front of or behind the solar disk are a few percent.* Because of this limb-viewing bias of coronagraphs, most CMEs observed to date could not be related uniquely to other observed kinds of solar activity. Using simple mathematical models, we investigated the *pB* properties of a typical CME as viewed in projection in the plane of the sky and at various angular distances away from the plane of the sky. The simulated CME extended from 2.5 R_{Sun} to 8.0 R_{Sun}. It was 35° wide in longitude, and the shell was 1 R_{Sun} thick (these numbers are representative of CME observations from LASCO C2 and C3). Figure 5a presents a view with the CME in the plane of the sky, while Figures 5b and 5c show the views when the CME is rotated 30° and 60° out of the plane of the sky, respectively. The CME appears fainter and smaller when rotated 30° from the plane of the sky. It appears as a halo when rotated to 90°. But our simulation shows that correct interpretation of the halo in terms of physical size or angular extent is almost impossible. Also, images from a single vantage point do not provide any information on the longitude of the CME. With two vantage points, one can ascertain its longitude and compare it directly to other solar disk observations.

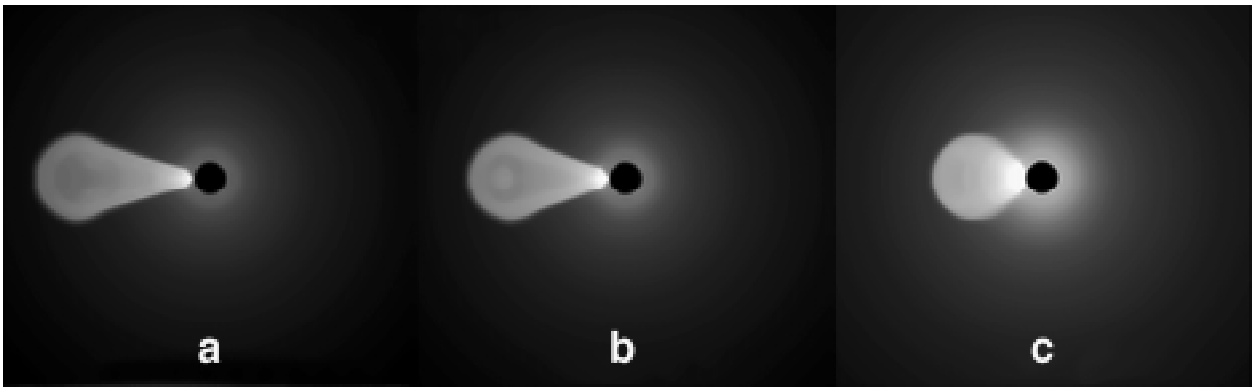

Figure 5. Three views of a simulated coronal mass ejection. (a) CME in the plane of the sky on the west limb of the Sun, (b) CME rotated 30° from the plane of the sky, and (c) CME rotated 60° from the plane of the sky.

CMEs in the Heliosphere

CME propagation and CME effects at Earth depend not only on the character of the coronal event but also on the state of the heliosphere. Even as a CME emerges from the corona, its motion is influenced by surrounding streamer belt structures and coronal holes. A fast CME propagating into a slow ambient wind compresses the wind in its path; the interplanetary magnetic field is intensified, its orientation changes as it is compressed, and it drapes around the advancing structure. If the speed of the CME is high enough relative to the ambient solar wind, a forward shock forms ahead of it. When a CME occurs near the boundary between fast and slow streams, part of it is accelerated and part of it is slowed down. In general, a CME can be accelerated, decelerated, deflected, distorted, attenuated, or amplified, depending on the details of its interaction with the ambient medium. Many of these interactions are of special interest because they produce occasional strong enhancement of geomagnetic effects.

To understand and predict the effects of CMEs on Earth, it will be necessary to map the inner heliosphere and reveal fast and slow streams, interaction regions, and the interplanetary magnetic field. These maps will be generated from numerical models of the solar wind based on the 3-D observations of coronal holes and streamers together with observations of the magnetic field at the surface of the Sun. *In situ* data obtained at STEREO spacecraft will be used to correct the heliospheric maps.

Current maps of the heliospheric magnetic fields are based on Carrington Rotation maps built up from line-of-sight magnetograms taken from ground-based observatories. The fidelity of the resulting models is suspect because the determining characteristics are partly global in nature. Consequently, some parts of the input data for the models are more than 3 weeks out of date. We know from Yohkoh and SOHO observations that even the quiet Sun during solar minimum changes on timescales measured in hours and days rather than weeks.

Maps derived from STEREO data will allow tests of a new generation of advanced models of interplanetary propagation of solar disturbances. The input requirements are relatively straightforward but also impossible to obtain with present capabilities. The crucial elements are the time and location of launch, the initial direction, the speed, the spatial extent, the magnetic configuration, and the mass.

Some tentative tests of CME propagation models are being undertaken with existing data, but the efficacy of such tests is severely constrained. For example, coronagraphs are sensitive only to the portion of the disturbance lying close to the plane of the sky and the relation of that special slice to the entire CME is generally ill defined.

Current models show that CME interaction with the heliosphere is likely to be very complex and to produce confusing results. An illustration is presented in Figure 6, which shows two slices through a 3-D hydrodynamic simulation of a CME interacting with a tilted-dipole background flow. Although the resolution of this exploratory calculation is crude and the model structures highly idealized, it suffices to show how an initially compact, spheroidal CME (characterized as a modest velocity and pressure

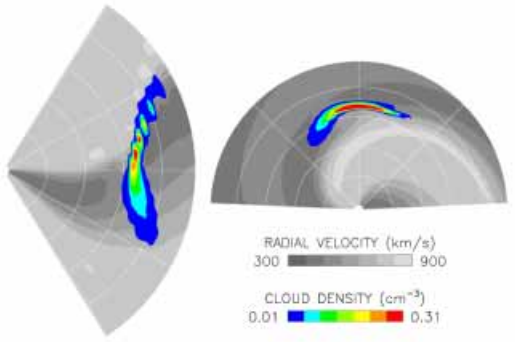

Figure 6. Simulation of a model CME pulse interacting with a tilted-dipole ambient solar wind flow structure. The panels represent slices through the solution in the ecliptic plane (left) and the central meridian plane (right) 10 days after CME launch from the Sun. The computational domain runs in heliocentric distance from 0.14 to 5.0 AU, with white semicircular gridlines every AU. The model CME was injected into the solar wind at the equator, at the base of the streamer belt. Note how the CME is compressed at the interface between the slow streamer belt flow and fast high-latitude flow above the equator, whereas the CME is drawn out and accelerated by the rarefaction flow ahead of it below the equator.

pulse injected at the base of the slow flow along the model coronal streamer belt) is subsequently distorted by variations in the flow structures it encounters. Such models predict certain patterns in the interplanetary evolution of CMEs that are directly related to the surrounding background flow structure. *STEREO observations will allow us to make a realistic assessment of the models.*

Tracking Disturbances from the Sun to Earth

Interplanetary disturbances will be detected remotely not only by heliosphere imagers but also by radio telescopes. Only two types of radio emission are generated far from the Sun in interplanetary space. These are (1) the quite common flare-associated type III bursts, and (2) the much rarer type II bursts associated with CME-driven shocks. Type III events are caused by energetic electrons traveling at speeds of 0.2 to 0.4 times the speed of light, so they move from the vicinity of the Sun to 1 AU in 20 to 30 minutes. For the type II events, typical speeds are 300–1000 km/s, so the travel time from the Sun to 1 AU is several days. For both types of emission, the disturbance (that is, the energetic electrons or the shock) generates radio emissions at the local electron plasma frequency or its second harmonic as it moves along.

With one spacecraft, parameters such as the electron density at the emission sites and the path of the disturbance through interplanetary space can be inferred but they are model dependent because it is not possible to determine exactly where along the measured line of sight the radio source lies. What is usually done in this case is to rely on a global model of interplanetary electron density, taking the point where the line of sight intersects the appropriate density (thus, plasma frequency) to be the emission point. An example of this type of source location determination can be seen in the top part of Figure 7.

As illustrated by Figure 7, reliance on a single spacecraft does not solve one of the outstanding and fundamental problems involved with predicting the terrestrial impact of CMEs, namely, determination of the propagation speed of the corresponding

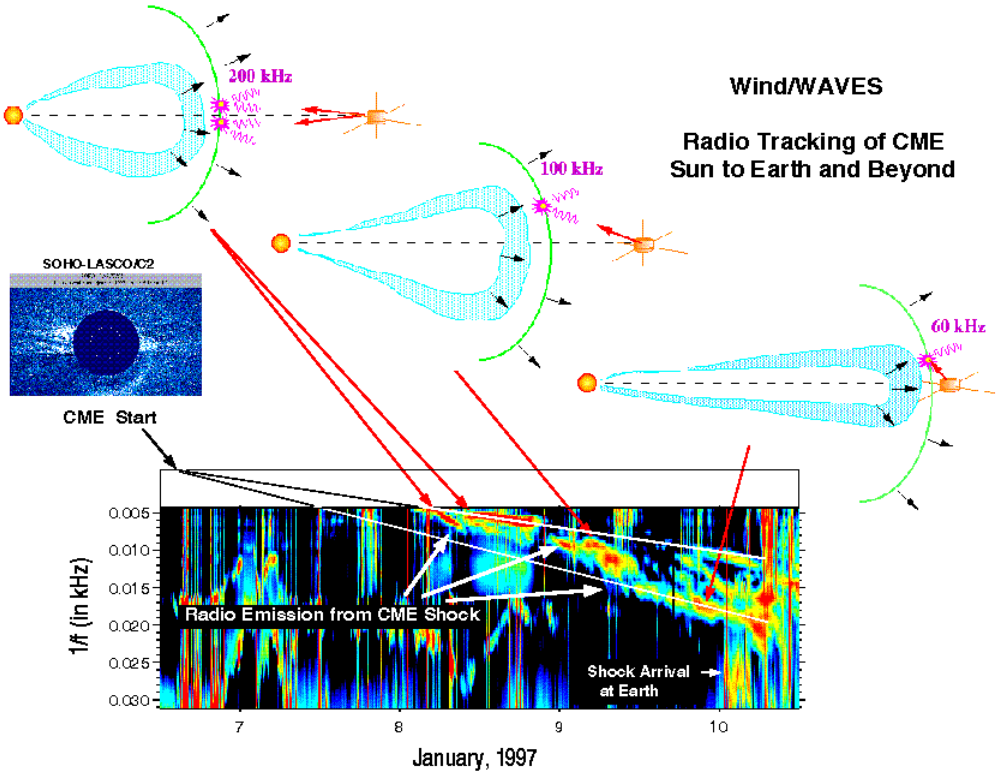

Figure 7. Radio tracking of a CME shock from the Sun to beyond Earth. The Wind/WAVES instrument was able to measure the azimuth and elevation of the type II emission associated with the spectacular January 1997 CME, but the actual location of the source could be found only by intersecting the lines of sight with the assumed position of the shock front. Since the speed of the shock front was not known until the shock passed by Earth, the sketches at the top could only be constructed *after the fact.*

disturbance through interplanetary space. For example, in the low corona, where CMEs are observed in visible light, their speeds and accelerations can be measured. However, these measured speeds are generally quite different from the speeds of propagation through the interplanetary medium and can, therefore, lead to predictions of the arrival time of the coronal disturbance at Earth that can be in error by a day or more. Similarly, single spacecraft radio measurements like those of Figure 7 of the shock front can lead to large errors because the electron density in the solar wind can vary over a wide range. *Radio telescopes on the two STEREO spacecraft will make reliance on models unnecessary because the radio source location is simply the intersection of the two measured lines of sight.*

The radio direction-finding capabilities, together with the wide separation between the STEREO spacecraft, will permit the type II radio source, at a given frequency, to be located by triangulation. A single triangulated source position is sufficient to establish the density scale and, therefore, determine the CME shock speed through the interplanetary medium. Once the shock speed and density scale are obtained, we can readily predict, to within about 2 hours, when Earth will encounter the disturbance. *By triangulating the type II radio source at many times and frequencies, the CME shock can be precisely tracked through interplanetary space and the predicted arrival time at Earth can be refined*.

With the stereoscopic observations, trajectories of kilometric type III radio bursts will be constructed and studied in a systematic way for the first time. The type III radio burst trajectory can be constructed from measurements made at a number of different frequencies. Stereoscopic observations will allow interplanetary densities along the radio burst trajectory and electron exciter speeds to be remotely measured and the average interplanetary magnetic field topology to be mapped. STEREO observations will also allow intrinsic properties of the radio source region, such as the brightness temperature, the source size, and the source effective beam width, to be derived and studied in an unambiguous manner.

Particle Acceleration by CMEs

Solar energetic particle studies with STEREO have two main objectives:

- To understand how and where CMEs accelerate charged particles
- To develop tools for greatly improved forecasts of large solar energetic particle (SEP) events and/or to warn of their onset

More than 95% of the largest solar energetic particle events are associated with CMEs, but only about one-third of CMEs produce shocks, and not all shocks result in large events. In the largest SEP events, the particle fluxes spread out over 180° in longitude. Since the particle flux at a given spacecraft depends on how well it is connected to the shock, the objectives above are best addressed by observations of particles and fields at several heliospheric longitudes, as emphasized in the recent NASA report "Foundations of Solar Particle Event Risk Management Strategies."

SEP events can be classified into two different types (see Figure 8): *impulsive* events, which have minor increases in particle flux, are rich in He^3, heavy ions, and electrons, and last from minutes to hours; and *gradual* events, which are major proton flux increases on timescales of hours to days. Impulsive events are associated with solar flares, and gradual events are associated with fast CMEs that drive. In both types of events the propagation and properties of the charged particles depend crucially on the structure of the coronal and interplanetary magnetic fields and plasmas, so particle flux measurements will allow a new kind of remote sensing of the acceleration and propagation regions, especially when the measurements are combined with stereoscopic images of the corona and heliosphere.

Compression, plasma turbulence, and shock acceleration of particles are expected to be strongest near the western face of fast CMEs, and the duration of the particle events should depend on the time that the shock and CME affect the field lines that connect the observer with the Sun. Thus, the particle experiments on the two STEREO spacecraft will

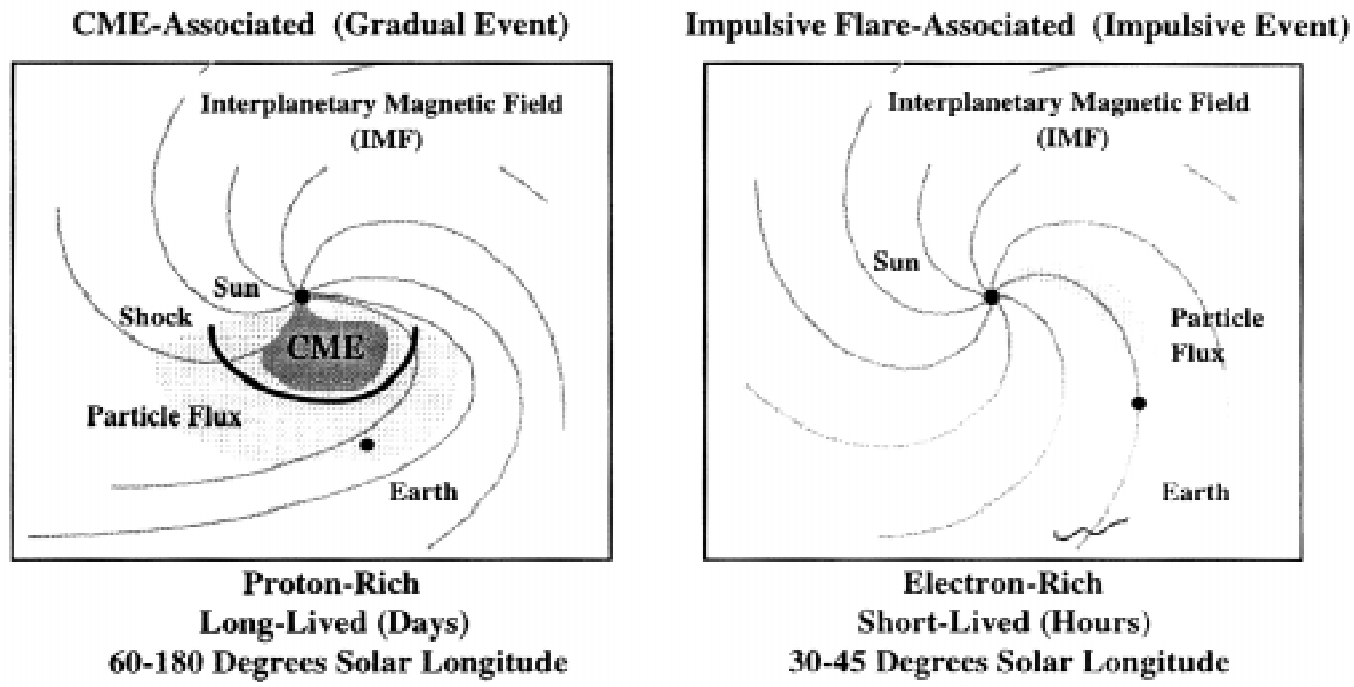

Figure 8. Impulsive and gradual solar energetic particle events. Particles accelerated in impulsive solar flares are generally detected only by observers that are well connected to the flare site. These events tend to be relatively small. They are rich in He^3, heavy elements, and electrons. In gradual events, the particles are accelerated by a CME-associated shock and are observed over a wide range of longitudes.

provide stereoscopic observations of the large-scale structure of CMEs, their effects on the ambient interplanetary medium, and their evolution in interplanetary space. The effects of shocks and CMEs can be sensed from CME onset up to and beyond the time when the CMEs or shocks pass over the spacecraft. Model calculations can then determine the large-scale structure and the position of the CME's center in the heliosphere. To test the models, it is important to be able to sense the different regions around CMEs and shocks on a large scale. This probing can be continued throughout the STEREO mission.

The particle detectors aboard the STEREO spacecraft trailing Earth will probe the corona and its dynamics near disk center (as seen from Earth). Here is where the most geoeffective CMEs start. Figure 9 shows an example of how particle measurements at different energies provide information from the onset of the CME at the Sun up to its arrival at Earth. Early in the event, the particle intensity peaks at MeV energies, followed by increases at keV energies up to and beyond the time the shock passes the observer. The MeV electrons and protons provide information on the dynamics of the corona and CME close to the Sun, and the keV particle measurements can be used to track the shock and CME on the way to Earth. In addition to helping profile CME-associated particles, the trailing spacecraft will detect steady interplanetary particle streams, such as those in co-rotating interaction regions, before they pass Earth.

Magnetic Clouds

Many CMEs are associated with erupting prominences (called filaments when seen against the bright solar disk). They often appear to be twisted strands, like ropes (see Figure 10). Interplanetary magnetic clouds are also flux ropes, as determined from fitting their *in situ* fields to flux rope models. Many, if not all, CMEs are associated with magnetic clouds. This may be a vital clue to their possible origins in helicity charged features in the corona.

Magnetic fields in astrophysical settings are usually filamentary and tend to concentrate as "magnetic flux

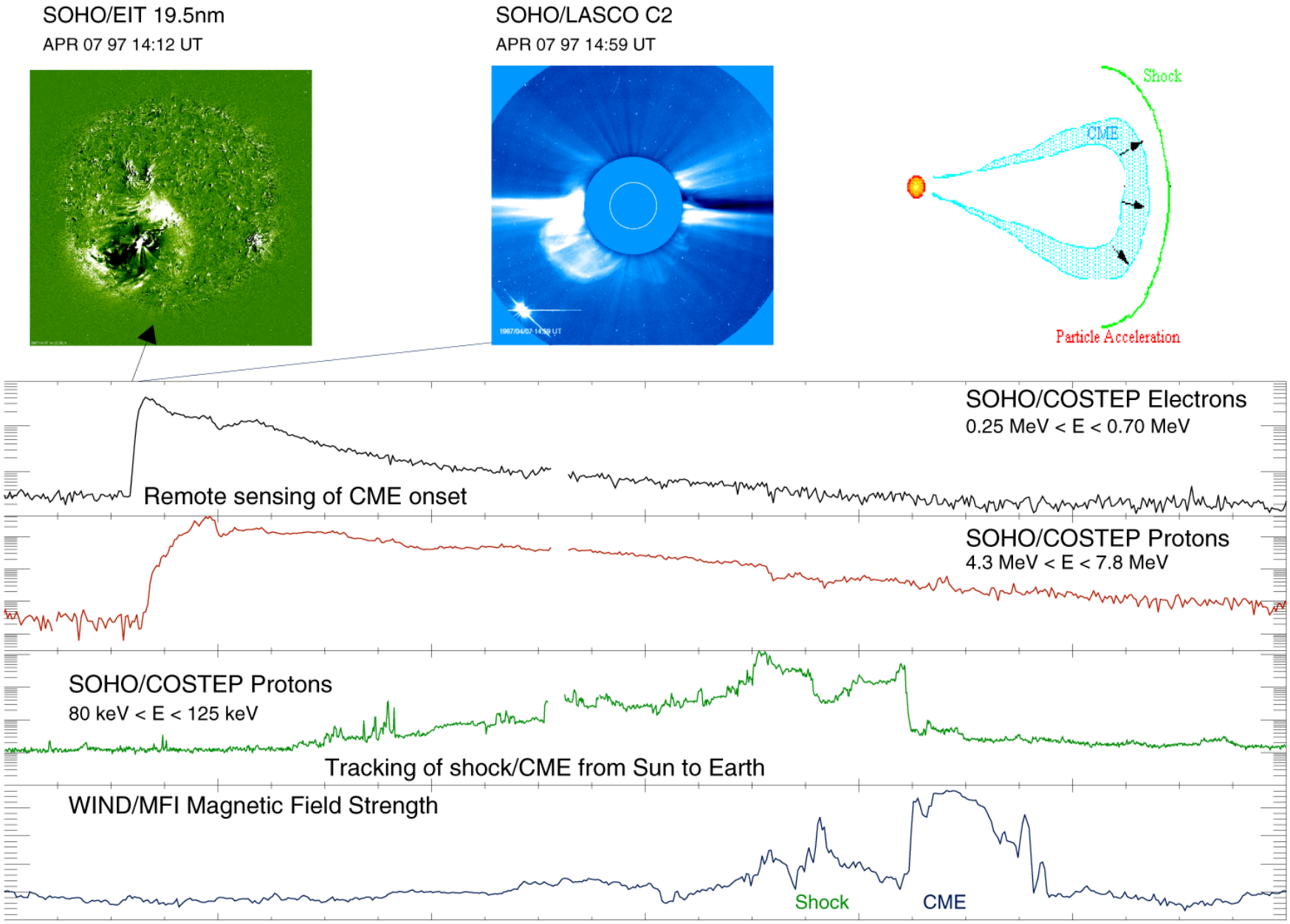

Figure 9. Collected SOHO/EIT/LASCO/COSTEP EUV, white-light, electron, and proton observations for the CME on 7 April 1997. EIT observations show the extent of the wave in the corona. The shock/CME passed the Earth on 10/11 April.

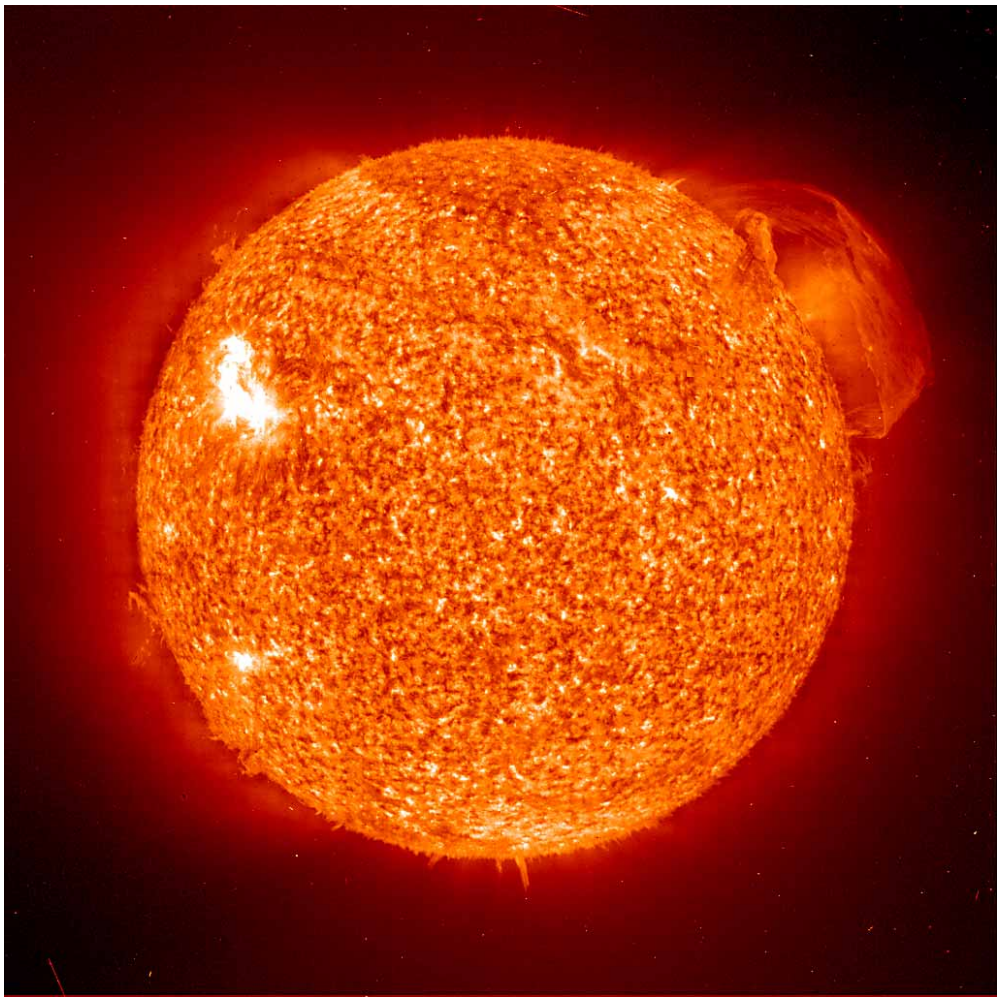

Figure 10. The Sun in He 304 Å emission as recorded on 26 August 1997 by the EIT telescope on SOHO. The prominence on the northwest limb demonstrates the twisted structure characteristic of eruptive events.

ropes." It is expected that magnetic helicity is conserved in such flux ropes once they leave the Sun. Magnetic helicity, H_m, is defined as

$$H_m = \int_V \mathbf{A} \cdot \mathbf{B}\, dV\,, \qquad (1)$$

where $\boldsymbol{A}$ is the magnetic vector potential and $\boldsymbol{B}$ is the magnetic field vector. With suitable specification of gauge and boundary conditions, H_m can be specified in practical terms. For example, the magnetic helicity of a twisted flux rope is $T\Phi^2$, where T is the total twist in radians and Φ is the magnetic flux in the rope. The STEREO chromospheric and low corona imagers should have enough spatial resolving power to allow determination of T in eruptive prominences, such as the one shown in Figure 10. Magnetograms will allow reasonable estimates of the flux. The imagers should also be able to test models that attribute CME onset to a helical kink instability.

Helicity-conserving flux-rope models have been constructed under the assumption that twisted filaments and their surrounding loops become the magnetic clouds seen in interplanetary space. The models fit the average thermodynamic and magnetic properties of magnetic clouds. If the helicity of eruptive prominences can be determined with STEREO observations, one should be able to predict the magnetic field structure and strength of magnetic clouds at 1 AU. This would represent a major advance in estimating the geomagnetic effects of the most potent CMEs.

Escape of Magnetic Flux and the Solar Dynamo

Two mechanisms can facilitate net flux escape from the Sun: helicity charging to push open the fields with reconnection to close them off. Measurements of the solar wind magnetic fields at 1 AU appear to show that 10^{24} Mx of azimuthal flux is ejected by the Sun in each solar cycle. This rate is the same as the expected rate of toroidal flux generation by the solar dynamo. This measured flux ejection rate is also consistent with estimates of flux escaping in CMEs and prominence eruptions and with the apparent rate of flux emergence at the solar surface, as measured by ground-based magnetographs. It appears that escaping toroids (idealized in Figure 11 as resulting from the net effect of many CMEs with helical fields) remove at least 20%, and possibly 100%, of the emerging flux in each cycle. *Flux escape can be checked with STEREO data, and it may prove to be the key to understanding the cyclic behavior of the Sun.*

Coronal Magnetic Fields

"Moreton waves," once also known as flare blast waves, were discovered by Gale Moreton, an observer at the Lockheed Solar Observatory in the 1960s. These waves propagate horizontally across the disk of the Sun at velocities up to 1000 km/s. They are fast-mode magnetosonic waves associated with large flares. Moreton waves are visible in the wings of the Hα line, and until the SOHO mission, they were known only by their effect on the chromosphere and by their correlation with type II radio bursts.

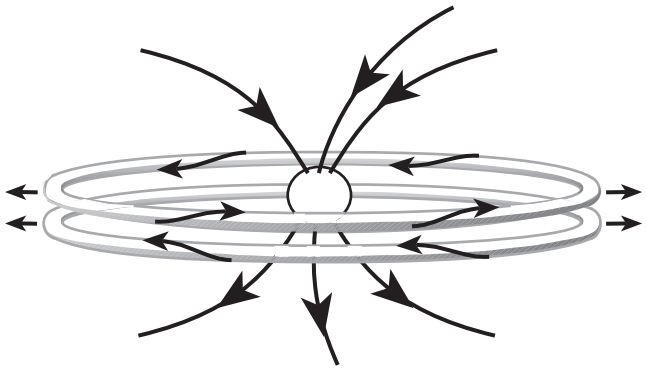

Figure 11. The escape of CME-associated helical fields from the Sun, idealized as northern and southern toroids. The net effect of the ejection of many CMEs with helical fields may be the removal of most of the dynamo-generated flux each solar cycle. The direction (arrows) of all the fields in the figure reverses at about the time of solar cycle maximum.

As Figure 12 shows, there are distinctive waves in coronal emission line images from the EIT instrument on SOHO. They sweep across almost the entire corona, and it is probably true but yet to be established beyond doubt, that the chromospheric manifestation, the Moreton wave, is just the skirt of the wave front (Figure 13). The waves in the EIT images ("EIT waves") have been seen throughout the low corona. Considering that the cadence of EIT images is only four per hour (at most) and that most of the SOHO mission to date has taken place near solar minimum, it is surprising that so many Moreton waves have been detected. The EIT observations make it clear that *two coronal emission-line imagers operating at higher cadence than is possible with SOHO would be able to specify the wave fronts in three dimensions.*

The motion and distortions of the wave fronts reflect the conditions for wave propagation in the corona. According to Uchida's theory of Moreton waves, propagation of the slow mode and the Alfvén mode wave packets is confined to local magnetic field lines, but the propagation of the fast mode wave packets can reveal the distribution of the field strength. The field strength distribution in the corona can be inferred by entering a field distribution and computing the paths of the wave packets, then adjusting the field distribution until there is agreement with the observed wave fronts. Thus, STEREO observations of the wave fronts can achieve a dramatic advance in measuring the coronal magnetic field. *This "seismology of the corona" may finally achieve what has been impossible with older approaches: a complete specification of coronal magnetic field strength.*

Coronal Loop Heating

At a temperature of several million degrees, the solar corona is 3 orders of magnitude hotter than the underlying photosphere. The reason for these extreme conditions has challenged solar physicists for decades and remains one of the great unsolved problems in space science. What is the physical mechanism responsible for heating the corona? A number of interesting ideas have been proposed, including the dissipation of electric currents in stressed magnetic

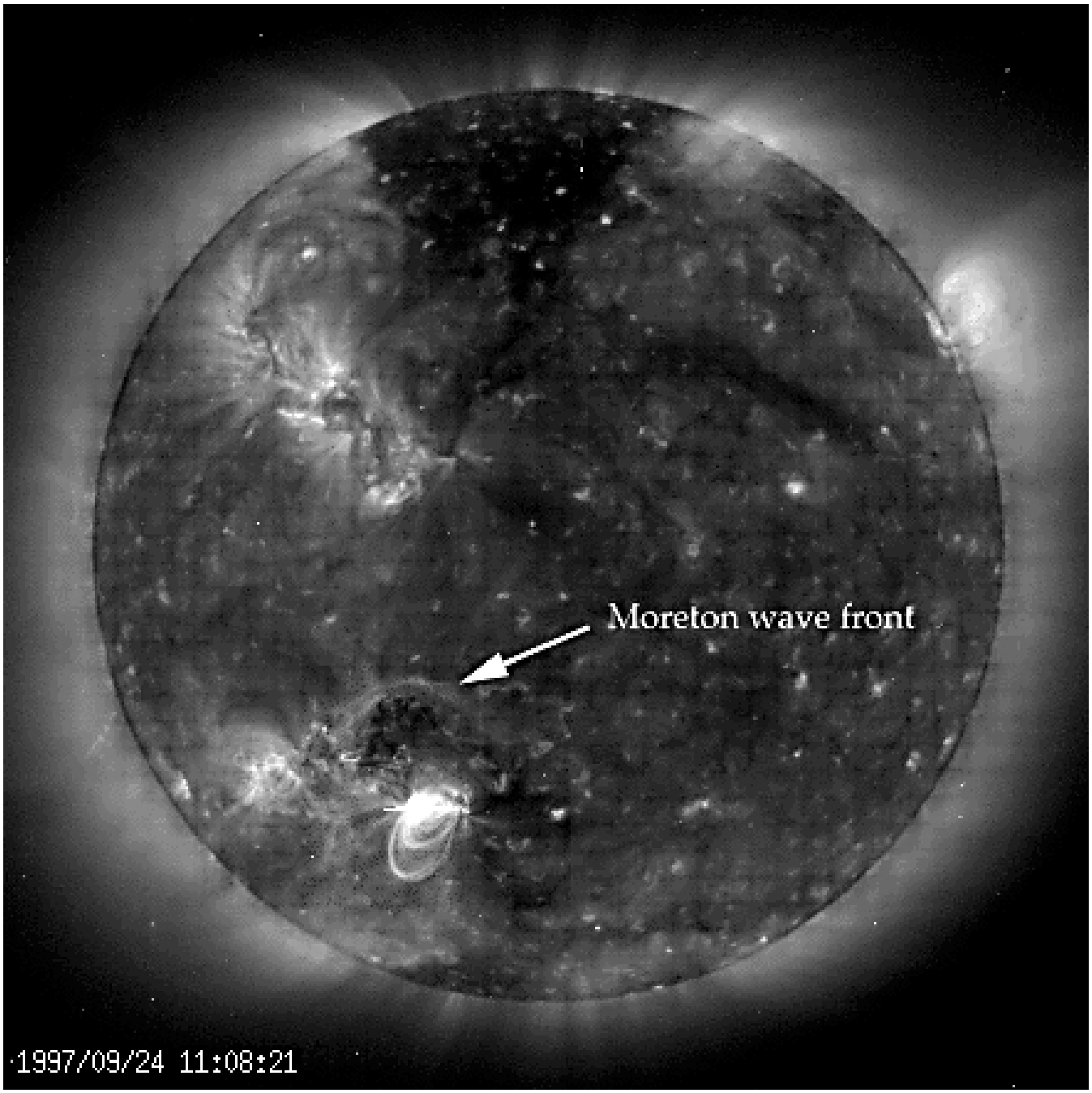

Figure 12. An EIT image of Fe XII 195 Å emission in the corona on 24 September 1997 showing the loops of a major flare and the EIT wave. Both the wave and the flare were associated with a CME.

fields and the dissipation of magnetohydrodynamic waves generated in the photosphere, but none of them has been demonstrated to be correct.

The solar corona is a highly structured medium. Coronal loops, which trace closed magnetic field lines, are the primary structural elements. Although magnetic fields fill the entire coronal volume, only those flux tubes that are filled with strongly heated plasma appear as bright loops. The existence of distinct loops is, therefore, a direct indication of spatial inhomogeneities in the rate of coronal heating. Clearly, if we are going to understand coronal heating, we must understand the nature and origin of coronal loops. Why do they exist, what are their properties, and how do they evolve?

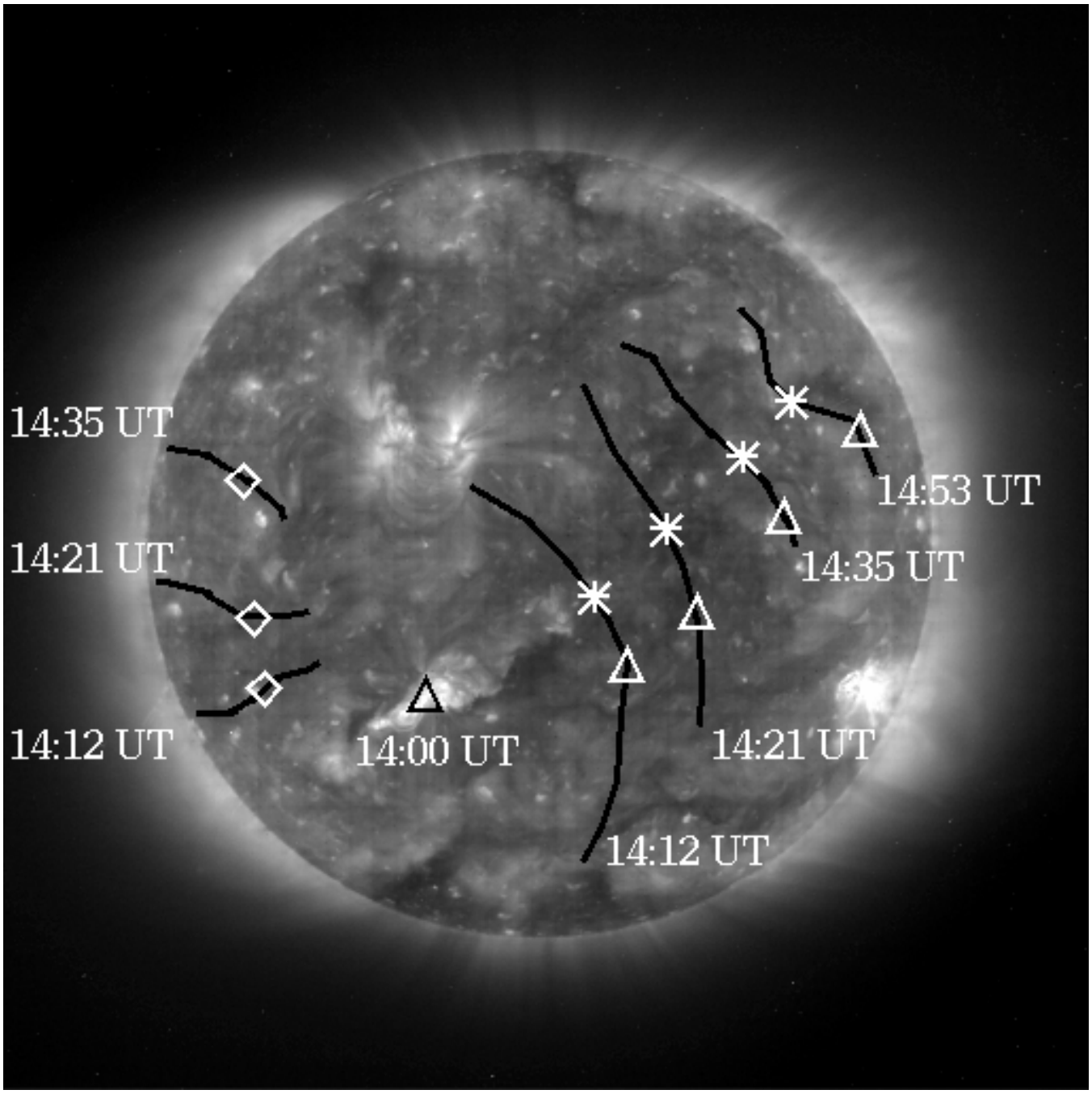

Figure 13. Wave fronts at various times after a CME event on 25 May 1997. Distortions of the wave front reflect variations in fast-mode wave velocity along ray paths from the site of the eruption. Stereoscopic observations of such wave fronts can be used to derive the distribution of magnetic field strength in the corona.

Loop Cross Sections

One of the basic properties of coronal loops is their cross section. The shape of the cross section is determined by the spatial distribution of the energy release and, to a lesser extent, by the transport of this energy within the loop. It thus provides valuable information about the spatial dependence of the heating process. If energy is released within thin layers, as might be expected for magnetic reconnection, for example, loops should be ribbon-like structures with highly noncircular cross sections. If energy is instead released axisymmetrically, loops should be more like the tubular structures that are commonly assumed. It is impossible to know which of these possibilities is correct in single-view observations, where loops are seen as projections onto the

flat plane of the sky. Their depth is completely unknown. *Only STEREO can provide the necessary information to determine the all-important 3-D structure of coronal loops*.

Scaling Laws

Scaling laws are very useful for studying the heating and equilibrium properties of coronal loops. These laws describe relationships among loop-averaged quantities. One well-known scaling law relates the product of the average temperature and pressure in a loop to the loop's length. Another relates the average pressure and length to the average heating rate. By comparing theoretically and observationally derived scaling laws, it is possible to determine if the heating is steady and how it differs among loops of different sizes. This information provides vital clues about the nature of the physical mechanisms involved. Current progress is hampered, however, by an inability to make accurate measurements of the fundamental loop parameters. Lengths can only be approximated because there is little information about the extent of the structures along the line of sight. Densities and pressures are also highly uncertain, since they are derived from emission measures with an assumption about the line-of-sight thickness of the emitting plasma. The situation will improve dramatically with the two-view observations from STEREO.

Axial Gradients

Many coronal loops observed in soft X-rays by Yohkoh appear to have far more variation along their axes than is predicted by theory. If this observation is correct, it has major implications for both the heating and transport of energy within the loops. It is difficult to know, however, whether the variations are real or merely a consequence of misunderstood projection effects. A bright loop section could be an indication of locally enhanced densities and temperatures or it could be a result of the loop geometry (a bend that increases the line-of-sight thickness). STEREO will resolve this ambiguity.

Loop–Loop Interactions

Both Yohkoh and ground-based coronagraphs have observed what have come to be known as "loop–loop interactions." These are transient events in which nearby loops concurrently brighten, with the greatest enhancement occurring at the presumed point of contact. It has been suggested that magnetic reconnection at the current sheet interface between the loops is responsible for the energy release, so these events may provide an excellent opportunity to study the details of the reconnection process. At this point, however, we cannot be certain that the loops are actually in contact, much less sort out the details of the overlapping structures. *STEREO observations will provide a definitive resolution of the loop–loop interaction issue.*

Solar Wind Origins

Two of the most important current questions in solar and heliospheric physics are how the solar corona is heated to temperatures in excess of a million degrees and how the solar wind is accelerated to speeds that range from approximately 300 to 800 km/s. There are at least three different types of solar wind: fast wind from coronal holes, slow wind from coronal streamers, and transient wind of any speed from CMEs. The slow wind from coronal streamers may also be essentially transient in nature. Solar wind might also originate on open field lines in other regions, such as the quiet, background corona. How is the wind accelerated? We cannot be sure we understand the processes responsible for solar wind acceleration until the theoretical models match conditions both in the solar corona and in the solar wind near 1 AU for each type of wind.

To determine the conditions at the source regions of the solar wind, we rely on white-light images and spectral information in the UV, extreme ultraviolet (EUV), and X-rays. These emissions contain information about the densities, temperatures, wave motions, and bulk flows of several ion species as well as the electron density. Because the plasma is tied to the magnetic field lines, imaging also provides information on the geometry of the magnetic field. Current models try to incorporate some of this information, but the problem is that the images and spectra are all obtained by integration of the emission of the optically thin plasma along the line of sight. This leads to fundamental ambiguities about the actual 3-D structure. *What is needed to make solar wind acceleration models more realistic is a model of the 3-D structure of the streamlines based on observations, rather than on assumptions.*

The STEREO mission will play an important role in improving our understanding of the acceleration of the solar wind and in testing models deriving from that understanding. Stereo images of the corona will help remove the ambiguities arising from observations along a single line of sight. When the angle between the two STEREO spacecraft approaches 90°, it will be possible to obtain both white-light coronal data and interplanetary data on the same streamline; currently, the *in situ* measurements must be combined with plane-of-sky observations obtained at a 90° separation in longitude, so that the correlation between white-light coronal observations and solar wind measurements can be done only on a statistical basis.

Solar-B Collaboration

The approved Japanese Solar-B mission (Table 1), due for launch in 2004, will overlap with STEREO and can provide sophisticated Earth-perspective context observations. The STEREO and Solar-B data sets will be highly complementary since Solar-B emphasizes high-resolution observations of the photosphere, transition region, and low corona, while STEREO provides an extended view of the corona and heliosphere. The Solar-B data will include vector magnetograms at 0.1-arcsec pixel size as well as sensitive EUV spectroheliography and whole-Sun X-ray imaging. The Solar-B vector magnetograph will provide the best possible sensitivity for studying the underlying magnetic fields and their evolution before, during, and after a CME-launching instability, and it will be operating when STEREO spacecraft are optimally positioned for recording those same CMEs.

Table 1. Solar-B key parameters.

Launch date	2004
Orbit	Sun-synchronous Earth orbit
Instruments	White-light telescope (0.2-arcsec resolution) – filter photometry – spectroscopy (vector B) UV stigmatic slit spectrograph X-ray imager

Similarly, STEREO will add a great deal to Solar-B science by helping to define the 3-D structure of any particular target of observation. Solar-B's science theme is a "systems approach" to the physical coupling of the photosphere and corona. To achieve this goal in a completely satisfactory manner requires additional knowledge, because the corona is mostly optically thin and one cannot accurately infer the true geometry from a single set of observations.

Collateral Research

The STEREO platforms offer opportunities for many unique kinds of observation in areas not directly related to the solar activity that affects Earth. We recommend that such observations should be accommodated to the extent that resources permit, providing that this does not compromise the primary mission objectives.

Helioseismology

Helioseismology has captured scientific and public attention because it actually provides views, graphic as well as quantitative, of the structure inside the Sun. Moreover, these views challenge some of our present concepts of the physics of the Sun and of the broader universe (e.g., the abundances of the elements). The current methods of observation in helioseismology, led by SOHO in space and GONG on the ground, have certain limitations. These include access to the lowest-frequency p-modes of low degree, which give the best information about the deepest interior, where we hope to resolve the puzzling solar neutrino problem. At low frequencies one finds high values of Q in the p-modes, with obvious benefits for mode identification and application to learning about solar structure.

Thus far, the existing helioseismic observations have not discovered g-modes, which propagate only in the radiative core of the Sun and, thus, would be the best guide to its structure. The present tools may not suffice to show the g-modes, and STEREO might offer the key help needed.

The low-degree p-modes, and possibly the g-modes as well, can be detected with simple photometry. From a single geometrical perspective, the different

modes of oscillation present foreshortened projections, which lead to crosstalk between modes. Stereoscopic observation can reduce both this crosstalk and noise in the measurement. *A pair of well-separated instruments would allow removal of the incoherent convective motions (which represent noise) and isolation of the almost strict coherence of the seismic effects*. Instruments on SOHO (MDI, VIRGO, and GOLF) provide some heritage for helioseismic observations from deep space. In the STEREO mission, these measurements would probably be done photometrically with irradiance instruments. If a more complex helioseismology instrument could be accommodated, velocity measurements could be made. These are superior to irradiance measurements for low-degree, low-frequency modes.

Solar Irradiance

The solar irradiance variability discovered in the 1980s provides a substantial challenge for solar physics. What are the mechanisms that produce such great output fluctuations in what was once called "the solar constant?" We had long known about the variability of spectral emissions such as the 10-cm or soft X-ray fluxes, but these relate to the corona, not to the photosphere of the star itself, and represent relatively minor energy fluctuations.

Several known mechanisms exist to explain different components of the observed variability of total solar irradiance but there remains a substantial unexplained variance, which may include secular terms linking one solar cycle with the next. One method of disentangling these different components of variability is to construct models that relate independent observations (for example, sunspot area) to the irradiance variations. The lack of data from above or around the solar limbs reduces the accuracy of these models and, thus, limits the study of the mechanisms of solar variability. Broad-band irradiance measurements can be carried out with minimal resource demands, and such measurements can also be used for seismic observations if specialized instruments are not available.

Stereoscopic observations represent an important next step in solar irradiance measurements. Instruments from SOHO and other deep-space missions provide some technical heritage. *Total irradiance measurements (and broad-band spectral measurements) require only minor resources and could easily be accommodated on a STEREO platform.*

X-ray and Gamma-ray Bursts

Hard X-rays, γ-rays, and radio bursts may help to characterize coronal structure and may represent energetically important components of major eruptive events. Solar flares and probably also developments at CME onsets accelerate high-energy particles. CMEs continue to accelerate particles as they propagate through the corona and the heliosphere. Thus, observations of the byproducts of these high-energy particles represent an important channel of information about the overall process involved.

Solar nonthermal radiation, including hard X-rays and γ-rays (>10 keV) may have anisotropic emission because they are nonthermal in origin. This property of the radiation provides a relatively simple remote-sensing tool that can help study particle distribution functions near the acceleration site. The directivity of hard X-rays from bremsstrahlung is closely related to the polarization, which is a very difficult measurement that has never been successfully carried off. Effectively, then, *the only way to observe the directivity of the hard X-ray bremsstrahlung is by stereoscopic viewing*.

Precise timing of γ-ray fluxes also provides some of the best position information for the enigmatic (nonsolar) γ-ray bursters, and this position information improves with the baseline separation for triangulation. Other techniques have recently become available for burster source localization, however, and it is not clear that this is a high-priority item any longer. There is considerable technical heritage for small high-energy instruments in deep space, starting with the Vela program and currently on Ulysses. An effective hard X-ray and γ-ray spectrophotometer for a STEREO platform would require modest resources.

Faint Objects

Unique studies of faint sources in the sky other than heliospheric plasmas can be undertaken with the STEREO coronagraphs and heliosphere imager:

- **Zodiacal light**. The imagers can help determine the dust distribution in the inner heliosphere.

- **Asteroids.** It is estimated that a heliosphere imager will discover between 10 and 100 asteroids per year with radii greater than 12 m.
- **Comets.** Images of comets and of the distribution of dust down to the level of the zodiacal cloud brightness will provide fundamental information about the dust replenishment of the zodiacal cloud.
- **Stars.** Stellar light curves with ~0.1% photometric precision and 1-day time resolution can be obtained for the 10^3 brightest stars.

3. Making the Best Use of STEREO Images

Determining the 3-D Structure and Dynamics of the Corona

The coronal plasma radiates strongly in X-rays and EUV. These emissions are sensitive to both plasma density and temperature, making them a powerful diagnostic of the coronal plasma. Moreover, because the plasma follows the magnetic field lines in the low corona, imaging in X-rays and EUV directly shows the structure of the magnetic field lines with hot plasma. Thus, stereoscopic observations of the corona in X-rays and EUV can be used to determine the 3-D structure and dynamics of the coronal plasma and magnetic fields.

Resolving Line-of-Sight Ambiguities with Stereo Observations

Coronal loops are not in general isolated. Other structures often lie along the line of sight, either in front of or behind the structure of interest, causing a "background" problem. Many Yohkoh images show loops apparently interacting with adjacent loops. Without a stereo view, however, it is not possible to resolve the ambiguity of whether the brightenings of the loops are a result of summing intensities along the line of sight or if the loops physically interact. In some eruptive event scenarios, the energy release is triggered by the interaction of neighboring flux systems, but a close neighbor in a 2-D view may be quite distant when the third dimension is considered. *Stereoscopic observations of the X-ray/EUV corona can resolve ambiguities in the interpretation of changes in the coronal structure.*

The effective depth resolution depends on the separation between STEREO #1 and STEREO #2 and the 2-D resolution of the imager. In the first year of the mission, the separation will dwell at 50°, so if the imager has 2000-km resolution in the plane of the sky, it will have 2600-km depth resolution.

Use of Triangulation to Determine the 3-D Coordinates of Coronal Features

It has not been generally appreciated that quantitative information on the 3-D magnetic fields can be found by using triangulation on coronal loops and other features. Using classic surveying techniques, the coordinates in three dimensions of a coronal feature can be determined from only two views as long as (a) one knows the stereo separation angle and spacecraft distances and directions to the Sun and (b) one can recognize the feature in both images. Condition (b) can be a serious limitation in studies of diffuse features or features in crowded fields, in a large active region, for example. Over the course of a year of observations, however, the Sun will present many opportunities to study a wide range of coronal features under near-ideal conditions.

The triangulation technique for a simple case is shown schematically in Figure 14, where it is assumed that both views are from the equatorial plane of the Sun. In this figure, the coordinates in the plane of the sky of the two views with stereo angle α are related by the simple rotational transform

$$T(\alpha) = \begin{pmatrix} \cos\alpha & \sin\alpha & 0 \\ -\sin\alpha & \cos\alpha & 0 \\ 0 & 0 & 0 \end{pmatrix}. \qquad (2)$$

The triangulation calculation from a pair of points in the stereo images can be done by determining the coordinate transformation between the telescopes and solar coordinate systems so that the rays from the points in the images can be traced back to the Sun. If there were no errors, the two points on the same feature in two images would map to a single point in solar coordinates. However, errors are introduced by the manual tiepointing (joint feature identification) itself. Therefore, what is actually computed is the point of closest approach (in solar coordinates) of the two rays traced back toward the Sun from the points on

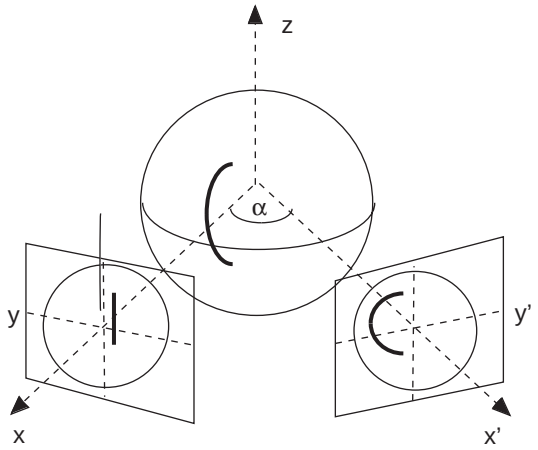

Coronal loop viewed from two angles separated by α

Coordinates of two views related by simple rotational transform

$$x = x'\cos\alpha + y'\sin\alpha$$

$$y = y'\cos\alpha - x'\sin\alpha$$

$$z = z'$$

Given y,y' , Solve for x,x'

$$x = \frac{y' - y\cos\alpha}{\sin\alpha}$$

Figure 14. Determination of 3-D loop geometry from two views via triangulation. Since both views of the loop are from the solar equatorial plane, the coordinates are related by a simple rotational transform that can be inverted to give the 3-D solar coordinates of the loop as shown.

the image pair. The location of the feature is then taken to be midway between the rays at closest approach.

The triangulation technique was tested on simulated STEREO observations of well-defined loops. A stereo image pair was created by viewing the loops from two angles separated by 15° (see Figure 15). Also shown in Figure 15 are the (*x,y,z*) location of points (crosses) determined by triangulation from the stereo pair plotted over the input test loops (solid curves). The agreement between the input loops and the inferred loops is excellent. When the same feature can be located in a time sequence of stereo pairs, one can also determine the 3-D velocity of the feature and, in this way, obtain information on loop expansion rates.

Automatic Feature Tracking

We recommend that studies be undertaken of stereo analysis techniques used in other fields, such as Earth

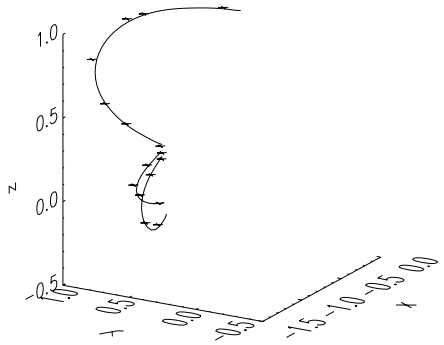

Figure 15. Test of determination of 3-D loop geometry: known loops. The test stereo image pair was created by viewing the known loops from two angles separated by 15°. The (*x,y,z*) location of points (crosses) determined by triangulation from the stereo pair are plotted over the known test loops (solid curves). The agreement is excellent.

and planetary surface imaging. Several fields have long had the benefit of stereo data, and some of their developed analysis techniques can probably be carried over to space physics. One example is automatic feature tracking in which patterns within many sections, or "patches," in one of the images are searched for and identified automatically in the other image. In contrast to the manual method described above, the relative offsets of matching points are computed with cross correlations, usually to subpixel accuracy. Then, using ray intersection techniques, a sophisticated algorithm determines the coordinates for conjugate points in the two images in three dimensions. While this is a standard technique in producing digital terrain models, much development remains before we will understand its full potential and limitations in interpreting the optically thin features of the corona.

Use of Magnetic Field Models in Conjunction with X-ray and EUV Observations

The use of magnetic field models with magnetograms supplying the photospheric boundary conditions will greatly enhance the information obtained from STEREO X-ray and EUV observations. Simultaneous stereo observations will allow a much better identification between features in the magnetic model and features in the observations. Loops and other features that have been determined by triangulation can also be compared to features in the 3-D magnetic field model. If a correspondence between the

model and observed features can be made, the magnetic field model can be tested.

Once a magnetic field model has been validated, field lines from the model form a skeleton to which emitting plasma can be attached to create a 3-D model of the corona. For whatever plasma model is chosen, the integrated line-of-sight emission calculated from the 3-D coronal model (field plus plasma) must agree with the X-ray and EUV observations from both viewpoints. Figure 16 shows results from such a 3-D corona model using an iterative technique to determine the spatial distribution of emissivity. In the figure, both the original Yohkoh/SXT view of a loop complex and an image rendered from the 3-D model are shown. The model is viewed from the same angle as the original SXT image.

The comparison in Figure 16 shows clearly that the magnetic models need to be improved and that vector magnetic field measurements will probably be needed to achieve convincing representations of observations. These enhancements will be available from Solar-B and the National Solar Observatory SOLIS magnetographs.

From a time series of STEREO images and magnetic models, a complete 4-D (three spatial dimension plus time) model of coronal features can be built. In this way, *the STEREO observations can be used to determine the magnetic field evolution that accompanies solar eruptions.*

Magnetic-Field-Constrained Tomographic Reconstruction of the Corona

Tomography can be used to directly determine the 3-D structure of the optically thin corona if one has many viewing angles. STEREO will provide images from only two angles. However, it is possible to make a tomographic-like reconstruction of the corona from only two views by assuming a magnetic field configuration *a priori*. In this approach, the spatial distribution of coronal emissivity is determined by constraining the stereo reconstruction with a 3-D magnetic field model. The technique is a modification of the multiplicative algebraic reconstruction technique. In it, the constraint is applied by assuming that emitting plasma only exists within a loose volume defined by the magnetic field model. Figure 17 illustrates the technique and shows results of a tomographic reconstruction both with and without a

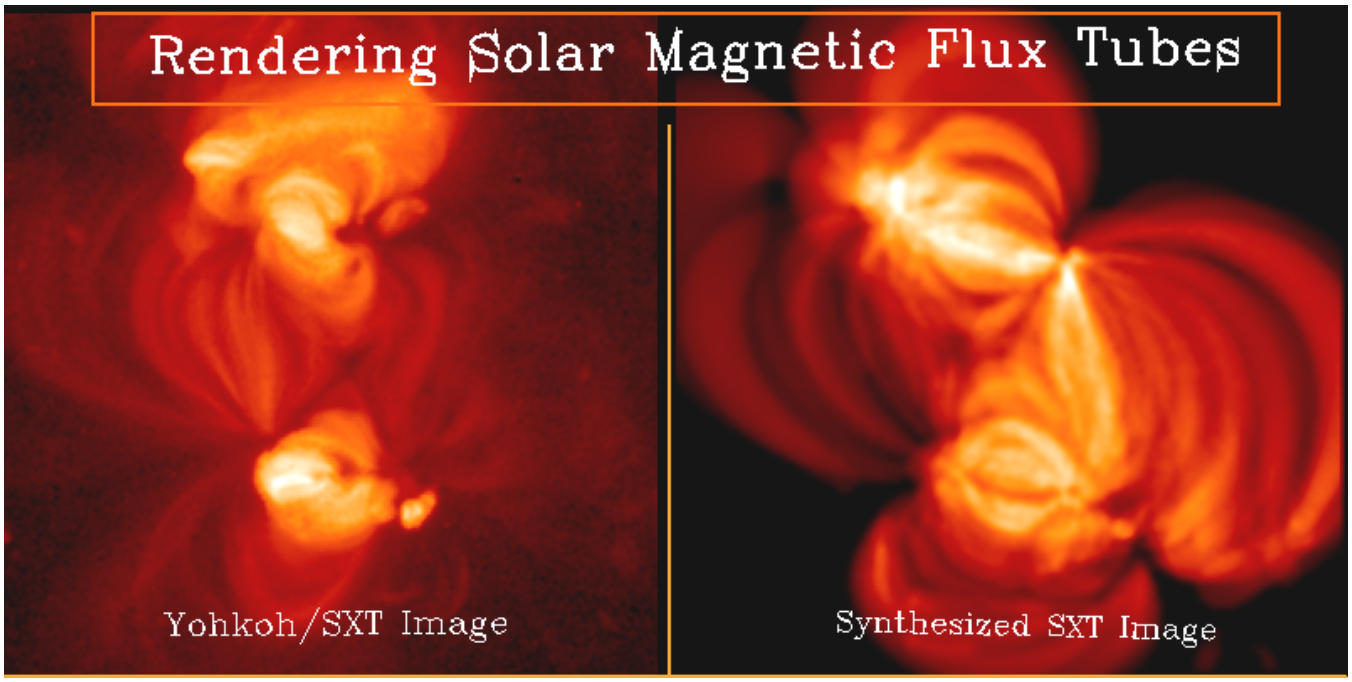

Figure 16. Yohkoh/SXT image and rendered image from 3-D magnetic-field-based model of an active region. The model assumes a potential magnetic field in the region. The 3-D model was rendered into the image on the right by computing the integrated line-of-sight emissivity.

magnetic field constraint. The top panel of Figure 17 shows the original test loops on the left and the magnetic field constraint to be applied on the right (viewed from a second angle). The middle panel shows two views of the result from a tomographic reconstruction of the test loops obtained *without* applying the magnetic field constraint. The bottom panel shows the result from the tomographic reconstruction *with* the magnetic field constraint applied. *The magnetic-field-constrained tomographic reconstruction has reproduced the original loops with very little smearing compared to the unconstrained reconstruction.*

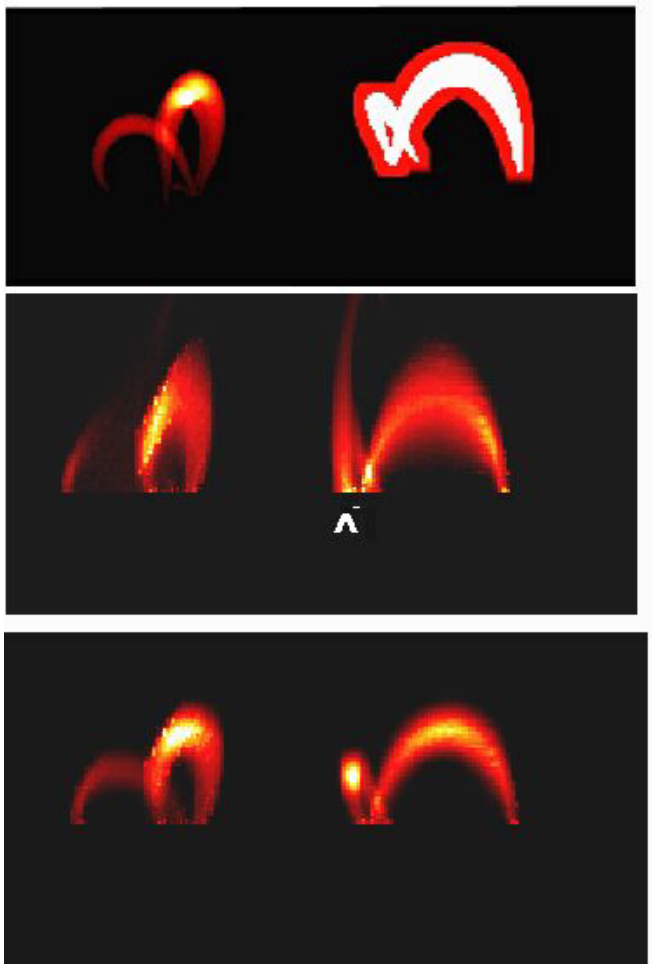

Figure 17. Magnetic-field-constrained tomographic reconstruction. (Top left) Original simulated X-ray loops. (Top right) The envelope is the magnetic field constraint applied. The view here is orthogonal to that on the left. (Middle left and right) Two views of the tomographic reconstruction of the simulated loops from a simulated pair of stereo X-ray images (28˚ separation angle) with no magnetic field constraint; the white arrow head points to the more badly smeared loop. (Bottom left and right) Reconstruction from the same image pair but with the added constraint that the loops are within the loose magnetic envelope shown in the top right frame. The magnetic-field-constrained tomographic reconstruction has reproduced the original loops with little smearing (considerably less than the range of the envelope), illustrating the importance of using *a priori* knowledge of the magnetic field.

Visual Evaluation of Stereo Images

Human beings are equipped with an exquisite computer that quickly evaluates stereo image pairs and develops an intense image in three dimensions. Just viewing stereo image pairs and time sequences of stereo pairs will provide valuable insights on the structure and dynamics of the phenomena we seek to understand. Examination of image pairs with stereo viewers may be enough to eliminate some models. For example, models of CME initiation involving buoyancy require that there be a cavity, but the absence of a cavity in a single image may be due to a line-of-sight effect. However, if stereo observations show some CME initiations with no cavity, buoyancy models can be eliminated.

To gain an impression of what can be gained from direct examination of stereo images, we have substituted sequential images for true angular separation of viewpoints. Figure 18 shows a simulated soft X-ray stereo image pair created from two Yokhoh/SXT images taken 6 hours apart. Solar rotation shifts

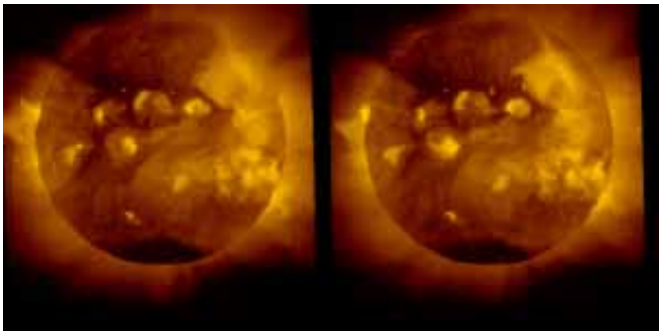

Figure 18. Simulated stereo pair of soft X-ray images of the corona. The Yohkoh/SXT image on the left was taken on 27 April 1992 at 23:16 and the other about 6 hours earlier. Some features can be seen in both images while others are unrecognizable due to temporal changes. These images may be viewed as a stereo pair by relaxing your eye focus or using a stereo viewer.

the effective viewpoint 13° per day. The simulated angular separation in Figure 18 is then 3.3°, so the viewer has a leverage on 3-D structures on the Sun similar to that achieved by examining something about 130 cm away.

Attempts to use such rotational synthesis to build a 3-D picture of the active corona are defeated by the constantly changing active regions. Even larger-scale and longer-lived structures such as polar streamers and quiet-Sun arcades are impossible to deconvolve because of slow evolution in brightness, shape, and size. Only simultaneous images can give an accurate impression of coronal structure.

On the back cover of this report is an anaglyph (an image in relief) constructed from two EIT images. To obtain the 3-D effect, the reader should view it with a red filter over the left eye and a blue one over the right eye. Examination of the back cover image brings out the dark veins in the corona, and one gains an especially clear impression of the extent of a coronal-emission-absorbing prominence that is near the northwest limb. Figure 18 suggests that the post-CME coronal arcade in the upper right quadrant of the Sun is extraordinarily high—higher than any other feature. Whether any physical insight can be gained from such simulated stereo observations using solar rotation depends on the features being static, but it is clear that *substantial insight can be gained from visual examination of the true stereo pairs that STEREO telescopes will produce*.

4. Space Weather

Besides the scientific reasons for studying the Sun and heliosphere, there is a practical reason. Solar activity influences our lives. In our era of heavy space utilization, many more solar-terrestrial-related problems occur than are commonly publicized or admitted, especially in telecommunications and defense satellites. Enterprises known to be affected are

Cellular telephone service
Weather satellite operation
Fusion and carbon dating experiments
Global Positioning System (GPS)
Ozone measurement program
Commercial airlines
Commercial TV relays
Communication satellite systems
Satellite reconnaissance and remote-sensing systems
Geophysical exploration and pipeline operations
Submarine detection
Power distribution
Long-line telephone systems
Manned space program
Interplanetary satellite experiments
VLF navigation systems (OMEGA, loran, etc.)
Over-the-horizon radar
Solar-terrestrial research and applications satellites
Satellite orbit prediction
Balloon and rocket experiments
Ionospheric rocket experiments
Short-wave radio propagation

NASA should not ignore the needs of space weather users. Of course, STEREO will greatly accelerate the development of reliable forecast techniques. STEREO data can be helpful almost from the first day of the mission. However, if STEREO data are to be used operationally in forecasting space weather, they must be available in real time and the STEREO spacecraft must be monitored continuously. This is outside the scope of a NASA research mission, but there could be a clear delineation of responsibility between NOAA and NASA, with NASA being responsible for collecting and transmitting the science data and NOAA being responsible for real-time tracking and forecasting, much as is done with the real-time solar wind data from ACE.

Although it would be impractical to transmit full-up STEREO science data continuously, STEREO could warn Earth of either coronal or interplanetary conditions indicative of impending disturbances. A network of modest antennas could detect the alert and even trigger real-time tracking of the spacecraft by the Deep Space Net to gain additional information and possibly lead to continuous monitoring of events during critical manned space activities, for example.

Solar Energetic Particles (SEPs)

In this era when man is always present in space, it is vital to improve our ability to forecast the energetic

proton events that can present a radiation risk to astronauts. In the immediate future, there is a need for warnings and short-term forecasts that might be used in scheduling astronaut extravehicular activity.

The energetic particle flux at Earth depends critically on how Earth is connected to the acceleration site at the shock. The degree of connection can change quickly as the shock moves outward. Figure 19 shows typical time-intensity profiles for observers viewing a large CME-driven shock from three longitudes. The observer seeing a western event is well connected early and sees a rapid rise and decline, while the observer seeing an eastern event is poorly connected until after the local shock passes. This represents an example where the well-connected observer can provide several days' warning of a particle event that will eventually affect observers to the west.

In the long term, as NASA considers manned missions to the Moon and/or Mars, it will be important to forecast SEP events as much as 2 weeks in advance. Such forecasts will require new approaches with improved accuracy. *The observations to be carried out on STEREO will provide the first test of what can be achieved with a future network of space weather stations, and they will provide the database, experience, and insight on which planning for such capabilities can be based.*

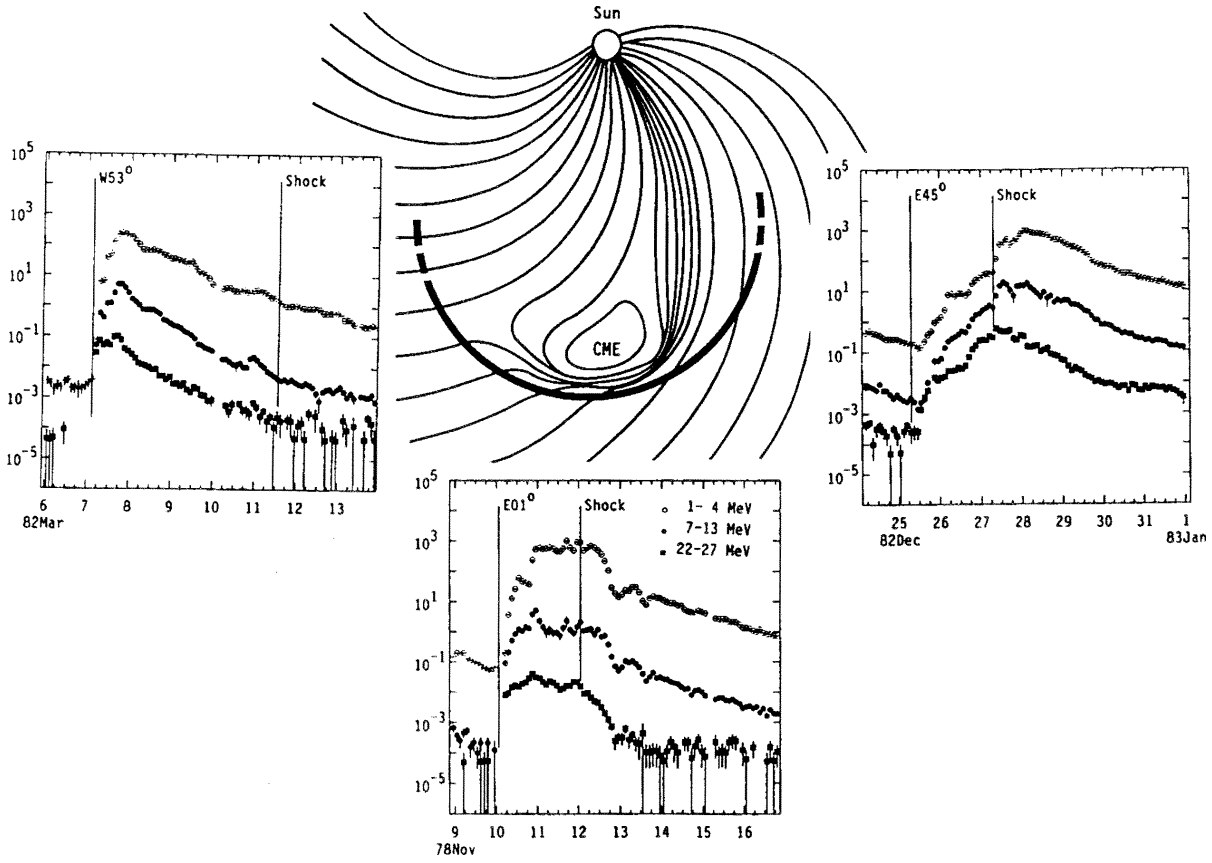

Figure 19. Longitudinal dependence of particles from CME-driven shocks. Typical intensity-time profiles for protons of three different energies as seen by observers viewing a large CME-driven shock from three different longitudes. The observer seeing a "western" event (left panel) is well-connected to the nose of the shock early on and sees a rapid rise and decline. The observer near central meridian is well-connected until the shock passes, and thus sees a flat profile. The observer viewing an "eastern" event is poorly connected until after the shock passes; it is not until then that he is connected to the nose of the shock. With a network of spacecraft at such locations it is possible to study the accelerated particle spectra and composition as the shock moves out into the heliosphere, to measure the plasma and magnetic field properties of the shock *in situ,* and to develop the necessary databases, understanding, and tools that can ultimately lead to a predictive capability.

CMEs and Space Weather Forecasts

Virtually all transient shock wave disturbances in the solar wind observed near Earth are driven by CMEs. In addition, the largest SEP events, the so-called gradual events, appear to be a consequence of particle acceleration occurring in the vicinity of strong CME-driven shocks. Finally, all of the largest (Kp > 7–) nonrecurrent geomagnetic storms are caused by CME-driven solar wind disturbances impacting Earth's magnetosphere. On the other hand, about two-thirds of all CMEs do not produce shock disturbances in the ambient wind near 1 AU, an even larger fraction do not produce gradual particle events in interplanetary space, and about five out of six CMEs directed Earthward do not produce large geomagnetic storms (Kp > 7–). Present evidence suggests that CME speed, in particular speed relative to the ambient wind ahead, is a key factor in a CME's ability to produce these phenomena. However, other factors, such as the mass and size of the CME, the strength and orientation of the magnetic field within both the CME and the ambient wind, the location of the observer (or Earth) relative to the disturbance center, and the availability of various particle seed populations for acceleration, enter into the disturbance equation as well. *It is not currently known which attributes of the CME/ambient wind combination are most influential in producing large shock wave, energetic particle, and geomagnetic disturbances*. In addition, we do not yet know how to translate observations of the ambient wind and CME characteristics close to the Sun into accurate predictions of effects at Earth.

The STEREO Beacon

Space Weather Forecast Data

Successful integration of STEREO into the national space weather forecast effort hinges on the implementation of simple but robust onboard processing schemes to automatically identify events of interest, broadcast an alert, and trigger the transmission of a pre-stored, high-cadence image and ancillary data stream necessary to sharpen the warning and maximize its utility.

A "beacon" mode of operation can be particularly useful in warning of dangerous solar particle activity. For example, a microprocessor could make real-time classifications of gradual or impulsive events based on the measured particle composition and other characteristics. The microprocessor would also determine the maximum particle flux, rate of rise, proton and helium energy spectra, and elemental composition. If these parameters exceed predetermined threshold levels, an alert could be sent to Earth.

If suitably designed, STEREO will provide a real-time capability for warning of Earthward-directed CMEs. For example, if an onboard microprocessor identifies a coronal transient, significant particle fluxes, or a strong interplanetary shock, an alert could be sent to Earth at a low bit rate. The immediate alert will need to provide positive identification of CME launch time and direction. Estimates of speed, mass, and relation to structures in the lower atmosphere (to provide an idea of the magnetic content of the CME) would be desirable but perhaps too difficult to include in a simple algorithm. Most likely, preliminary values will have to be derived from the first few images sent down, and more accurate ones would follow from analysis of the full series of event images.

The immediate alert algorithm will presumably be based on some form of image differencing scheme. Detection of change beyond some threshold value will be required but, in addition, it will be necessary to judge whether the motion is, in fact, toward Earth. The fastest CMEs travel approximately 5 R_{Sun} per hour, so the underlying image cadence needs to be quick enough to catch these events before they pass entirely out of the field of view.

It is important that the false alarm rate of the immediate alerts be kept low lest their utility be compromised. This will be no trivial task, since the detection scheme will have to be run in real time and autonomously. These difficulties are compounded by the desire to track as far from the Sun as possible (to get the best estimate of CME properties and arrival time), out where accurate subtraction of the F-corona

becomes an issue. In addition, although the fastest and most energetic CMEs are generally associated with the most dramatic geomagnetic disturbances, some CMEs that start out slow and unimpressive can also be geoeffective. For these reasons, *an effective forecast scheme will have to rely heavily on the instruments that can track CMEs to 1 AU*.

STEREO could improve upon predictions of SEPs from X-ray observations provided directional inferences can be drawn in real time. That is, if STEREO in the beacon mode can distinguish the location of the parent X-ray flare, it could at the very least sort out sources too far removed from the Earth–Sun line to be effective (thereby reducing false alarms), and it might be able in a statistical sense to narrow the probabilities of the prediction by virtue of the more accurate locations.

The value of the STEREO mission in pioneering and developing the use of deep space monitors at large angles to the Sun–Earth line cannot be overemphasized. *The work here is truly exploratory, since although we now have some idea of what is involved in gathering observations relevant to space weather applications, the full scope of what is required can only be determined by direct experience.*

Maximizing the Science Return

In addition to modern data compression strategies (see Appendix II), the STEREO mission can use a unique new strategy for maximizing the data return by taking advantage of the beacon mode and of simultaneous observations from Earth-orbiting and ground-based solar observatories. The concept is to store much more imaging data on board than can be downlinked; data from periods of interest are then selectively downlinked. Using this strategy, very high-cadence data on the initiation and explosive phases of CMEs or other eruptive events can be obtained. This data strategy requires that mission operations include scientists monitoring the data provided by other observatories and by the STEREO beacon.

To implement this strategy on a STEREO mission with a downlink of about 1 Gbit per day, the onboard data storage capacity would be sized at about 10 to 20 Gbits. This does not cause a large mass or cost penalty because 10- to 20-Gbit erasable disk mass memory devices weighing about 5 kg are now available. Data would be recorded at a much higher cadence than 1 Gbit per day. Scientists would determine which portions of the data should be downlinked and which portions should be marked for deletion. This information would be uplinked to the spacecraft during the daily uplink/downlink period. Since the data could remain on the recorder for several days before being downlinked, this strategy can be implemented within a low-cost 40-hour/week mission operations schedule.

5. Mission Overview

STEREO must lead to a depth of understanding of solar activity that is incisive enough to predict solar eruptions and their effects throughout the heliosphere. To accomplish this, each STEREO spacecraft must carry a cluster of state-of-the-art telescopes and environmental sensors. Images from STEREO's solar telescopes will be combined with solar magnetograms and other data from ground-based or Earth-orbiting observatories to document in detail both the buildup of magnetic energy and CME liftoffs. Other STEREO telescopes will track CMEs and their shocks through interplanetary space. Onboard sensors will sample particles accelerated by the shocks as well as the disturbed plasmas and magnetic fields themselves.

We recommend that the STEREO mission consist of two identically instrumented Sun-pointed spacecraft at 1 AU. The spacecraft should slowly drift away from Earth, so that after 2 years, STEREO #1 will lead Earth by 45° and STEREO #2 will lag by 60°. Each spacecraft will generate at least 250 images per day plus *in situ* magnetic field and particle data. The solar images should be simultaneous ±1 s. Science data should be transmitted once a day, and both spacecraft should provide real-time alerts (beacon mode). When needed, a quick response by the Deep Space Network (DSN) to an alert of especially important or dangerous events could provide details on Earth-bound CMEs.

As described in Appendix I, the two spacecraft can be launched in 2003 either separately by Taurus rockets or together by a Delta rocket. Solar and interplanetary instruments on and near Earth will provide a third vantage point from which to study the Sun and heliosphere together with the STEREO spacecraft. Solar-B will be launched in 2004. There will be improved ground-based telescopes, and the NOAA GOES satellites will carry solar X-ray imagers. It is possible that the Solar and Heliospheric Observatory (SOHO), WIND, and the Advanced Composition Explorer (ACE) will be operating still, although those programs are expected to end before 2003. The Yohkoh satellite, with its outstanding X-ray telescopes, will reenter the atmosphere in 2002.

We have defined a STEREO mission that will determine the origins and propagation of solar activity that affects Earth. We assumed that only a network of ground-based observatories and the Solar Terrestrial Probes will be available to provide synergistic data. We particularly considered the possibility that SOHO could serve as one of the STEREO eyes on space. We decided against relying on SOHO because if it should fail during the years leading up to launch or shortly after, reliance on SOHO would result in the loss of the stereoscopic mission. As our study made clear, *the scientific value of another single-viewpoint mission is dramatically lower than for a mission with stereoscopic capability.*

The mission is divided into four phases, as described in Section 6 of this report. Primary science operations will occupy the first 2 years. The goal for total mission lifetime is 5 years. The schedule, with a launch in 2003, is based on the Solar Terrestrial Probe strategic plan developed for the Sun-Earth Connection Roadmap. *The scientific program does not depend on the phase of the solar cycle because CMEs and the other phenomena to be studied are common to all phases of the cycle.*

To achieve the scientific goals outlined in Section 2 of this report, the STEREO instruments must reflect state-of-the-art technology and achieve quite high spatial and temporal resolution. The technology to achieve the STEREO goals is available now, but implementing it within the cost guidelines for Solar Terrestrial Probes will be a challenge. We believe the measurement objectives summarized in Table 2 are necessary and sufficient to achieve the science goals. A preliminary cost study (Appendix I) carried out at the Goddard Space Flight Center indicates that

Table 2. STEREO measurement objectives.

Phenomenon	Feature Size Resolved (and/or Timestep)	Physical Properties
CMEs near Sun	40,000 km = 2×10^{-4} AU (6 min)	Density, velocity, internal structure, extent
Flares	2,000 km	Position, density, structure
Moreton waves	5,000 km (1 min)	Wave front shape, velocity, underlying magnetic field
Coronal loops	2,000 km	Temperature, density, structure, deflection by waves
Coronal streamers	40,000 km	Distortion by CMEs, extent
Coronal holes	2,000 km	Footprint, spreading
SEPs	2 min	3-D distribution function
CMEs near Earth	0.01 AU (images) (plasma) 1 min	Magnetic field, density, velocity, shape, extent, temperature
Interplanetary shocks	0.02 AU (5 s)	Extent, velocity, strength

the measurement objectives can be achieved within those cost guidelines.

As detailed in Appendix I, the STEREO mission can be implemented with a mission cost (phase C/D) at the $120M (FY97 dollar) cap for Solar Terrestrial Probes. Costs can be minimized by a deft execution of phase C/D, which, according to the study, lasts only 32 months, and by early selection of an instrument team.

As detailed near the end of Section 2, there are many interesting and important investigations, beyond those baselined, that can be carried out from the STEREO platforms. The principal restriction on added investigations is the Solar Terrestrial Probe cost cap. Hence, *instruments provided by non-NASA-supported institutions may be included to strengthen the overall science program*.

What is the Optimum Angular Spacing Between the Two Spacecraft?

There is no single angular spacing that is best for all instruments and science goals. The coronagraphs effectively detect only the corona within ±60° of the plane of the sky. This implies that for triangulation on CMEs aimed at Earth, the spacecraft should be at least 60° apart. Other CMEs will be detectable by both coronagraphs for spacecraft separations ranging between 0° and 120°. On the other hand, it is best to have the high-resolution chromosphere and low corona imagers separated by only 15°–60° so that features can be identified in the images from both spacecraft. Triangulation on shock fronts with the radio receivers is likely to be most accurate when the spacecraft are separated by ~60°. If ACE or WIND or other near-Earth spacecraft are not available, then a STEREO spacecraft near Earth would be desirable to monitor the fields and particles input to the magnetosphere. The Science Definition Team's solution is the four-phase plan, which focuses on different mission objectives at different times. Thus, we recommend that the two spacecraft be launched into slightly elliptical orbits at 1 AU, one leading Earth and one lagging (see Figure 20), so that the angles between the spacecraft and the Sun–Earth line increase gradually with dwells at selected angles (see Appendix I). STEREO #1, leading Earth, will dwell near 20° between 200 and 400 days into the mission, and near 45° between 600 and 800 days. STEREO #2, lagging Earth, will dwell near 30° and 60°, respectively. After this period, the two spacecraft will move to larger angles and focus on support of other Solar Terrestrial Probe missions.

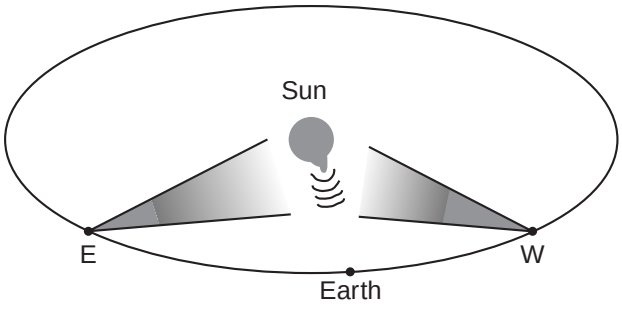

Figure 20. Position of the STEREO spacecraft after about 1 year. STEREO #1, leading Earth, can see around the west limb; STEREO #2, lagging Earth, can see around the east limb.

6. Phases of the STEREO Mission

The studied STEREO mission will have four distinct phases corresponding to different scientific and practical applications of the data and to the angle α separating the two spacecraft.

Phase 1: The 3-D Structure of the Corona (first 400 days, $\alpha \leq 50°$)

While the angular separation α is small and the satellites are close to Earth, telemetry is hardly restricted, and the STEREO satellite configuration is optimum for making rapid-cadence high-resolution 3-D images of coronal structures. The coronal imagers will be able, for the first time, to unambiguously determine the important physical properties of coronal loops and to determine whether coronal loop interactions include reconnection. Stereoscopic image pairs and sequences will capture the 3-D structure of the corona before, during, and after CMEs. They will also allow us to delineate the subtle swelling and the sigmoid features that often foreshadow CME onset. Solar-B will be able to show the corresponding magnetic developments in the photosphere. The period when the STEREO spacecraft are close together will also be used to intercalibrate the instruments.

Phase 2: The Physics of CMEs (days 400 to 800, $50° \leq \alpha \leq 110°$)

As the two spacecraft drift farther apart, they become ideally placed to triangulate on CMEs to determine their true dimensions and trajectory. These will be breakthrough measurements. Further, each spacecraft will be able to image CMEs directed toward the other. Detectors on each spacecraft will measure the magnetic field and plasma properties of CMEs tracked by the other spacecraft, thereby linking the characteristics of a CME (composition, magnetic field orientation, density, and velocity at 1 AU) with its launch and propagation parameters (size, velocity, and source region characteristics).

Phase 3: Earth-Directed CMEs (days 800 to 1100, $110° \leq \alpha \leq 180°$)

In Phase 3, the viewing angles become ideal for observing CMEs aimed at Earth. The coronagraphs, heliosphere imagers, and radio receivers will track the development of CMEs and their shocks as they propagate to Earth, where the Magnetospheric Multiscale and Global Electrodynamics missions will measure their geoeffectiveness.

At this phase of the STEREO mission, the spacecraft will have nearly a 360° view of the Sun, allowing the longitudinal extent of CMEs and other activity to be determined. There have been tantalizing suggestions from Yohkoh soft X-ray images and from the SOHO/LASCO experiment that CMEs can stretch over more than 180° of longitude. STEREO will not only test this suggestion but will also provide global maps of the coronal structures that participate in the activity.

Phase 4: Global Solar Evolution and Space Weather (after day 1100, $\alpha > 180°$)

When the separation of each STEREO spacecraft from the Sun–Earth line becomes greater than 90°, events on the far side of the Sun that launch particles toward Earth will be visible for the first time. Active regions can be tracked and studied for their eruptive potential from their emergence, wherever it occurs on the Sun. The results will have a tremendous impact on our ability to anticipate changes in solar activity and to predict changes in space weather conditions. Such a predictive capability is vital if we are to build permanent lunar bases or send astronauts to Mars.

7. Observational Approach

Based on our study of the scientific potential of a STEREO mission, as described in Section 2, and on the practical limitations, as described in Appendix II, we recommend that the baseline instrument complement for each of the two STEREO spacecraft consist of seven instruments as summarized below.

- *Chromosphere and low corona imager:* an extreme ultraviolet (EUV) and/or X-ray telescope that images 1 R_{Sun} to 1.5 R_{Sun}
- *Coronagraph:* a white-light coronagraph that images 1.5 R_{Sun} to 30 R_{Sun}
- *Radio burst tracker:* a radio receiver that tracks shocks from the outer corona to beyond Earth
- *Heliosphere imager:* a visible-light telescope that images 30 R_{Sun} to beyond Earth

- *Solar wind analyzer:* a plasma analyzer that samples CME and ambient plasmas at 1 AU
- *Magnetometer:* a sensor that detects magnetic fields inside and outside CMEs
- *Solar energetic particle detector:* detectors of prompt and delayed electrons and ions from 0.1 to 50 MeV

*All the instruments needed for accomplishing the STEREO objectives can be built with available technology***.** In some cases, instruments essentially identical to previously flown instruments will meet the objectives and mission constraints. In other cases, some customizing will be needed. The instrument descriptions given below are intended to demonstrate that there is at least one well-established approach to each of the baseline instruments. The actual STEREO instruments will be selected through a competitive review process, and *the instrument descriptions here are not intended in any way to restrict the possible approaches, nor do we intend by our list to preclude consideration of other instruments, such as a magnetograph* (see Appendix III). We believe, however, that the baseline instrument complement will meet the mission science objectives.

Chromosphere and Low Corona Imager

This telescope should be able to obtain images in at least one coronal and one chromospheric emission line. The EIT multilayer normal-incidence extreme-ultraviolet telescope on SOHO, for example, provides the kind of images needed. However, STEREO's focus on solar activity will require a much higher cadence of observations than EIT provides. The images should show solar prominences and coronal loops and other coronal structures from the base of the corona to 1.5 R_{Sun}.

The capabilities of the chromosphere and low corona emission-line imager should include tunability, so that Doppler shifts can be measured. One approach studied at the NASA Goddard Space Flight Center would include two mirrors, multilayer-coated to have a peak reflectivity chosen to observe He II 304 Å at 301 and 307 Å. Each of the two mirrors would form images of the Sun on the same area of the detector. A movable shutter could switch between the two multilayer passbands. The difference in intensity between the two images would provide a measure of the Doppler velocity for each pixel. The instrument should be able to measure velocities in the range of 10 to 3000 km/s. The spatial resolution should be at least 3 arcsec, or 2000 km on the Sun.

Coronagraph

The white-light coronagraph should be capable of observing the current sheet, streamers, CMEs, streamer blow offs, and the acceleration of inhomogeneities in the solar wind from ~1.5 R_{Sun} to ~5 R_{Sun}. A substantially larger field of view, to at least 30 R_{Sun}, is important for studying the three-dimensional structure of streamers, the evolution and acceleration of streamer blow offs, and the acceleration of inhomogeneities in the solar wind.

Coverage of the corona from about 1.5 R_{Sun} to 30 R_{Sun} will likely require two channels if conventional externally occulted designs are used. The detector format should be 1024 × 1024 or better and the dynamic range must be better than 10^4 in order to track the two orders of magnitude change in the signal and background while detecting the ~1% contrast of coronal features against the background.

Certain aspects of the coronagraph design peculiar to the specific objectives of the STEREO mission must be carefully considered. The usual background light rejection limitations affecting the determination of the field of view of an externally occulted white-light coronagraph designed for the inner corona is complicated by the orbit eccentricity, the separation angle of the two spacecraft, and the spatial resolution function in the inner field of view. While the orbital eccentricity affects the apparent diameter of the Sun, and hence the occulter inner cutoff R_1, by a relatively small (~10%) amount, its effect on the background light rejection can be very pronounced.

The spacecraft separation significantly affects the co-observed field of view for separation angles above about 30°. A feature observed in the plane of the sky and an altitude h by one coronagraph will be co-observed by the second coronagraph only if $h > R_1 \sec \alpha$, where α is the spacecraft separation or stereo angle. The science objectives of STEREO indicate $R_1 \sim 1.5\ R_{Sun}$ is desirable. The co-observed h is 1.55 R_{Sun}, 1.73 R_{Sun}, 2.12 R_{sun}, and 3.00 R_{Sun} for 15°, 30°,

45°, and 60°, respectively. The effects at the outer field of view cutoff, R_2, scale similarly. Using standard design methods, a coronagraph with R_1 = 1.5 R_{Sun} could be expected to have R_2 ~ 5–6 R_{Sun}. The coronagraph spatial resolution function, due to the varying obstruction of the entrance aperture by the external occulter with changing altitude, is asymmetric and deteriorates rapidly near R_1. The SOHO/LASCO/C2 coronagraph with an R_1 of about 1.5 R_{Sun} has a nominal spatial resolution of about 8 arcsec at 6 R_{Sun}, but only about 110 arcsec by 2 R_{Sun}. The effects that the low and radially varying resolution function will have on three-dimensional image reconstruction in the inner corona must be carefully examined.

Radio Burst Tracker

The STEREO spacecraft should carry two identical radio receivers so that triangulation of solar events can become routine rather than fortuitous as for Wind-Ulysses. A simple receiver like that to be flown on Cassini connected to a triaxial antenna system also similar to (but simpler than) that being flown on Cassini can track solar radio disturbances to within ±1° from 1 to 2 R_{Sun} to 1 AU. The corresponding radio frequency range is ~15 MHz to ~30 kHz. A key scientific objective for the radio burst tracker is to triangulate on radio emission from shock-accelerated particles, 20 MHz to 30 kHz sweep, with a few seconds' time resolution. This should effectively allow tracking of the location of particle acceleration sites through interplanetary medium

Heliosphere Imager

The heliosphere imagers should have 100 times the spatial resolution of those on Helios and a cadence of about one image pair per hour. These capabilities will be adequate to map the solar wind and CMEs at heliospheric distances between 30 R_{Sun} and 215 R_{Sun}. Resolutions of ~1° in heliospheric latitude and longitude are feasible with current technology, so STEREO should achieve the goal of approximately 1-hour time resolution in CME tracking.

One design that has been studied has an optical imager to view a hemisphere of sky starting within a few degrees of the solar disk and roughly centered on the spacecraft-to-Earth line. Strictly speaking, this is a "half-sky" camera, although it covers nearly all the path traveled by material going from the Sun to beyond Earth. A hemispherical imager with a multi-element light baffle, a wide-angle optical system, and a CCD camera has been designed and its components have been tested. The baffle works like a coronagraphic external occulter and consists of five knife-edge walls spaced about 1 cm from one another, with each wall top placed in the shadow of its next outer neighbor. The optical system further reduces background-light contamination, down to below the equivalent of one 10th magnitude star per square degree. This optical system consists of a toroidal mirror enclosing a simple thick lens, which maps the sky onto the CCD photometer; it is the equivalent of a "fish-eye lens," but without a protruding glass element that can intercept stray light crossing over the edge of the baffle.

Solar Wind Plasma Analyzer

The solar wind plasma analyzer should measure the distribution functions (to provide density, vector velocity, temperature, and anisotropy) of ions and electrons over the energy ranges of 300–8000 eV (for positive ions) and 1–1000 eV (for electrons). The required time resolution is a few minutes.

One approach to the solar wind plasma analyzer is an ion-electron spectrometer comprising two top-hat toroidal electrostatic analyzers that share a common collimator and steering lens. This design allows simultaneous measurement of electrons and ions with an overall reduction of mass and volume over two discrete instruments. With no potential placed on the steering lenses, the analyzer provides up to 360° field of view in the plane perpendicular to the axis of symmetry through the entrance aperture. By placing a potential across the steering lens, the field of view of the instrument is changed to a cone, the apex of which is located on the analyzer's axis of symmetry. By sweeping the steering lens voltage, elevation angles through ±40° can be observed during an effective field of view of 2.6 π steradians. The elevation can be servo-controlled to follow deviations in the solar wind direction.

If sufficient mass, power, and funding are available, the plasma analyzer could be enhanced by the addition of a time-of-flight section capable, at a

minimum, of determining the ionization temperature of the plasma through measurement of the ratio of O^{6+} to O^{7+} ions. A second objective would be to determine the relative abundances of ions with high and low first-ionization potentials, such as the Mg:O ratio. The ionization state and the composition provide clues to the coronal sources of the plasma. The energy-per-charge filtered ions would be accelerated through a carbon foil floating at a high negative potential. Secondary electrons emitted from the foil would provide a start pulse, while accelerated ions would be detected after passing through the time-of-flight region to provide a stop pulse.

Magnetometer

A candidate magnetometer for STEREO is a single miniature triaxial fluxgate magnetometer using ring-core magnetic sensing elements. The magnetometer low-noise ring core sensors are derived from the same technology used in the Voyager, Magsat, Giotto, CLUSTER, GGS, AMPTE, and MGS. A dynamic range of ±65,536 nT can be achieved with a resolution of 0.125 nT in one channel, and ±655 nT with a resolution of 0.00125 nT in a second channel. The vector magnetic field can be obtained at a rate of 20 vectors per second, but such high temporal resolution is not necessary for the STEREO mission. If the magnetometer sensor is mounted on a boom, the orientation of the boom must be chosen to avoid interference with the field of view of other instruments.

Solar Energetic Particle Detector

Only rather modest instrumentation based on proven approaches is required to address the mission objectives for energetic particles. The instrumentation should be able to distinguish impulsive from gradual events based on the characteristics in Table 3.

Table 3. Characteristics of impulsive and gradual particle events.

Impulsive	Gradual
Enriched in He^3	Normal isotopic composition
Electron-rich	Proton-rich
Enriched in Fe & other heavy ions	Coronal abundances
Rapid rise & decay	More extended

It should be able to measure the absolute intensity and energy spectra of energetic nuclei at the energies (10 to 100 MeV/nuc) that pose a potential risk to astronauts. The following list gives the observational and scientific objectives of the energetic particle detector and representative energy ranges to be covered:

Observational Objectives	Scientific Objective
Sample *in situ*, with 1-min time resolution • Energetic electrons: ~0.1 to 3 MeV • Protons: ~0.1 to ~100 MeV • Helium: ~1 to 100 MeV/nuc • Heavy ions ($6 < Z < 28$): ~2 to 30 MeV/nuc He^3 identification	Understand the mechanism for the production of CME shock-accelerated particles

Using modern approaches to low-power, lightweight instrumentation, the required measurements can be provided with a package of several small detectors that would require ~3 kg and ~2 W. These particle telescopes could be based on silicon solid-state devices, which provide precise measurements with good long-term stability. An average bit rate of ~200 bits per second should be adequate if onboard processing and data compression techniques are used.

8. Conclusions

We have reviewed recent progress in understanding CMEs and identified the major scientific questions to be answered. The key questions and many of our conclusions are highlighted by italics throughout the text. We concluded that two spacecraft at 1 AU, one drifting well ahead of Earth and one well behind, will serve the objectives of NASA's Sun-Earth Connection Initiative by (1) enabling fundamental research on the three-dimensional structure and dynamical processes of CMEs, (2) providing the science base for greatly improved forecasts of disturbances at Earth, and (3) providing comprehensive measurements of the interplanetary environment in support of follow-on Solar Terrestrial Probes.

We recommend that the STEREO spacecraft carry identical complements of instruments, including chromosphere and coronal imagers, a heliosphere

imager, a radio telescope, and sensors of interplanetary particles and magnetic fields. We believe that the recommended complement of instruments will accomplish the goals of the STEREO mission.

Together with the Goddard Space Flight Center, we studied orbits, vehicles, programmatic requirements, and funding needed to carry out a 2-year science mission with a 3-year extension for support of other Solar-Terrestrial Probes. We concluded that the needed technologies are available now and that the mission can be launched in mid-2003 within the cost restrictions of the Solar-Terrestrial Probe line of missions. We also considered how existing or planned space assets, such as ACE and Solar-B, might add to the scientific potential of the mission. We particularly considered the possibility that SOHO could serve as one of the STEREO eyes on space. We decided against relying on SOHO because if it should fail during the years leading up to launch or shortly after, then reliance on SOHO would result in the loss of the stereoscopic mission. As our study made clear, *the scientific value of another single-viewpoint mission is dramatically lower than for a mission with stereoscopic capability.*

In order to maximize the scientific return from the unique opportunity provided by STEREO, further studies should be conducted to maximize the information that can be extracted from stereo observations. Such studies, which will include simulated observations of prescribed structures (e.g., CMEs, streamers, loops), will help assure the optimum design and selection of STEREO instrumentation. We also recommend that studies of various telescopes, including magnetographs, be pursued vigorously to minimize eventual costs and maximize capabilities.

As a result of this study, the Science Definition Team concludes that:

1. Two suitably instrumented spacecraft in elliptical solar orbits, leading and lagging Earth at 1 AU, will provide the measurements needed to solve the fundamental scientific issues surrounding coronal mass ejections.
2. The technology for the STEREO mission is ready, and NASA should act promptly to implement it. The spacecraft can be launched by 2003 within the cost cap of the Solar-Terrestrial Probe program.
3. NASA should act, in cooperation with other agencies, to implement a "beacon mode" that would enable STEREO to provide near-real-time warnings of impending geomagnetic disturbances.

9. Bibliography

The scientific literature dealing with solar activity and its effects is extensive. We have drawn on that literature in discussing the scientific goals of the STEREO mission, but for brevity we have not explicitly cited the works. Several recent conference proceedings are particularly helpful in explaining the scientific issues motivating the STEREO mission:

Coronal Mass Ejections, Geophys. Monogr. Ser., vol. 99, edited by N. Crooker, J. A. Joselyn, and J. Feynman, 1997, AGU, Washington, D. C.

Magnetic Reconnection in the Solar Atmosphere, edited by R. D. Bentley and J. T. Mariska, 1996, *Astron. Soc. Pacific Conf. Ser*., Vol. 111, San Francisco, Calif.

Solar Wind Eight, edited by D. Winterhalter, J. T. Gosling, S. R. Habbal, W. S. Kurth, and M. Neugebauer, 1996, *AIP Conf. Proc*., Vol. 382, AIP Press, Woodbury, N. Y.

Solar Dynamic Phenomena and Solar Wind Consequences, Proc. Third SOHO Workshop, 1994, ESA SP-373.

The recommended Sun-Earth Connections program is available on the Web:

Sun-Earth Connection Roadmap. Strategic Planning for the Years 2000–2020, Roadmap Integration Team (J. L. Burch, chairman), 1997. Website: http://espsun.space.swri.edu/~roadmap/index.html.

In the bibliography below, we offer a sample of recent papers that are representative of current thinking in the field and that will lead the interested reader to earlier works and to other works on the research frontier.

"Acceleration of energetic particles which accompany coronal mass ejections," Reames, D. V., 1994,

in *Proc. Third SOHO Workshop—Solar Dynamic Phenomena and Solar Wind Consequences*, ESA SP-373, pp. 107–116.

"Coronal mass ejections and large geomagnetic storms," Gosling, J. T., S. J. Bame, D. J. McComas, and J. L. Phillips, 1990, *Geophys. Res. Lett.*, **17**, 901–904.

"Coronal mass ejections and magnetic flux ropes in interplanetary space," Gosling, J. T., 1990, in *Physics of Magnetic Flux Ropes*, Geophys. Monogr. Ser., vol. 58, edited by C. T. Russell, E. R. Priest, and L.-C. Lee, pp. 343–364, AGU, Washington, D. C.

"Coronal mass ejections: A summary of SMM observations from 1980 and 1984-1989," Hundhausen, A. J., 1997, in *The Many Faces of the Sun: Scientific Highlights of the Solar Maximum Mission*, edited by K. T. Strong, J. L. R. Saba, and B. M. Haisch, Springer-Verlag, New York, in press.

"Coronal mass ejections: The key to major interplanetary and geomagnetic disturbances," Webb, D. F., *Rev. Geophys., Supplement*, pp. 577–583.

"Disruption of coronal magnetic field arcades," Mikic, Z., and J. A. Linker, 1994, *Astrophys. J.*, **430**, 898.

"EIT: Extreme-Ultraviolet Imaging Telescope for the SOHO Mission," Delaboudinière, J.-P. and others, 1995, *Solar Phys.*, **162**, 291–312.

"The ejection of helical field structures through the outer corona," House, L. L., and Berger, M. A., 1987, *Astrophys. J.*, **323**, 406-413.

"Eruptive prominences as sources of magnetic clouds in the solar wind," Bothmer, V., and R. Schwenn, 1994, *Space Sci. Rev.*, **70**, 215.

"The escape of magnetic flux from the Sun," Bieber, J. W., and D. M. Rust, *Astrophys. J.*, 1995, **453**, 911.

Foundations of Solar Particle Event Risk Management Strategies, Findings of the Risk Management Workshop for Solar Particle Events, M. Acuna, Chair, July 1966.

"Geomagnetic activity associated with Earth passage of interplanetary shock disturbances and coronal mass ejections," Gosling, J. T., D. J. McComas, J. L. Phillips, and S. J. Bame, 1991, *J. Geophys. Res.*, **96**, 7831–7839.

"Great geomagnetic storms," Tsurutani, B. T., W. D. Gonzalez, F. Tang, and Y. T. Lee, 1992, *Geophys. Res. Lett.*, **19**, 73–76.

"Heliospheric observations of solar disturbances and their potential role in the origin of geomagnetic storms," Jackson, B. V., 1997, in *Magnetic Storms*, Geophys. Monogr. Ser., vol. 98, edited by B. T. Tsurutani, W. D. Gonzalez, Y. Kamide, and J. K. Arballo, pp. 59–76, AGU, Washington, D. C.

"The implications of 3D for solar MHD modelling," Antiochos, S. K., and R. B. Dahlburg, 1997, *Solar Phys.*, **174**, 5–19.

"The initiation of coronal mass ejections by magnetic shear," Mikic, Z., and J. A. Linker, 1997, in *Coronal Mass Ejections*, Geophys. Monogr. Ser., vol. 99, edited by N. Crooker, J. A. Joselyn, and J. Feynman, pp. 57–65, AGU, Washington, D. C.

"In situ observations of coronal mass ejections in interplanetary space," Gosling, J. T., 1992, in *Eruptive Solar Flares, Lecture Notes in Physics*, edited by Z. Svestka, B. V. Jackson, and M. E. Machado, vol. 399, pp. 258–267, Springer, Berlin.

"Interplanetary magnetic clouds, helicity conservation and intrinsic-scale flux ropes," Kumar, A., and D. M. Rust, 1996, *J. Geophys. Res.*, **101**, 15,667.

"Interplanetary origin of geomagnetic activity in the declining phase of the solar cycle," Tsurutani, B. T., W. D. Gonzales, A. L. C. Gonzales, F. Tang, J. K. Arballo, and M. Okada, 1995, *J. Geophys. Res.*, **100**, 21,717–21,733.

Lagrange: The Sun and Inner Heliosphere in Three Dimensions, Schmidt, W. K. H., and others, 1996, a proposal to the European Space Agency for the next medium size mission (M3), ESA SP-1180, 116.

"The Large Angle Spectroscopic Coronagraph (LASCO)," Brueckner, G. E., and others, 1995, *Solar Phys.*, **162**, 357–402.

"Magnetic chirality and coronal reconnection," Canfield, R. C., A. A. Pevtsov, and A. N. McClymont, 1996, in *Magnetic Reconnection in the Solar Atmosphere*, edited by R. D. Bentley and J. T. Mariska, pp. 341–346, Astron. Soc. Pacific, San Francisco.

"Magnetic field structure of interplanetary magnetic clouds at 1 AU," Lepping, R. P., J. A. Jones, and

L. F. Burlaga, 1990, *J. Geophys. Res.*, **95**, 11,957–11,965.

"Problems and progress in computing three-dimensional coronal active region magnetic fields from boundary data," McClymont, A. N., L. Jiao, and Z. Mikic, 1997, *Solar Phys.*, **174**, 191–218.

"Quasi-stereoscopic imaging of the solar X-ray corona," Batchelor, D.,1994, *Solar Phys.* **155**, 57–61.

"Rendering three-dimensional solar coronal structures," G. Allen Gary, 1997, *Solar Phys.*, **174**, 241–263.

"Scaling of heating rates in solar coronal loops," Klimchuk, J. A., and Porter, L. J., 1995, *Nature*, **377**, 131.

"The sizes and locations of coronal mass ejections: SMM observations from 1980 and 1984-1989," Hundhausen, A. J., 1993, *J. Geophys. Res.*, **98**, 13,177–13,200.

"Solar activity and the corona," Low, B. C., 1996, *Solar Phys.*, **167**, 217.

"The solar flare myth," Gosling, J. T., 1993, *J. Geophys. Res.*, **98**, 18,949.

"Solar flares—An overview," Rust, D. M., 1992, in *Life Sciences and Space Research XXIV/2/ Radiation Biology; Proc. Topical Meet. Interdisciplinary Scientific Commission F/Meetings F3*, **12**, 289–301.

"Solar tomography," Davila, J. M., 1994, *Astrophys. J.*, **423**, 871.

"Spatial and temporal invariance in the spectra of energetic particles in gradual events," D. V. Reames, S. W. Kahler, and C. K. Ng, 1997, *Astrophys. J.*, in press.

"The spatial distribution of particles accelerated by coronal mass ejection-driven shocks," Reames, D. V., L. M. Barbier, and C. K. Ng, 1996, *Astrophys. J.*, **466**, 473.

"Spawning and shedding helical magnetic fields in the solar atmosphere," Rust, D. M., 1994, *Geophys. Res. Lett.*, **21**, 241–244.

"Stereoscopic viewing of solar coronal and interplanetary activity," Schmidt, W. K. H., and V. Bothmer, 1996, *Adv. Space Res.*, **17**, 369–376.

"Three-dimensional reconstruction of coronal mass ejections," Jackson, B. V., and H. R. Froehling, 1995, *Astron. Astrophys.*, **299**, 885–892.

"Tomographic inversion of coronagraph images," Zidowitz, S., B. Inhester, and A. Epple, 1996, in *Solar Wind Eight*, edited by D. Winterhalter, J. T. Gosling, S. R. Habbal, W. S. Kurth, and M. Neugebauer, pp. 165–166, AIP Conf. Proc. 328, Woodbury, N. Y.

APPENDIX I

Mission Requirements and Proof of Feasibility

I. Observatory Concept

A. Overview

The uniqueness of the Solar STEREO mission concept lies simply in the geometry of the observations and consequently the drifting heliocentric orbit requirement. The science instrumentation utilizes proven, relatively straightforward designs. The spacecraft requires modest three-axis stabilization and a reasonably high performance communication system. It must be rather lightweight, radiation hard, and inexpensive. All of these requirements can be met using current designs such as the newly developed SMEX•*Lite* architecture[1]. Though admittedly state-of-the-art today, this type of small spacecraft performance will undoubtedly be readily available by the 2003 timeframe in which STEREO will fly. Consequently, the SMEX•*Lite* architecture is cited in this study as an ample demonstration (a case study) of the ease in which this mission could be assembled.

B. Spacecraft Background

The SMEX•Lite architecture is currently being developed by the SMEX Project at NASA/GSFC under the context of the NASA Explorer Program Technology Infusion Program. This design will be built to protoflight standards, qualified for flight, and performance demonstrated by early 1998. Prototype integration began in October 1997. This new spacecraft architecture has been optimized for versatility, ease of change, and low cost. A three-axis stabilized version of this design is no more than one-foot tall, 38 inches in diameter, and is anticipated to cost approximately $10M per mission to obtain. This study makes no presumption as to who or where the spacecraft are produced, but only presumes ready availability of this class of technology and the acceptance of aggressive project management and systems engineering techniques. Full cost accounting techniques have been utilized in estimating mission costs. The current development activity is proceeding very well, meeting nearly all of its cost and performance objectives. This provides the confidence to cite this architecture as a proof of feasibility concept for the STEREO mission concept definition study.

C. Mission Orbit

The STEREO mission requires two spacecraft to make their observations separated within the ecliptic plane by approximately 60 degrees from each other in their respective viewpoints of the Sun. This is an optimum viewing geometry for the selected science instrumentation package, not an absolute geometry—meaning that good science can be obtained from smaller as well as larger angles, but the best observations will occur as this angle approaches approximately 60 degrees. In fact, there are reasons to argue that a variety of viewing geometries will yield more information on CME structures and behavior than a fixed viewing geometry. When you couple the science viewing requirements with the recognition that it takes a great deal of propulsive energy and resulting spacecraft weight and complexity to position a spacecraft in a fixed position in deep space such as a libration point, this study recommends a slowly drifting heliocentric orbit in which the spacecraft can be directly inserted by the launch vehicle as the optimal low cost solution for this mission. This approach has the added benefit of only requiring two spacecraft configurations (or operating conditions) during the mission—the launch configuration and the science observation configuration. With no intermediate orbit transfer or parking configuration and no propulsion system requirements to be met, the spacecraft design becomes very straightforward.

The heliocentric orbit, which was chosen, has an energy requirement of approximately 0.78 km^2/s^2. A C_3=1.0 km^2/s^2 was used for launch vehicle performance analysis. One spacecraft would be placed in a leading trajectory ahead of the Earth in its orbit and the other would be placed in a lagging trajectory following the Earth in its orbit. This combination of trajectories will yield a spacecraft separation angle of ~60 degrees that persists from about day 210 to day 460 of the mission (see Figure 1, Figure 2, Figure 3, and Figure 4).

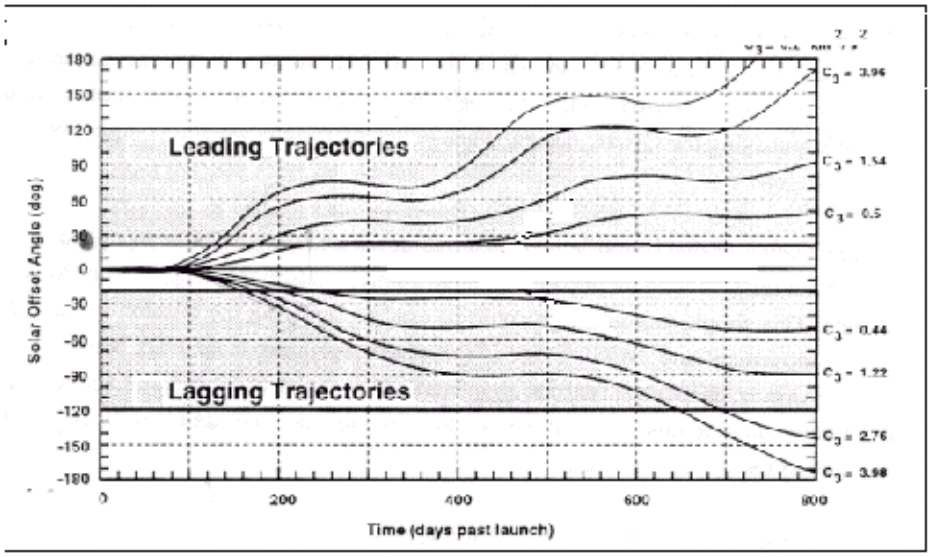

Figure 1. Reference Orbit Selection

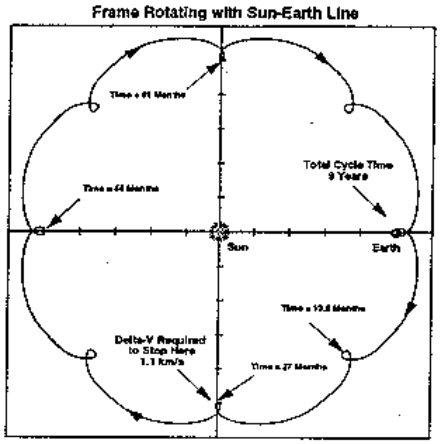

Figure 2. 9/8 Lagging Transfer C_3=1.2

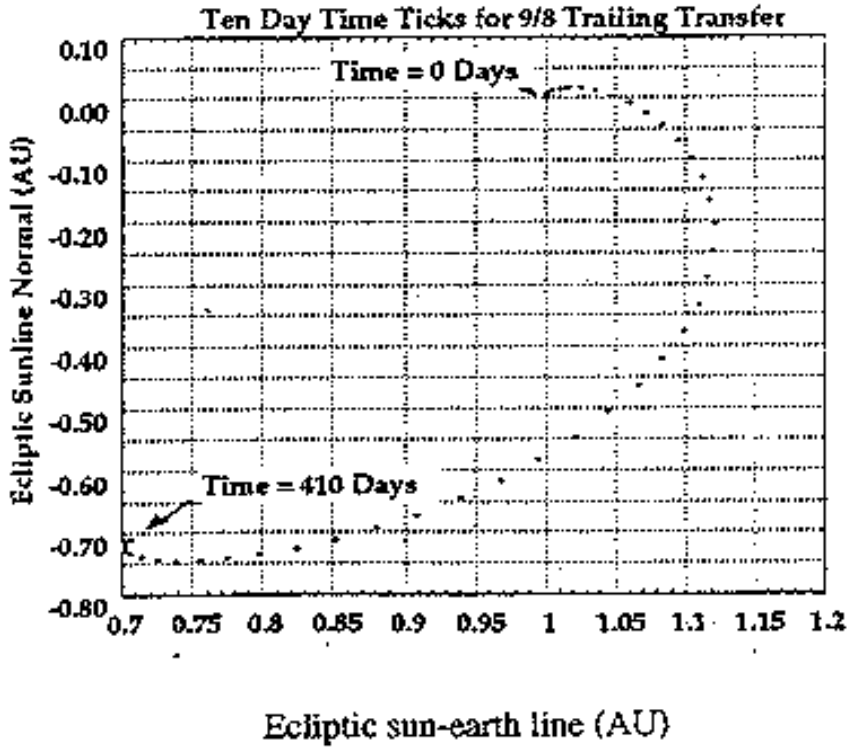

Figure 3. Ten-Day Time Ticks for 9/8 Trailing Transfer

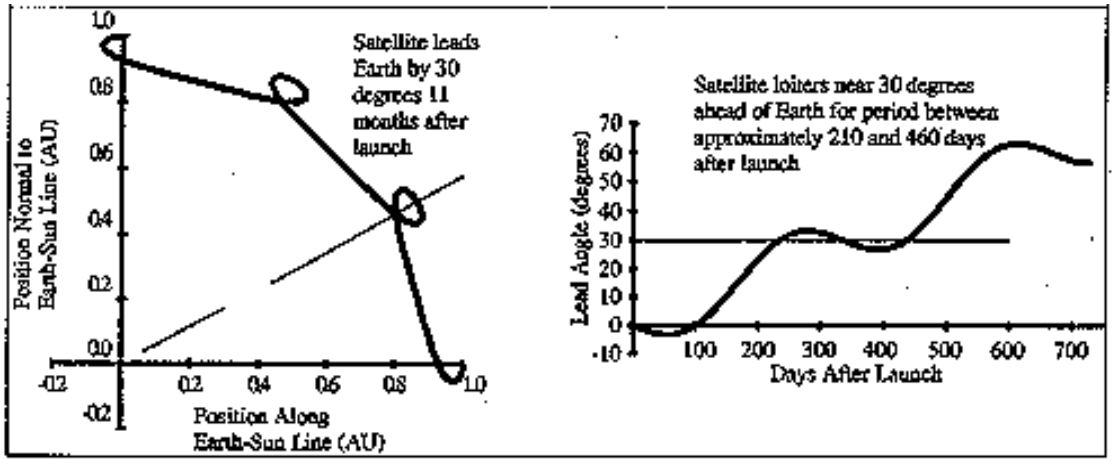

Figure 4. Parameters for the STEREO Orbit C_3=0.78

These trajectories are very straightforward to obtain and relatively insensitive to insertion errors (see Figure 5).

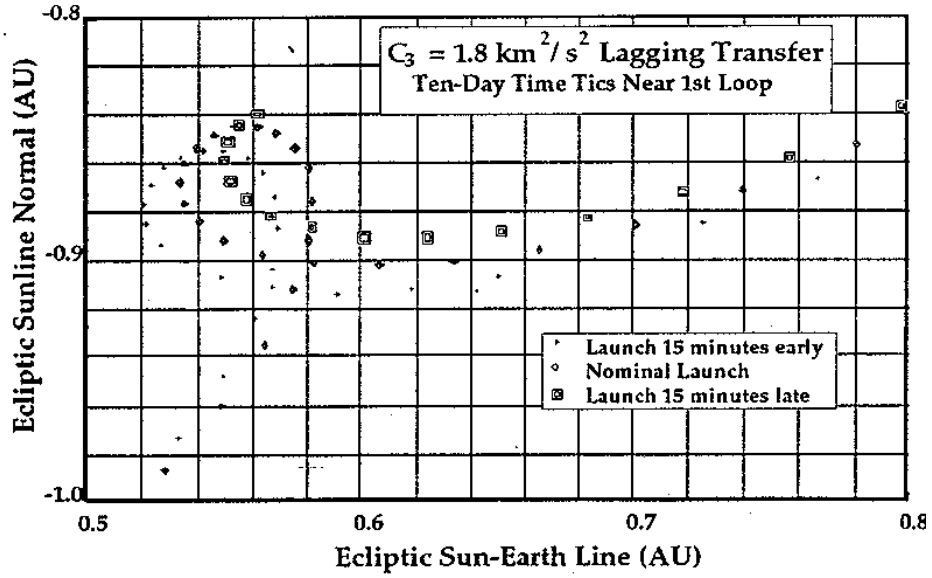

Figure 5. Effects of Launch Time Variations on Heliocentric Transfer

The resulting orbital geometry has the added advantage of minimizing the distance from the Earth (simpler RF communications) and of putting all other Earth orbiting as well as ground based solar observatories in a good position to provide collaborative data.

D. Launch Vehicle Selection

Launch vehicle options ranging from the Pegasus to the DELTA were evaluated for this mission. Vehicle technical capabilities and cost were considered. Two options were studied in detail—launching both spacecraft together on a DELTA or launching each spacecraft separately on a TAURUS.

The DELTA vehicle does not have the capability to provide separate 3rd stages to multiple payloads. Consequently, at least one, if not both of the spacecraft would require their own kick motors. The DELTA 7326 could lift a 600 kg combined payload mass into a transfer orbit, leaving one spacecraft there, and subsequently boost the other into its heliocentric orbit (C_3=1.0) using a STAR 37 upper stage. The other spacecraft would need to provide its own propulsive element to boost to the heliocentric orbit.

A single TAURUS vehicle could directly insert a single 350 kg payload into the required heliocentric (C_3=1.0) orbit for approximately half the cost of the DELTA. The TAURUS configuration would utilize the 63 inch diameter fairing (54 inch useable payload diameter), the Star 37FM upper stage, and the standard 3712 payload adapter fixture/separation system (see Figure 6). The upper stage is spin stabilized (~50 rpm) and includes an integral despin system. Launch would be from the Kennedy Space Center (KSC) range. It is assumed that all launch support facilities would already be in place. Two separate launches would be used for STEREO.

The TAURUS option was selected as the most practical for its simplicity in mission operations, least impact on the spacecraft design, and for spreading the risk of catastrophic failure by utilizing separate launches.

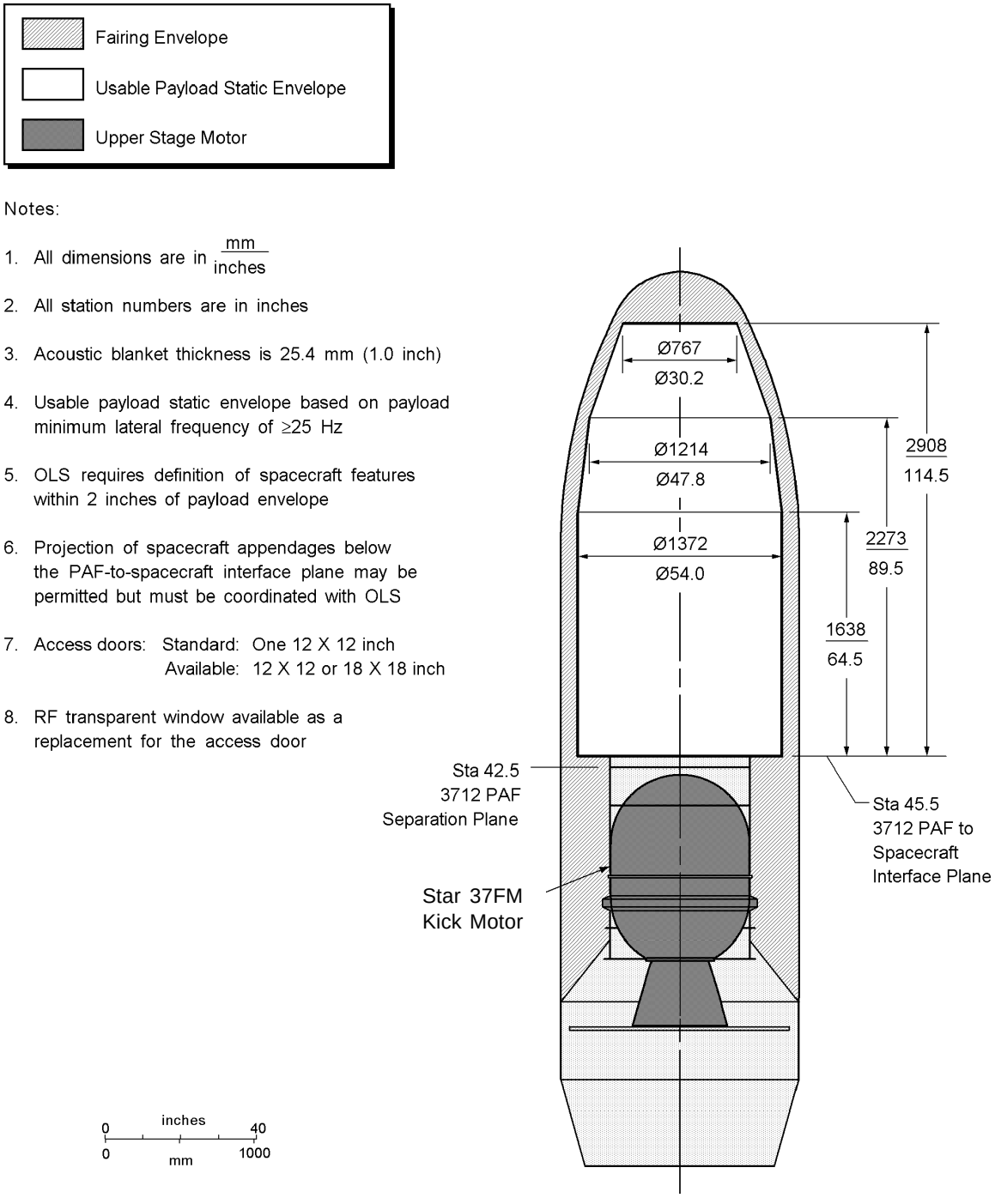

Figure 6. TAURUS Payload Envelope

E. Mission Lifetime and Reliability

The STEREO mission concept is optimized for the 60-degree separation angle science observations between days 210 and 460 and the 110-degree separation between days 600 and 800. Observations after this angle expands outward are considered an extended mission opportunity. Any additional science data gathered in the extended mission is considered a bonus and will be relayed back to Earth at diminished data rates as the spacecraft gradually drifts further and further away from Earth. This approach eliminates the need for a propulsion system on-board the spacecraft. It also greatly simplifies the data system requirements, both on-board the spacecraft as well as on the ground. It yields a design life of approximately 2 years—implying that a single string observatory is a reasonable design approach.

F. Spacecraft Configuration

The STEREO observatory was configured for maximum simplicity. The sunward facing platform was balanced so as to minimize the separation of the Center of Pressure (CP) and Center of Gravity (CG) in order to keep secular momentum build-up as small as possible. The spacecraft must be balanced in its launch configuration due to the spin stabilized upper stage. Balance mass has been allocated to simplify the implementation of this requirement. No attempt was made to provide a balanced torque couple configuration of the spacecraft thrusters since there are no stringent trajectory maintenance requirements. The science magnetometer was placed in the spacecraft shadow in order to minimize thermal distortion of its boom. The instrument electric dipole antennas were placed to prevent interference with not only the sunpointed instruments, but also the high gain antenna and the star tracker. The Heliosphere Imager is deployed on-orbit to a slightly outward and aft position in order to clear its expansive FOV from shadowing by the high gain antenna.

The spacecraft assembly was decoupled as much as possible from the instrument module in order to provide for the use of an accelerated development schedule (see Section VI) that minimizes mission cost. The instrument module is a separate, fully integrated sub-assembly. The spacecraft components are housed in or attached to the one-piece integral spacecraft structure (see Figure 7, Figure 8, Figure 9, Figure 10).

Figure 7. STEREO Launch Configuration

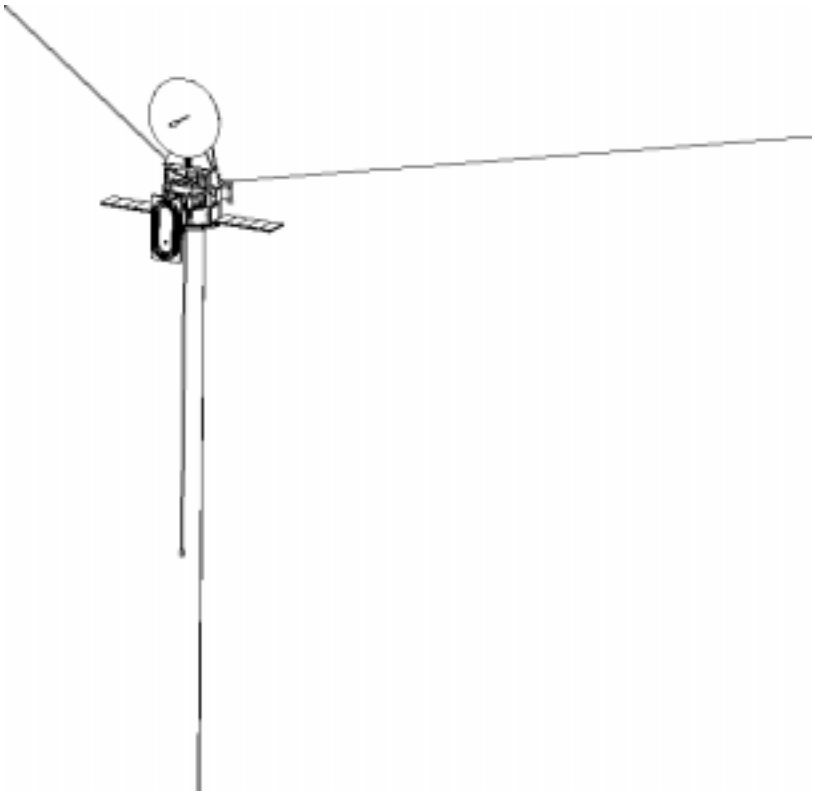

Figure 8. STEREO On-Orbit Configuration Overview

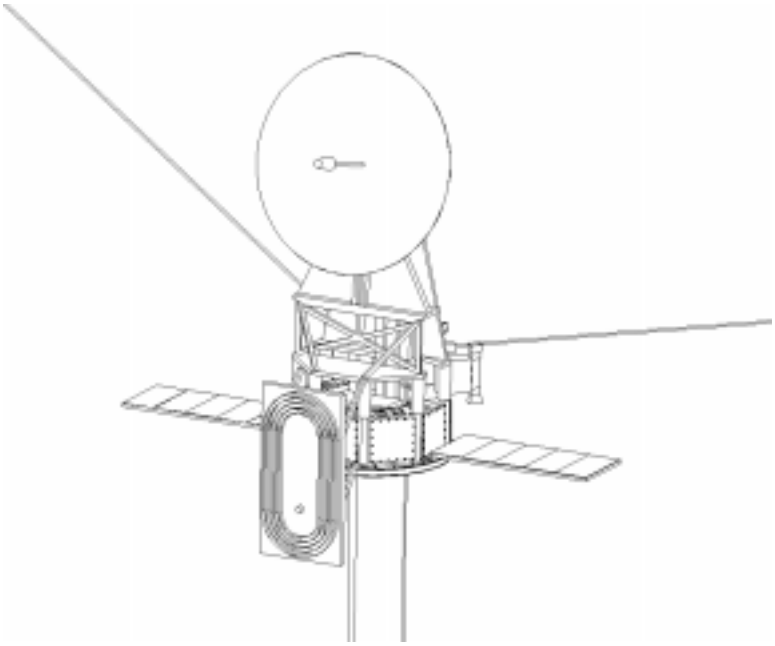

Figure 9. STEREO On-Orbit Configuration Close-up

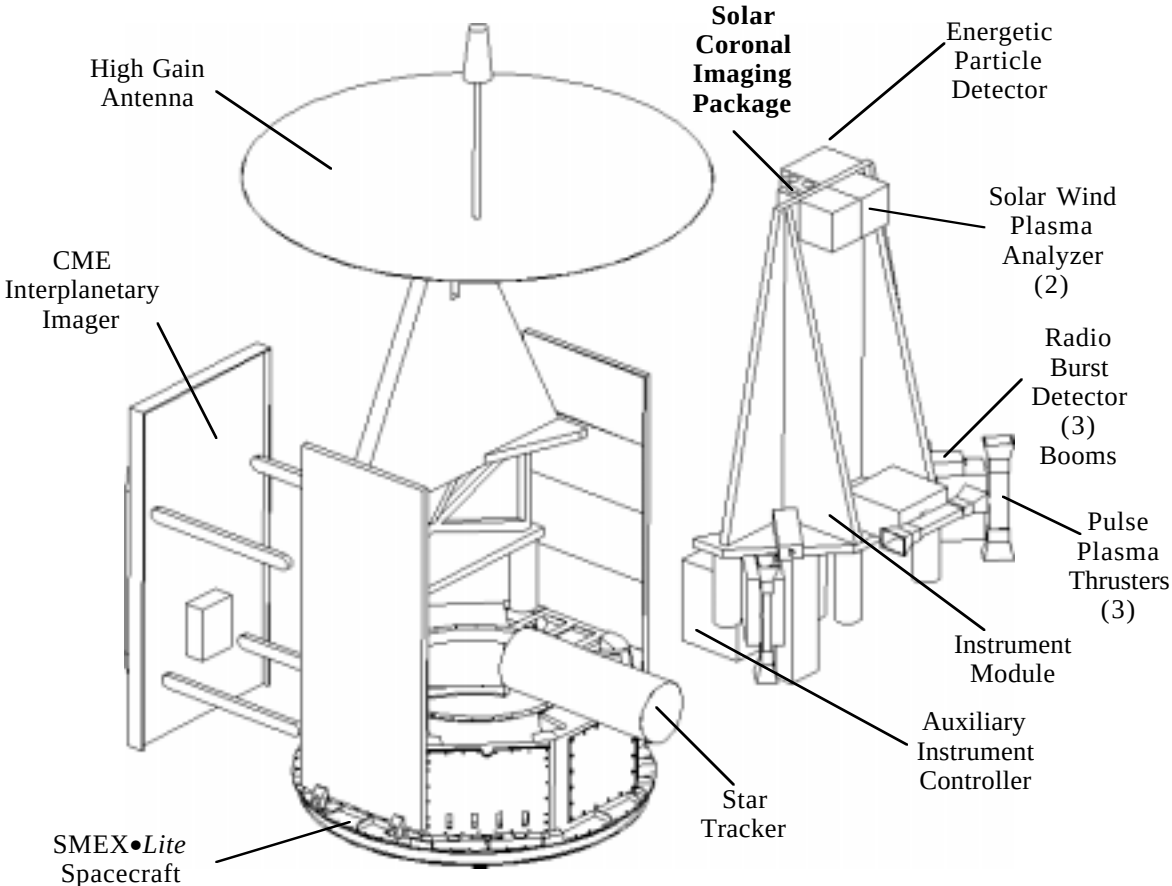

Figure 10. STEREO Configuration Details

The internal architecture of the STEREO observatory (see Figure 11) utilizes the standard interfaces and basic performance of the SMEX•*Lite* architecture[2]. Command and control, as well as housekeeping and low rate telemetry are managed on the MIL-STD-1553 Data Bus. A single RSC6000 radiation hard, 32-bit microprocessor controls all observatory functions. A single serial port is used to transfer the high data volume from the SCIP instrument. The remaining instruments are interfaced by a single Auxiliary Instrument Controller (AIC) to the spacecraft.

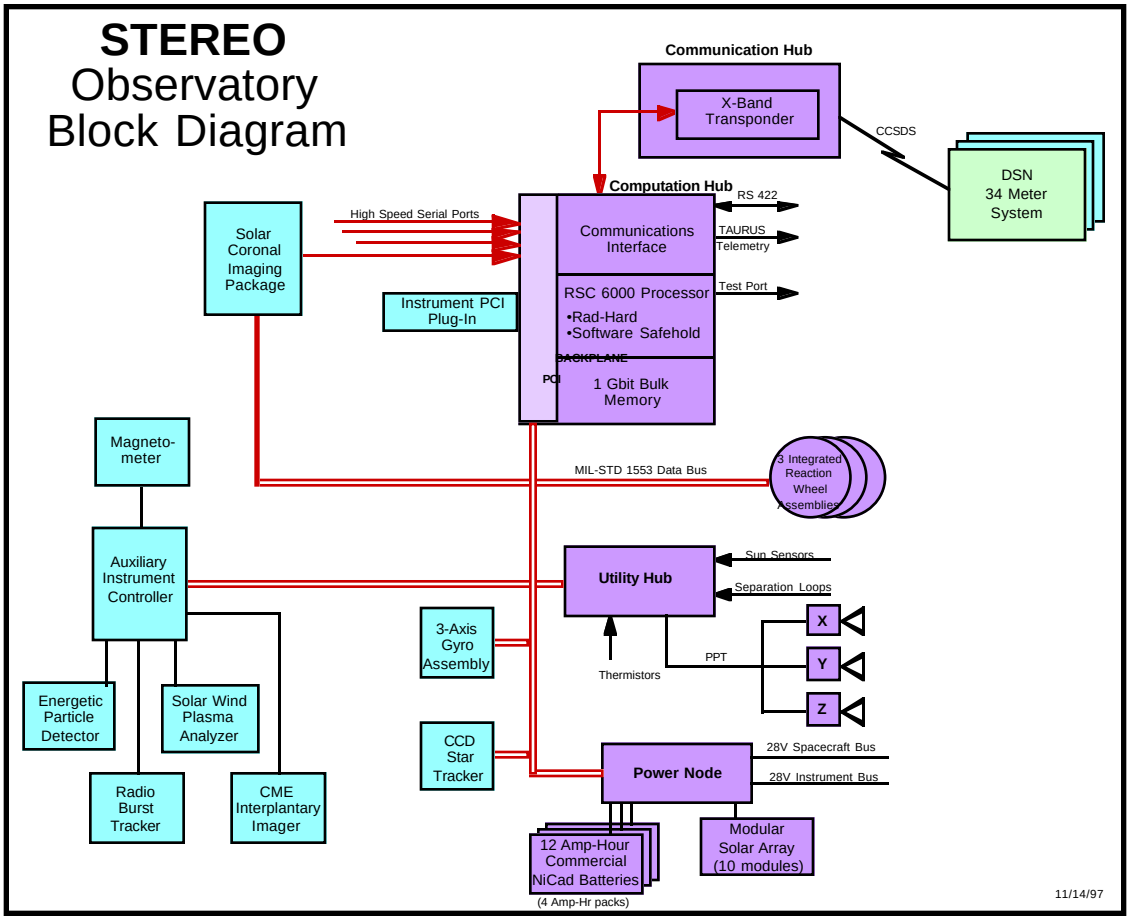

Figure 11. STEREO Observatory Block Diagram

G. Attitude Control System (ACS)

The STEREO mission requires a three-axis stabilized pointer that maintains the instrument line of sight viewing the Sun with a ±30 arc-sec, 3-sigma accuracy. Jitter must be limited to within ±5 arc-sec. The coronograph provides a pitch/yaw pointing error signal accurate to approximately 0.1 arc-sec that is used by the ACS for its solar reference. Roll about the sunline is unimportant to the science data collection, but is important for post flight data analysis. The solar roll angle must be known to 0.1 degrees. The spacecraft roll angle must be controlled such that the high gain antenna is pointed towards the Earth ±0.10 degrees.

All of these pointing requirements can easily be accommodated by an ACS configuration similar to that used on the NASA/SMEX Transition Region and Coronal Explorer (TRACE)[3] mission. Three orthogonal reaction wheels are used to adjust the attitude of the

spacecraft and to provide a bias momentum vector oriented towards the Sun. This bias momentum provides gyroscopic stability to the system, resisting disturbance torque perturbations and providing short-term stability in the case of system upsets.

Three orthogonal Pulsed Plasma Thrusters (PPT) are utilized to manage secular momentum build-up. These devices function as illustrated in Figure 12. They have been successfully flown on the US Navy NOVA satellites. Further background data is available in Reference 2. The PPT was chosen over the more traditional liquid or cold gas propulsion system because of its simplicity and small size. Once out of Earth orbit the spacecraft disturbance torques are very small, dominated by solar pressure forces and weak gravitational pulls. The estimated disturbance torques were increased by a factor of 3 for the purposes of this study. Designing the sunward face of the spacecraft to have a small CG/CP displacement (≤1.0 in) further minimizes the effects of the solar pressure forces; however, the ACS design is not dependent upon this assumption. Increasing the CG/CP separation to 1.0-foot approaches the practical limitation of the PPT, increasing the average power and Teflon propellant mass by a factor of twelve. However, it is rather straight-forward to balance the spacecraft projected area to within a few inches of the CG, so this is of little concern. This low torque environment is the ideal place to use PPT's since the devices themselves produce relatively small impulses. The PPT for STEREO were sized using the assumptions outlined in Table 1. The resulting calculations specified a very modest PPT size that is well within the experience base of these devices. The NASA EO-1 spacecraft of the New Millennium Program will fly similar devices in 1999.

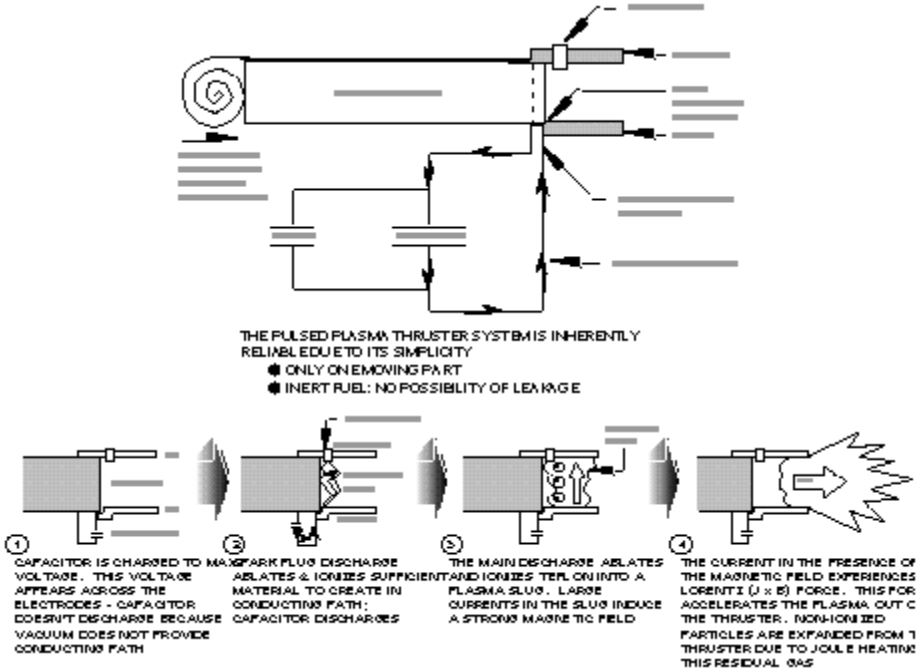

Figure 12. Pulsed Plasma Thruster System

Table 1. PPT Sizing Assumptions

Assumption			Comment
Environment	Solar radiation pressure	1.3×10^{-4} N	Solar flux = 1358 w/m^2
	Solar radiation pressure Torque	3.3×10^{-4} N-m	Spacecraft CP/CG offset = 1.0 in
	1 min. accumulated momentum	1.98×10^{-4} N-m-s	
	Spacecraft surface area	6.0 m^2	Sun face
	Spacecraft surface reflectance	0.6	Sun face q
Thruster Characteristic	1.5 amp source	29.4 W	70% efficiency
	Max. capacitor charge	29.4 J	
	Time for max. charge	1.0 sec	
	Min. capacitor charge	5.0 J	
	Time for min. charge	0.1701 sec	
Calculated	Required thruster impulse	3.97×10^{-4} N-s	
	Required mass per firing	4.05×10^{-8} kg	Isp = 1000 seconds
	Required thruster force	3.97×10^{-4} N	at 1 Hz firings
	Required capacitor charge	22.62 J	
	Required capacitor charge time	0.7694 sec	at power level
	Average power over 1 hour	0.377 W	
	Firings over 2 years	1,051,200	0.0167 Hz frequency
	Teflon mass over 2 years	0.0426 kg	
	Length of Teflon cylinder	0.0389 m	1 in. diameter
Performance			

Sun acquisition attitude signals are provided by a moderate Field of View (FOV) fine Sun sensor further aided by 2π steradian coverage coarse Sun sensors. Fine Sun pointing error signals come from the coronagraph.

Roll attitude information is provided by a star tracker oriented perpendicular to the spacecraft Sun axis, opposite the high gain antenna. The ecliptic plane is richly populated with stars, providing an easily recognizable roll reference throughout the mission. The orientation of the Earth will be computed on-board utilizing this roll reference and an orbital ephemeris updated by mission controllers. The ACS will also compute the required high gain antenna pitch angle necessary to maintain an effective communication link to the Earth.

The ACS will also provide safe pointing at the start of the mission. Once released from the launch vehicle, the spacecraft will autonomously deploy the solar arrays and enable the ACS to seek and point towards the Sun and orient the high gain antenna axis towards the Earth. This initial Sun acquisition utilizes all three reaction wheels and should be accomplished in a few minutes time. The wheels must be sized to have sufficient momentum storage capability to absorb the full tip-off momentum from launch vehicle separation. Once stabilized in position the spacecraft will await ground command to initialize the science instrumentation. This autonomous acquisition approach has been successfully utilized on all SMEX missions.

Attitude control algorithms are executed within the spacecraft processor. The required system performance is well within prior SMEX mission capabilities and is not a driver for this mission.

H. Data and Communication System

The STEREO data system must be capable of collecting one Gbit of science data per day and relaying it to the ground. This can easily be handled with two hours per day of 150 Kbps downlink transmission to the Deep Space Network (DSN) 34 meter ground system during the prime mission period (i.e., ~60 degree spacecraft separation angle). Later in the mission the data rate must be reduced in order to maintain an adequate link margin (see Figure 13) as the spacecraft-Earth separation distance increases. Reduced data volume must be incorporated to balance the data flow. Downlink time can also be increased as long as a positive energy balance is maintained within the spacecraft power system. A third option of maintaining data volume during the extended mission would be to switch to the DSN 70 meter ground system; however, system availability may make this impractical. The spacecraft will have 8 selectable data rates in order to support this flexibility.

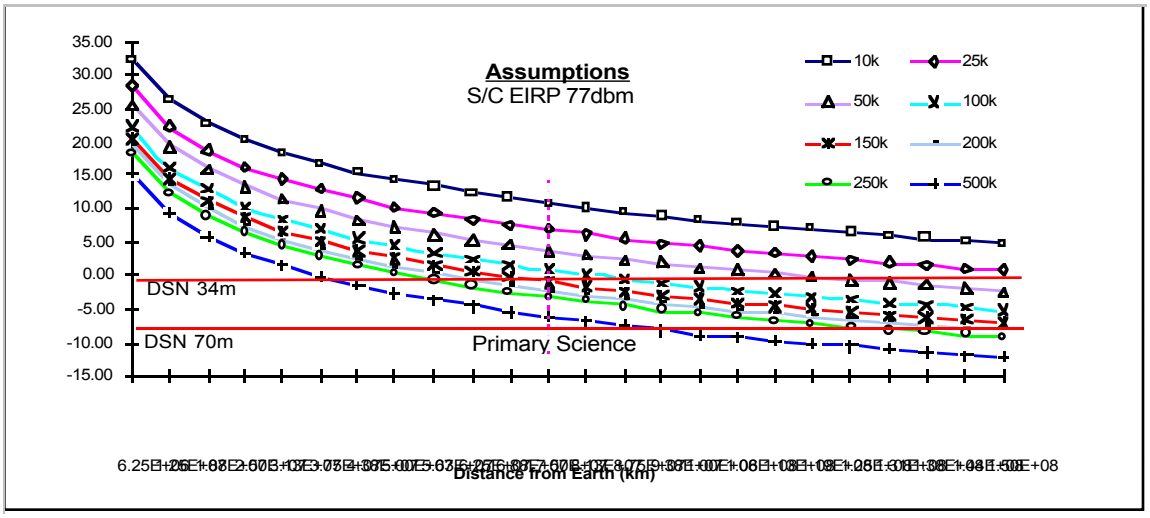

Figure 13. STEREO Link Margins

A full day's data set can be stored in a relatively modest solid state recorder. Spacecraft command loads can be received concurrent with the downlink.

In order to support these data flow requirements as well as to maintain the theme of spacecraft simplicity, a 1.3 meter rigid antenna with 39 dB gain and a Field of View (FOV)

of ±0.25 degrees was chosen for the high gain downlink and beacon mode broadcast. This is the largest fixed antenna that could be easily packaged in the payload volume without utilizing an elaborate deployable mechanism or antenna system. The antenna is stowed above the spacecraft for launch and rotated into the operational position after separation from the launch vehicle. The spacecraft will roll in order to orient the antenna towards the Sun-Earth line. The antenna will be oriented along the Sun-Earth line to point at the Earth by a small stepper motor that will pivot the antenna elevation axis relative to the spacecraft body. The elevation angle (see Figure 14 and Figure 15) changes slowly throughout the mission and consequently will only require periodic adjustment, rather than active pointing. The antenna elevation angle will therefore be controlled to ±0.1 degree. If the mission is extended much beyond two years the spacecraft will need to offset point from the Sun in order to place the Earth within the antenna FOV since elevation angle adjustment is limited. Two low gain omni-directional antennas will provide coverage for health and safety contingencies as well as initial Launch and Early Orbit (L&EO) activities.

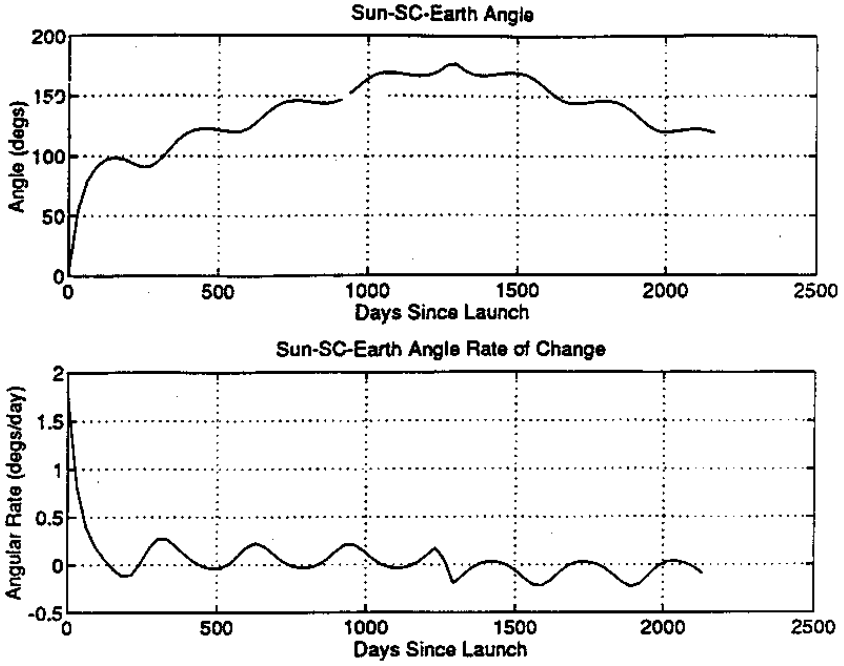

Figure 14. Earth-Sun-Spacecraft Angle Variation (C_3=2.01)

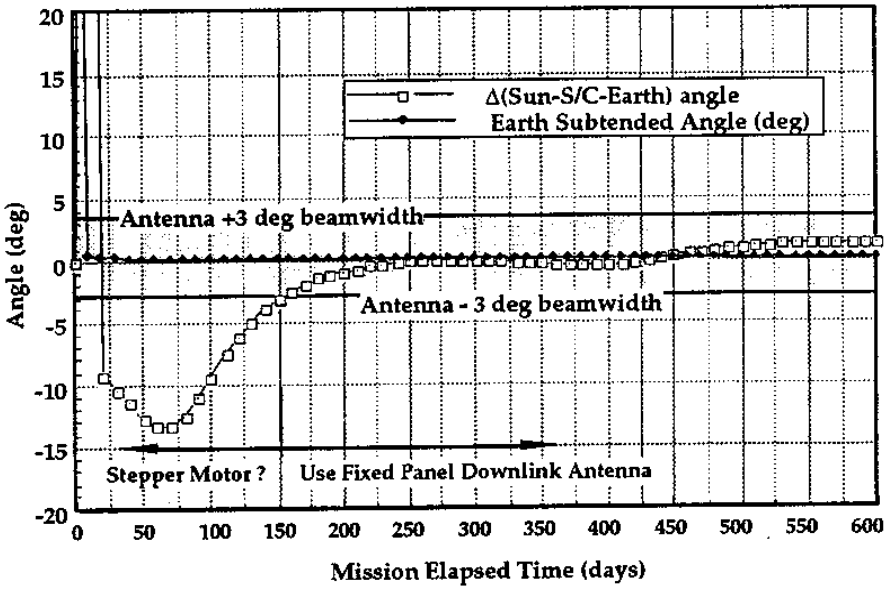

Figure 15. Typical Sun-Spacecraft-Earth Angle Variation (C_3=2.01)

The data system will utilize a 20 watt X-band transponder for RF communications. X-band allows for a smaller size antenna and avoids the frequency access issues which are becoming more pronounced in the crowded S-band arena. DSN is already equipped to handle X-band communications. This configuration meets the command and telemetry requirements as well as satisfying the orbit tracking requirements for two-way Doppler and ranging data. Orbit knowledge can easily be derived for this trajectory using this approach to better than ±200 km along track and ±100 km across track, more than sufficient for science data analysis and ground station antenna pointing.

The data management functions as well as the ACS functions can be easily handled by the single spacecraft R6000 processor and interfaces integral to the SMEX•*Lite* architecture. The Command and Data Handling (C&DH), ACS and spacecraft health and safety flight software requirements can easily be supported by existing SMEX software with an estimated reuse factor of 85%. This code is highly structured and utilizes C+/C++ high level language modules. The processor, running at 33 MHz, will only be ~15% utilized to support the spacecraft requirements of this mission.

I. Power System

The STEREO power system is only required to provide ~150 watts of 28 volt power to the observatory. This requirement can be met with 1.08 square meters (12 SMEX•*Lite* solar array platelets) of GaAs solar array. A 12 Amp-hr Nickel Cadmium battery is incorporated to provide a power reserve for transmitter operation as well as to act as the primary power source during L&EO prior to solar array deployment and Sun acquisition.

J. Power and Weight Budgets

Item	Mass (kg)	Average Power (watt)	Comments/Heritage
Primary Structure	24.0	–	SMEX•*Lite*
Balance Weights	10.0	–	
Solar Array	7.2	–	SMEX•*Lite*
Battery	12.0	–	Sanyo D-cell
Transponder	5.0	15.0	20 watt RF output (daily average)
Antenna Support Structure	11.0	–	
Harness	7.2	–	SMEX
High Gain Antenna	5.5	–	TRMM
Low Gain Antennas	0.8	–	SMEX
Computation Hub	5.5	18.5	SMEX•*Lite*
Utility Hub	2.3	5.0	SMEX•*Lite*
Power Node	5.4	9.7	92% efficiency
Reaction Wheels	12.0	12.0	SMEX•*Lite*
Pulsed Plasma Thrusters	10.5	3.5	Factor of 3 power margin
Sun Sensors	1.0	0.7	Adcole DSS, CSS
Gyros	5.0	12.0	SMEX Incosym
Star Tracker	8.0	7.6	Lockheed AST
Thermal	2.0	10.0	SMEX
Spacecraft Subtotal	134.4	94.0	
Combined Emission-Line Imager and Coronagraph	20.0	20.0	LASCO, EIT
Magnetometer	2.0	2.0	Existing versions
Solar Wind Analyzer	3.0	2.0	Existing versions
Energetic Particle Detector	3.0	2.0	Existing versions
Radio Burst Telescope	5.0	2.0	Existing versions
Heliosphere Imager	15.0	20.0	New development
Aux. Instrument Controller	5.0	10.0	
Instrument Support Structure	10.0	–	
CME Structure Deployment Mechanisms	8.0		
Instrument Harness	6.0		
Instrument Subtotal	69.0	58.0	
TOTAL	**211.4**	**152.0**	
Mission Capability	**350.0**	**156.0**	

II. Mission Operations Concept

The SMEX Program has been actively pursuing and promoting the concepts of automated spacecraft operations. By combining the safing capabilities of the spacecraft and the advancements in ground control software, the TRACE and Wide-Field Infrared Explorer (WIRE) missions are setting precedence for unattended spacecraft operations.

The location of the control center is somewhat arbitrary when considering these advancements in telecommunications. The SMEX control center is centrally located at GSFC with access to ground support resources as well as access to other solar physics observatories for coordinated science observations. Communications services between Jet Propulsion Laboratory (JPL), the primary source of data, and GSFC are already in place and would simply require bandwidth allocation. GSFC Flight Dynamics Facility (FDF) would provide tracking and navigation services which would allow STEREO to take advantage of the PC based FDF systems being developed for TRACE and WIRE. These systems will process and distribute required FDF products.

The STEREO control center could easily be modeled after the TRACE and WIRE systems. The primary ground control software requirements can be met by the Integrated Test and Operations System (ITOS). ITOS has 7 years of SMEX heritage and takes advantage of cost effective automation features. The automation features allow for unattended health and safety monitoring, data processing, and anomaly notification. Anomaly notification is accomplished with automated configuration monitoring and limit checking which activate pre-programmed paging systems. Spacecraft safing sequences ensure that all mission critical responses to anomalies are issued by the onboard computer.

Armed with the confidence that mission critical responses are satisfied and that the spacecraft will be in a stable condition at the next ground contact, the operations will be reduced primarily to mission planning and post-pass data evaluation. This will enable operations support to be constrained to a standard 40 hour week. The size of the team will depend primarily on the expertise of the staff and the spacecraft real-time requirements. A skilled team of four could reasonably support this mission as long as the instrument operations can be simplified to a consistent data acquisition mode. Operations of both STEREO satellites will be kept as identical as possible to minimize the operation to simple station contact differences. A baseline of 1 Gbit per day at the primary science distance of .5 AU will require DSN station support for 2 hours @ 150 Kbps per day. This could be supported in multiple passes or one single pass. Additional pass coverage could be scheduled to increase science data volume. Much of this depends on station availability; however, either approach can be accommodated. The spacecraft will have selectable data rates to accommodate link margin restrictions. This will give the operations personnel considerable flexibility in mission planning. The DSN 34 meter system is the baseline for the STEREO communication system; however, in times of conflict the 70 meter system can be used to dump science data faster and to conserve spacecraft power.

Command uploads will cover a one week period which once again will reduce operations. This upload should consist primarily of station contacts, science data dump commands and orbital ephemeris updates. The Command Management System (CMS), modeled after the TRACE system, will take ground station contact schedules and science command inputs to

produce spacecraft command loads. If routine operations are necessary these actions will be done with the on-board Absolute Time Sequence (ATS) and Relative Time Sequences (RTS).

On-board science data analysis could identify data as a priority for near real-time transmission and set off the “Beacon Mode” that would attempt to call for ground support. This mode would initiate a request for ground support by sending a low rate beacon to scheduled listening stations. Once the signal is detected the station would activate a paging request to the operations personnel. The flight operations team would then schedule a DSN station contact and issue the data collection commands. This concept does have drawbacks in that it would require constant ground monitoring. Ground stations with reasonable antenna gains of 52 dB (5.5 meter) could support a beacon mode surveillance concept. There are numerous commercial companies that are currently developing the ground station infrastructure that would be needed.

III. Mission Cost Estimate

The STEREO mission cost estimate is based partially on actual SMEX mission historical data[4], and partially on comparative evaluations of similar type instrumentation. SMEX-*Lite* mission costs are derived from the ongoing technology development expenditure history. The technical maturity of most elements of this mission make this a realistic method to assess mission viability.

The STEREO mission cost estimate is based on an accelerated development cycle (see Figure 16) beginning in October 1999 and ending with a launch of the first spacecraft in February 2003, and the second spacecraft in April 2003.

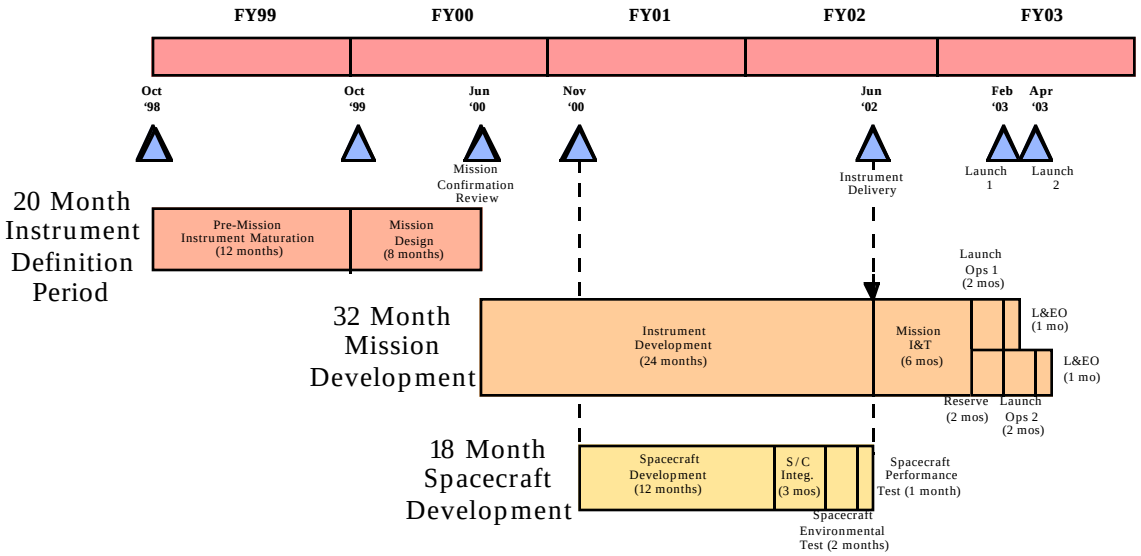

Figure 16. Development Cycle

Postponing the spacecraft development is a valid technique for reducing system cost given the straightforward requirements for this mission. It is assumed that an existing spacecraft design could be incorporated with very minor mission unique modifications. The mission design period and the pre-mission development instrument definition period will focus on defining the instrument configuration and interface specifications.

The STEREO mission total cost is summarized in Table 2 and Table 3.

Table 2. STEREO Mission Cost Summary (FY97 $M)

	Phase A/B & Technology & Ground System	Phase C/D	Non-Flight
Instrument Definition			
Maturation	3.0		
Definition	5.0		
Instrument Development		60.0	
Reserve (20%)		12.0	
Subtotal		72.0	
Spacecraft Development	5.2	26.5	
Reserve (20%)	1.1	5.3	
Subtotal	6.3	31.8	
Mission Integration	1.6	11.6	
Reserve (10%)	0.2	1.2	
Subtotal	1.8	12.8	
Launch Segment			56.0
Ground System	8.0		
Reserve (20%)	2.0		
MO&DA			20.0
Plan Subtotal	22.8	96.1	76.0
Reserve Subtotal	3.3	20.5	0.0
Subtotal	**26.1**	**116.6**	76.0
GRAND TOTAL		**218.7**	

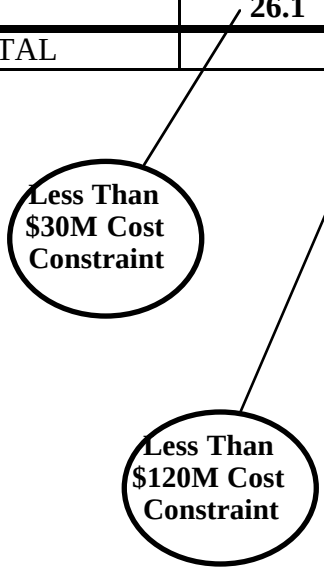

Table 3. STEREO Mission NOA Phasing Estimate (FY97 $M)

Mission Segment (including reserve)	FY99	FY00	FY01	FY02	FY03	FY04	FY05
Instrument Definition	3.0	5.0					
Instrument Development		14.4	26.4	21.6	9.6		
Spacecraft Development		6.3	17.2	12.7	1.9		
Mission Integration		1.8	4.4	5.8	3.9		
Launch Segment			23.0	24.6	8.4		
Ground Segment			2.0	5.0	3.0		
MO&DA					8.0	11.0	11.0
TOTAL	3.0	27.5	73.0	69.7	34.8	11.0	11.0

A. Launch Segment Costs

The TAURUS vehicle configured for STEREO is estimated by the NASA/GSFC Orbital Launch Services (OLS) Project to cost ~$28M. This includes payload support and integration costs. Consequently the STEREO mission launch cost is $56M. The vehicle is ordered 30 months prior to launch with a payment schedule as outlined in Table 4.

Table 4. Payment Schedule

Milestone Event No.	Amount (% of Price)	Estimated Date of Completion (Months)
1	10%	L-30
2	5%	L-27
3	8%	L-24
4	9%	L-21
5	9%	L-18
6	9%	L-15
7	12%	L-12
8	12%	L-9
9	11%	L-6
10	5%	L-3
11	5%	Launch
12	5%	L+3

B. Instrument Costs

1. Instrument Definition

Instrument definition costs include all instrument expenditures associated with Pre-Phase A, Phase A, and Phase B activities leading up to the Mission Confirmation Review.

The projected instrument costs are summarized in Table 5, along with some indication of the heritage of the instrument design.

Table 5. Summary of the Estimated Instrument Costs for the STEREO Instrument complement.

Instrument	Heritage	Estimated Cost ($M) for Each Instrument*
Solar Coronal Imaging Package (SCIP) Coronagraph and emission-line imager combined	Coronagraph is similar to the SPARTAN 201 coronagraph with offset occulter Coronal and Chromospheric Imager is a simplified version of the multi-layer imaging technology of TRACE and EIT	18
Energetic Particle Detector	ACE	2
Radio Burst Tracker	Similar to the instruments on Ulysses and WIND	2
Magnetometer	Similar to instrument on GIOTTO, CLUSTER, Mars Global Surveyor	1
Solar Wind Plasma Analyzer	WIND	2
Heliosphere Imager	SMEI (Air Force prog.) NEAR	5
Total Cost	**—**	**30**

*All costs given are for a single instrument. The total mission instrument cost can be obtained by simply doubling these amounts since two instruments are required.

The cost for the SCIP is based on the cost for comparable but more complex instruments from the TRACE and SOHO missions. TRACE is a much more sophisticated, much

larger instrument than the SCIP with sub-arcsecond pointing, active focusing, multiple bandpass optics. Additional basis for this cost is obtained by comparing the SCIP with the Solar X-ray Telescope (SXT) on Yohkoh. But again, the instrument is much more challenging than the SCIP with very expensive grazing incidence optics and a filter wheel. In addition, SXT had one of the first CCD cameras built for a solar physics mission, and significant development cost were incurred. Since that time, several groups have developed working, inexpensive CCD cameras, which could be used for the SCIP.

2. Instrument Development and Integration

Instrument development and integration costs include all costs incurred during Phase C/D associated with the instruments and the preparation of the Science Operations Center (SOC). This includes support to observatory Integration and Test (I&T) through launch + 30 days.

C. Spacecraft Costs

Spacecraft costs (see Table 6) begin with supporting the mission design. They include all costs associated with spacecraft design, build, and qualification testing as an assembled single component up to the time of instrument integration. Spacecraft hardware is obtained in a "protoflight" status, meaning that Engineering Test Unit (ETU) and spare units are generally not procured. This approach obviously presents some schedule risk, but is consistent with the low cost approach that is recommended for the STEREO mission. Significant reserve is carried on the spacecraft, not because it is a risky development, but simply because the aerospace industry has only infrequently demonstrated cost performance similar to that of the SMEX Program. Better performance is expected over the next few years as the newer technology subsystems and interface standardizations become the norm.

Table 6. Spacecraft Cost Itemization

	FY00		FY01	FY02	FY03		Mission Tota
Mission Element	**$M**		**$M**	**$M**	**$M**		**$M**
Mechanical	0.111		0.810	0.280	0.105		1.306
Power Node	0.017		0.190	0.020	0.010		0.237
Battery	0.000		0.120	0.020	0.010		0.150
Solar Array	0.187		0.320	0.210	0.000		0.717
Harness	0.000		0.130	0.040	0.000		0.170
Thermal	0.153		0.160	0.150	0.040		0.503
Contamination	0.017		0.020	0.080	0.020		0.137
Utility Node	0.000		0.110	0.010	0.010		0.130
ACS Analysis	0.391		0.363	0.262	0.175		1.191
ACS Hardware	0.170		1.500	1.190	0.010		2.870
ACS Software	0.136		0.288	0.257	0.050		0.731
C&DH Software	0.204		0.400	0.300	0.070		0.974
C&DH Hardware	0.034		0.670	0.310	0.000		1.014
Communications	0.051		0.740	0.340	0.020		1.151
I&T GSE	0.357		0.440	0.340	0.200		1.337
EEE Parts	0.578		0.170	0.010	0.000		0.758
Spacecraft I&T	0.000		0.200	1.100	0.000		1.300
SUB-TOTAL	2.406		6.631	4.919	0.720		14.676
8% G&A	0.192		0.530	0.394	0.058		1.174
TOTAL	**$2.598**		**$7.161**	**$5.313**	**$0.778**		**$15.850**
	Phase B (Design)		**Phase C/D (Development)**				

D. Mission Integration Costs

Mission integration costs (see Table 7) begin with managing the mission design activities and include all costs associated with integration of the instruments to the spacecraft and all subsequent observatory testing and engineering support up through the initial 30 days on orbit. It also includes all project management costs including administrative, project support, financial, flight assurance, Reliability and Quality Assurance (R&QA), inventory management, preparation of the flight operations team for mission operations, mission systems engineering, and launch operations support.

The STEREO mission integration costs are based on actual SMEX mission[5] historical data. Though the STEREO mission requires the construction of identical observatories, the mission integration costs assume an activity level consistent with prior SMEX missions that were unique and distinctly separate.

Table 7. Mission Integration Cost Itemization

	FY01	FY02	FY03	FY04	Mission Total
Mission Element	**$M**	**$M**	**$M**	**$M**	**$M**
Scheduling	0.017	0.025	0.045	0.010	0.097
Configuration Management	0.068	0.100	0.100	0.030	0.298
Management, Systems Engineering and Administrative	0.306	0.430	0.510	0.410	1.656
Travel	0.020	0.048	0.059	0.150	0.277
Mission I&T	0.000	0.000	0.580	0.590	1.170
Field Operations	0.000	0.000	0.050	0.100	0.150
Quality Assurance	0.068	0.130	0.230	0.050	0.478
Misc. Flight Assurance	0.000	0.080	0.020	0.000	0.100
Reliability	0.000	0.040	0.080	0.030	0.150
EEE Parts Support	0.170	0.200	0.060	0.000	0.430
Flight Operations Preparation	0.085	0.540	0.460	0.130	1.215
Miscellaneous	0.000	0.050	0.050	0.000	0.100
SUB-TOTAL	**0.734**	**1.643**	**2.244**	**1.500**	**6.121**
8% G&A	0.059	0.131	0.180	0.120	0.490
TOTAL	**0.793**	**1.774**	**2.424**	**1.620**	**6.611**
	Phase B (Design)	**Phase C/D (Development)**			

E. Mission Operations and Data Analysis Costs

The STEREO MO&DA activities are very straightforward. Except for the routine use of the DSN 34 meter system, the mission operations activities are very similar to those planned for the upcoming TRACE mission. These include not only the conduct of the STEREO mission and analysis and distribution of its data products but also coordination with other orbiting and ground based solar observatories. For the purposes of this study the Mission Operations and Data Analysis (MO&DA) requirements were assumed to be approximately twice the scale of those of the TRACE mission. This is a very conservative assumption.

IV. Study Conclusion and Recommendations

This study finds the STEREO mission to be very doable with today's progressive technologies. The spacecraft and instruments can be developed with minimal technical risk. Cost and technical (power, weight, volume, and performance) margins are robust.

The STEREO mission is an excellent starter mission candidate for the new SEC initiative. The three-dimensional measurements of coronal structures will provide new and unique research tools to investigate the physics and evolution of the Sun. These will have tremendous public appeal, helping to communicate the excitement of this science to members of other scientific disciplines and to the public at large.

---

[1] James G. Watzin. "SMEX•Lite–NASA's Next Generation Small Explorer". 10th Annual AIAA/USU Conference on Small Satellites, 16-19 September 1996.
[2] Same as number 1.
[3] Darrell Zimbelman. "The Attitude Control System Design for the Transition Region and Coronal Explorer Mission". 9th Annual AIAA/USU Conference on Small Satellites, 18-21 September 1995.
[4] Same as number 1.
[5] Same at number 1.

Appendix II. Data Compression

The STEREO mission science objectives require transmission of at least 250 images per day from each spacecraft. Since the spacecraft distances from Earth range up to ~1 AU during the prime science phases, the capacity of the available resources to handle the demand must be carefully examined. We studied the issue using reasonable assumptions for the onboard computer, compression algorithms, transmitter power, high-gain antenna dimensions, and use of the NASA DSN. The results of the study are presented *quantitatively* in tabular form as unit images received per DSN contact as a function of spacecraft distance from Earth and *qualitatively* as actual compressed SOHO/LASCO and images.

The onboard resource assumptions for the study were as follows. The nominal imaging detector was assumed to be a 1024 × 1024 pixel format charge-coupled device (CCD) operated with 16-bit analog-to-digital conversion. A single full-resolution image acquired with such a detector is treated as a unit image. Other image rates with subframe images or larger CCD pixel formats can be obtained by scaling the tabular unit image rates as appropriate.

The onboard computer was assumed to be able to handle the computational compression demand without significantly affecting the telemetry rate. This is a reasonable assumption based on earlier studies. These had indicated that, when the spacecraft are very near Earth, the telemetry rate is so high that either the instruments themselves or the onboard storage tends to limit the images per contact, while at large spacecraft distances from Earth telemetry limits the rate. The compression algorithms assumed and used for the sample images were Rice and the H-transform. Onboard storage was assumed to be adequate to hold up to 3 days of compressed images.

A 50-W X-band transmitter coupled to a 1.3-m-diameter parabolic high-gain (38 dB) antenna was assumed for the study. The power level appears to be practical for the anticipated launch date, and the antenna diameter is reasonable for the overall spacecraft design.

Use of the DSN assumed a 34-m dish, an 8-hour contact, and a 6-dB margin, all standard values.

The results of the study are presented in Table 1, which shows the number of unit images transmitted per 8-hour DSN contact as a function of spacecraft lead (lag) angle from Earth and as a function of the applied compression factor (CF). The CFs were chosen on the basis of actual experience with SOHO/LASCO. A CF of 1.0 indicates no compression; a CF of 2.4 is typical of the compression achieved with the lossless Rice compression; and CFs of 10 and 28 are for H-compression and were chosen to match the compression applied to the sample compressed images shown in Figure 1.

The images shown in Figure 1 are SOHO/LASCO C2 and C3 coronagraph images compressed with the lossless Rice compression (CF = 2.4) and the lossy H-compression (CF = 10 and 30). The images show that the lossy compression values cited in Table 1 are acceptable for the coronagraph images and probably also for the heliosphere imager. Similar tests with SOHO/EIT images indicate that H-compression with a CF of 10 produces acceptable image quality.

We conclude that one 8-hour DSN contact per spacecraft every 3 days will provide ~200 to 600 stereographic image pairs per day around a 60° lead angle and ~100 to 300 stereographic image pairs per day around the 90° lead angle. This quantity of stereographic image pairs will be sufficient to meet the STEREO science objectives. The onboard storage requirement for 800 images per day compressed by a factor of 28 is ~1 Gbit.

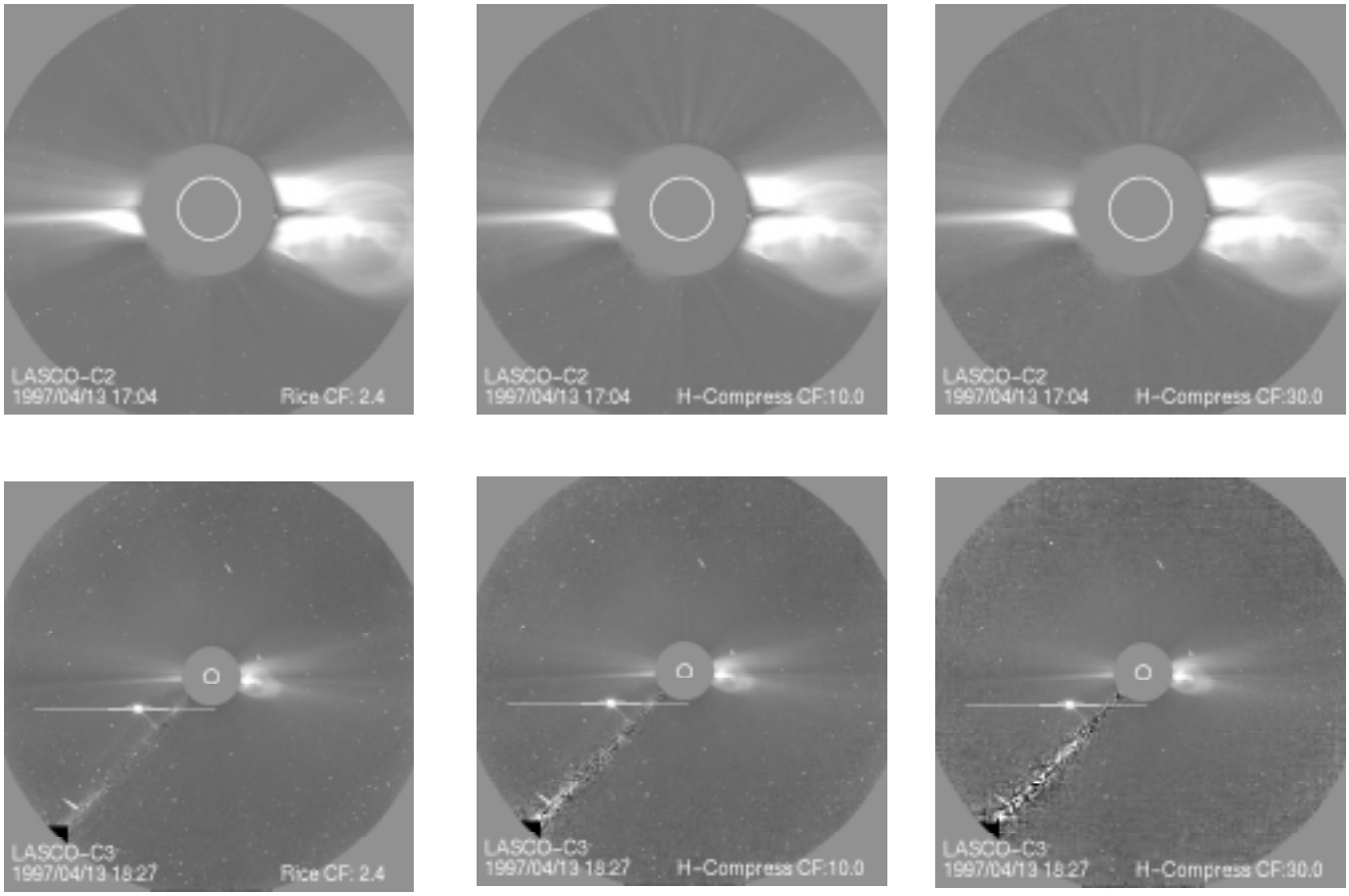

Figure 1 Comparison of coronagraph images compressed by various factors. Even with a compression factor of 30, it is difficult to detect any image degradation.

Table 1. Unit images per DSN contact as a function of spacecraft lead angle and compression factor (CF).

Angle (deg)	Telemetry (kbits/s)	CF = 1	CF = 2.4	CF = 10	CF = 28
30	142	243	585	2437	6823
60	38	65	156	653	1827
90	19	32	78	326	913

Appendix III. The Case for Magnetographs

Should the STEREO spacecraft carry a magnetograph? If so, what type of magnetograph—vector or line-of-light (LOS)? In this appendix, we make the case that it is important for STEREO to carry a magnetograph of some form on both spacecraft.

Vector versus LOS Magnetographs

A simple, low-resolution longitudinal magnetograph would add immensely to the scientific return of the STEREO mission, but is there a strong case for including a vector magnetograph? It is a more complex and expensive instrument and would take more telemetry resources so would have a lower cadence than a longitudinal instrument.

A vector magnetograph would enable us to see the transverse component of the photospheric magnetic fields as well as measure the line-of-sight magnetic field. It could help in understanding the role of helicity in the processes that form magnetic structures in the corona and their relative instability.

However, we need to investigate what sensitivity is possible on an instrument compatible with the size, mass, telemetry, and budget restrictions of the STEREO mission. If it can only measure the transverse component in strong-field regions, i.e., active regions, it will not add greatly to the mission. Equally, if the spatial resolution is too low, we run the danger of adding too much of the fine structure together and ending up with a low-fidelity reconstruction of the coronal fields.

LOS magnetographs would provide valuable information on the general structure of the photospheric field, and having three views (including ground-based magnetographs) would provide some information on the transverse component, at least in the plane of the ecliptic. If these data can be combined with the 3-D data on coronal magnetic field structure from the coronal imager, it might be possible to model the structure of the field from the photosphere to the corona. However, this could be a very computationally challenging project, and how well conditioned the problem is would have to be studied.

Scientific Objectives of Magnetic Field Measurements from STEREO

Vital to our understanding of the propagation of interplanetary disturbances is the ability to model the solar wind flow. Such models currently are based on Carrington Rotation maps built up from LOS magnetograms taken from ground-based observatories. The fidelity of the resulting models are suspect because the determining characteristics are partly global in nature. Consequently, some parts of the input data for the models are more than 3 weeks out of date. We know from Yohkoh and SOHO observations that even the quiet Sun during solar minimum changes on timescales measured in hours and days rather than weeks. Having the multiple views of the Sun that STEREO spacecraft would provide, especially when they are more than 90° apart, none of the data that the solar wind models were based on would be more than a few days old. This would provide significantly more reliable models of the solar wind and, hence, a firmer basis for understanding the propagation of CMEs in the solar wind.

These types of measurements impose some basic requirements on the magnetograph. It can be relatively low resolution (>5 arcsec) over the full solar disk, but it does need to have high accuracy at low field strengths (≤ 100 G). The observations would be required every ~6 hours.

The global measurement of the solar magnetic field would enable us, for the first time, to see its continuous evolution. From a single, Earth-bound perspective we only see about 30% of the Sun's magnetic evolution due to foreshortening effects near the limb, and we are blind to what happens on the far side of the Sun. Hence, our understanding of the emergence and evolution of magnetic fields is based on a statistical montage of the partial evolution of many regions. We do not know, for example, whether there is simultaneous global emergence of field (as implied by outbreaks of X-ray bright points seen by Yohkoh and sympathetic flaring observed by SMM). This would imply a large-scale (global) interconnectivity of the field. We have been surprised by the Yohkoh images showing how widely interconnected active regions are, but do these images reflect

a global phenomenon? STEREO, with a combination of a magnetograph and coronal imager, especially in Phase 4, would be able to address this problem.

The evolution of large-scale structures, although slower than active regions, still cannot be followed with a sufficient temporal coverage to understand or predict their course. The appearance and evolution of coronal holes, particularly transequatorial coronal holes, is hard to understand without continuous coverage. They can last for several rotations, and some seem to be sheared by differential rotation while others do not. Are they a structure in their own right or are they formed and controlled by other global forces? Again, only STEREO, with a magnetograph and coronal imager, can answer this question by providing continuous spatial coverage of them.

Polar plumes, polar-crown arcades, filaments, and extended neutral lines are further examples of large-scale structures that can only be effectively studied using STEREO, but it is vital that the two spacecraft carry magnetographs to address the problems associated with these globally related phenomena.

Magnetographs can also make helioseismology measurements, either in Doppler mode or by tuning to the local continuum. Data taken from multiple spacecraft and the Earth–Sun line (e.g., from SOHO or ground-based observatories) can be combined so that the entire Sun is in view; this will allow precise frequency measurements without crosstalk between the modes. In the low-l, global-mode regime, the mode frequencies and rotational splittings that probe the energy-generating core may be measured much more precisely than is currently possible.

If it were possible to obtain time series over a few months, we could make advances in g-mode studies. Another potentially interesting application of this type of observation would be to obtain somewhat higher-resolution velocity measurements, perhaps in the range of l = 50–100. This is the direction of systematic, long-lived flows in and below the photosphere by the technique of time-distance helioseismology. Observations with the Michelson-Doppler Imager on SOHO have demonstrated that this approach is feasible but is limited by the solar rotation, which removes any given portion of the Sun in less than 2 weeks. By following a region around the Sun for a rotation or more, the technique could discover the long-sought giant cells in the convection zone beneath the photosphere.

Conclusion

The baseline instrument complement does not include a magnetograph simply because of cost limitations. However, we have explored the potential advantages of stereoscopic magnetography, and *we recommend that studies of lightweight vector magnetographs and line-of-sight magnetographs be initiated*. If a magnetograph can be developed that is compatible with the STEREO mission restrictions and science requirements, it should be seriously considered.